

**UNIVERSIDAD SAN FRANCISCO DE QUITO
USFQ**

Colegio de Ciencias e Ingeniería

6 [kg] Cargo UAV with Modular Seed Distribution System

Gabriel Alejandro Gómez Guerra

Mateo José González Estrella

Nicolás Alejandro Herrera León

Mateo Sebastián Ormaza Jurado

Ingeniería Mecánica

Trabajo de fin de carrera
presentado como requisito para la
obtención del título de
Ingeniero Mecánico

Quito, 16 de mayo de 2022

**UNIVERSIDAD SAN FRANCISCO DE QUITO
USFQ**

Colegio de Ciencias e Ingeniería

**HOJA DE CALIFICACIÓN
DE TRABAJO DE FIN DE CARRERA**

6 [kg] Cargo UAV with Modular Seed Distribution System

Gabriel Alejandro Gómez Guerra

Mateo José González Estrella

Nicolás Alejandro Herrera León

Mateo Sebastián Ormaza Jurado

Nombre del profesor, Título académico

Patricio Chiriboga, PhD

Quito, 16 de mayo de 2022

© DERECHOS DE AUTOR

Por medio del presente documento certifico que he leído todas las Políticas y Manuales de la Universidad San Francisco de Quito USFQ, incluyendo la Política de Propiedad Intelectual USFQ, y estoy de acuerdo con su contenido, por lo que los derechos de propiedad intelectual del presente trabajo quedan sujetos a lo dispuesto en esas Políticas.

Asimismo, autorizo a la USFQ para que realice la digitalización y publicación de este trabajo en el repositorio virtual, de conformidad a lo dispuesto en la Ley Orgánica de Educación Superior del Ecuador.

Nombres y apellidos: Gabriel Alejandro Gómez Guerra

Códigos: 00204438

Cédula de identidad: 1721837084

Lugar y fecha: Quito, 15 de mayo de 2022

© DERECHOS DE AUTOR

Por medio del presente documento certifico que he leído todas las Políticas y Manuales de la Universidad San Francisco de Quito USFQ, incluyendo la Política de Propiedad Intelectual USFQ, y estoy de acuerdo con su contenido, por lo que los derechos de propiedad intelectual del presente trabajo quedan sujetos a lo dispuesto en esas Políticas.

Asimismo, autorizo a la USFQ para que realice la digitalización y publicación de este trabajo en el repositorio virtual, de conformidad a lo dispuesto en la Ley Orgánica de Educación Superior del Ecuador.

Nombres y apellidos: Mateo José González Estrella

Códigos: 000200474

Cédula de identidad: 1722376538

Lugar y fecha: Quito, 16 de mayo de 2022

© DERECHOS DE AUTOR

Por medio del presente documento certifico que he leído todas las Políticas y Manuales de la Universidad San Francisco de Quito USFQ, incluyendo la Política de Propiedad Intelectual USFQ, y estoy de acuerdo con su contenido, por lo que los derechos de propiedad intelectual del presente trabajo quedan sujetos a lo dispuesto en esas Políticas.

Asimismo, autorizo a la USFQ para que realice la digitalización y publicación de este trabajo en el repositorio virtual, de conformidad a lo dispuesto en la Ley Orgánica de Educación Superior del Ecuador.

Nombres y apellidos: Nicolás Alejandro Herrera León

Códigos: 00201713

Cédula de identidad: 1724401474

Lugar y fecha: Quito, 16 de mayo de 2022

© DERECHOS DE AUTOR

Por medio del presente documento certifico que he leído todas las Políticas y Manuales de la Universidad San Francisco de Quito USFQ, incluyendo la Política de Propiedad Intelectual USFQ, y estoy de acuerdo con su contenido, por lo que los derechos de propiedad intelectual del presente trabajo quedan sujetos a lo dispuesto en esas Políticas.

Asimismo, autorizo a la USFQ para que realice la digitalización y publicación de este trabajo en el repositorio virtual, de conformidad a lo dispuesto en la Ley Orgánica de Educación Superior del Ecuador.

Nombres y apellidos: Mateo Sebastián Ormaza Jurado

Códigos: 00204684

Cédula de identidad: 1724802788

Lugar y fecha: Quito, 16 de mayo de 2022

ACLARACIÓN PARA PUBLICACIÓN

Nota: El presente trabajo, en su totalidad o cualquiera de sus partes, no debe ser considerado como una publicación, incluso a pesar de estar disponible sin restricciones a través de un repositorio institucional. Esta declaración se alinea con las prácticas y recomendaciones presentadas por el Committee on Publication Ethics COPE descritas por Barbour et al. (2017) Discussion document on best practice for issues around theses publishing, disponible en <http://bit.ly/COPETHeses>.

UNPUBLISHED DOCUMENT

Note: The following capstone project is available through Universidad San Francisco de Quito USFQ institutional repository. Nonetheless, this project – in whole or in part – should not be considered a publication. This statement follows the recommendations presented by the Committee on Publication Ethics COPE described by Barbour et al. (2017) Discussion document on best practice for issues around theses publishing available on <http://bit.ly/COPETHeses>.

RESUMEN

En las últimas décadas la rápida expansión y el crecimiento poblacional han causado la deforestación de los bosques y montañas aledañas a la ciudad de Quito, lo que ha causado un incremento de los incendios forestales en estas zonas. El impacto más notorio es en el volcán Ilaló en el valle de Tumbaco. El propósito de este trabajo es desarrollar un vehículo aéreo que sea capaz de distribuir semillas de plantas con alto contenido de humedad por rutas predefinidas, las cuales van a ayudar a detener o ralentizar la expansión del fuego en la zona del Ilaló. El vehículo diseñado es un dron que es capaz de hacer rutas de 15 minutos con una carga paga máxima de 6 kilogramos. El sistema diseñado es completamente modular, por lo que se adapta a las necesidades de cada misión y existe la opción de reemplazar piezas que se puedan dañar fácilmente. La estructura está diseñada para poder soportar la carga máxima de despegue de 22 kg y para resistir posibles accidentes que se pueda ocasionar durante la misión. Del mismo modo, la aeronave está diseñada para ser controlada por un piloto en tierra o por un piloto automático controlado por telemetría. En trabajos futuros se propone realizar un enjambre de este tipo de naves que sea capaz de cubrir más terreno en el mismo tiempo de vuelo.

Palabras clave: Dron, UAV, Distribuidor de semillas, piloto automático, control de vuelo, cortafuegos, reforestación, misión.

ABSTRACT

On the last decades, the population growth has increased the deforestation of forest and mountains near the city of Quito. This phenomenon has increased the wildfires in these zones. The most critical location is the Ilaló volcano in Tumbaco. The scope of this document is to design and develop an aerial vehicle capable of distribution seed pods of vegetation with high humidity around predefined routes, to stop or slow down the wildfire spread rate, giving firemen more time to control the emergency. The designed vehicle is a UAV capable of completing 15 minutes missions with a maximum payload of 6 kg. The system design is modular, meaning it can adapt to any mission requirements and there is the option to change damaged parts due to possible accidents. The structure is designed to endure the maximum take off weight of 22 kg and possible accidents that can occur during a mission. The UAV is designed to be controlled by an operator on land or by an autopilot module controlled by telemetry. For future work it is recommended to develop a UAV swarm to cover a larger surface area on the same flight time

Keywords: Drone, UAV, Seed Pod Distribution, Automatic Pilot, Flight controller, Firebreaks, Deforestation.

GENERAL INDEX

INTRODUCTION	18
Problem Statement and Project Specification	18
Client requirements	20
Design alternatives	20
UAV Size.....	21
General design	23
Frame Materials.....	25
Seed distribution system.....	27
Project management	29
Engineering Standards.....	30
ASTM D638-14.....	30
1939.1 Standard for Framework for Structuring Low Altitude Airspace for Unmanned Aerial Vehicle Operation	32
Standard Specification for Design and Construction of a Small Unmanned Aircraft System.....	32
Resolution DGAC-DGAC-2020-0110-R	32
ASTM D7127-13.....	33
ASTM A1087-16.....	33
Tolerance ISO system.....	33

	11
Material Selection and Design.....	34
Methods	34
Material and component selection.....	35
Motors, propellers, and ESC.....	35
Flight controller and telemetry	37
Batteries	38
Frame Materials	39
Seed distribution container	41
Design for Manufacturing	41
Engineering experiment.....	42
PETG stress strain tests	42
Thrust calculation through motor rotational velocity	45
Results and discussion	47
Engineering analysis.....	47
Propeller lift calculation	47
Seed distribution system calculations.....	51
Bolts joining seed tank with UAV frame	51
Fastener Stiffness.....	51
Member stiffness	53
Tension joints	55

	12
Maximum allowable forces	56
Seed Pod Container Size	57
Seed Distribution Carrousel Speed.....	58
Container axial loading.....	59
Container bottom force analysis	61
Stepper motor torque	64
Dynamic analysis of the seed pod	66
UAV frame calculations	68
Drone arm analysis	68
Data and calculations.....	69
Location of the C profile Centroid	70
Second moment of inertia.....	70
$F_y = 0$ $R_y - W \cdot l + L - WM = 0$ Analysis at the maximum force ..	71
Shear force and bending moment diagram.....	72
Analysis at the minimum force.....	73
Shear force and bending moment diagram when minimum force is applied	74
Fatigue stress analysis at the arm of the UAV	75
Stress Concentration.....	76
Average stress and Amplitude Stress	77

$\sigma_m = \sigma_{max} + \sigma_{min}$ $\sigma_a = \sigma_{max} - \sigma_{min}$ Gerber Failure Criteria ..	77
First cycle failure safety factor	77
Bolts joining the drone arms with the brushless motor	78
Stress analysis on the upper plate	80
Analysis with maximum propeller thrust	81
Shear and Moment diagram.....	82
Landed analysis	84
Fatigue stress analysis	86
Results and discussion	89
Safety Through Design.....	92
Maintenance and Operating Manual	92
References	93
APendixes.....	96
Manufacture flow diagram	96
Risk Analysis.....	97

Table List

Table 1: UAV size selection table	22
Table 2: General design selection table	25
Table 3: Score table for material selection.	26
Table 4: Score for the seed distribution system.....	29
Table 5: Summarized Gantt diagram.....	30
Table 6: Summarized project budget.....	30
Table 7: Summary of flight system components	39
Table 8: List of Parts and Manufacturing Technologies.	41
Table 9: Results of the mechanical properties of 3D printed pieces	44
Table 10: Experimental thrust calculation.....	45
Table 11: Risk Assessment.....	97

Figure List

Figure 1: Hexacopter model.	21
Figure 2: Quadcopter model.	22
Figure 3: First design option.....	23
Figure 4: Second design option	23
Figure 5: Third option design.....	24
Figure 6: Fourth option design	24
Figure 7: Rotatory cylinder	27
Figure 8: Rotatory vertical plate.....	28
Figure 9: Piston-funnel	28
Figure 10: Dimension for tensile strength tests specimens.	31
Figure 11: Selected motor for the UAV	35
Figure 12: Selected propellers.	36
Figure 13: Selected ESC.....	37
Figure 14: Pixhawk 5x.....	38
Figure 15: Telemetry radios	38
Figure 16: Selected battery.	39
Figure 17: Aluminum profile for the UAV arms (Cedal, s.f.).....	40
Figure 18: Stress strain graph for the first test specimen.	43
Figure 19: Stress strain graph for the second test specimen.	43
Figure 20: Stress strain graph for the fourth test specimen.	44
Figure 21: Thrust in function of throttle graph.....	46
Figure 22: Tank bolted joint schematic.	51

Figure 23: important dimensional parameters for bolts.....	52
Figure 24: Frustum division of the material layers.	54
Figure 25: Design of the carrousel rotor.....	58
Figure 26: Container axial loading.	60
Figure 27: Distributed load on the bottom of the tank.	61
Figure 28: Clamped circular plate representation.....	62
Figure 29: Infinitesimal Element 3D.....	63
Figure 30: Infinitesimal Element 2D.....	64
Figure 31: Carrousel diagram.....	65
Figure 32: Seed pod motion diagram.	67
Figure 33: Beam Free body diagram (Maximum force).....	69
Figure 34: C profile dimensions.	70
Figure 35: Shear forces and Moment diagram (Maximum Force).....	72
Figure 36: Maximum Shear Force Diagram.....	72
Figure 37: Maximum Moment Diagram	73
Figure 38: Beam Free body diagram (Minimum force)	73
Figure 39: Shear forces and Moment diagram (Minimum Force).....	74
Figure 40: Minimum Shear Force Diagram	74
Figure 41: Minimum Moment Diagram	75
Figure 42: indeterminate joint ((Budynas & Nisbett, 2014).....	78
Figure 43: Plate model.....	80
Figure 44: One-dimensional beam model.	81
Figure 45: AB beam section.	82
Figure 46: Beam section BC.....	83

Figure 47: Shear force diagram for maximum thrust.	83
Figure 48: Moment diagram for maximum thrust.	84
Figure : Landed analysis model.	84
Figure 50: Shear force diagram with landed UAV.	85
Figure 51: Moment diagram with landed UAV.	85
Figure 52: Safety factors for a plywood plate.	88
Figure 53: Safety factors for an aluminum plate.	88
Figure 54: complete set of designed pieces of the seed distribution system.	90
Figure 55: designed control circuit of the seed distribution system.	90
Figure 56: final design of the UAV.	91

INTRODUCTION

Problem Statement and Project Specification

For the last decade the rapid and uncontrolled expansion of Quito has accelerated the deforestation process of the surrounding mountains. One of the most severe examples is the Ilaló volcano located near the valley of Cumbayá. Here people enjoy recreational activities, grow crops, and is the habitat of multiple species of plants and animals (Alarcón, 2019). Additionally, wildfires have devastated the region, contributing to the destruction of the primary forest. This environment is of great importance to the city, given that it purifies and cools the air of Cumbayá, Tumbaco, Los Chillos and Alangasí. In addition, the native species of the region depend on the conservation of it to survive and regulate their population (Curipoma, 2015).

Due to human intervention, the mountain has been infested by introduced species that increase the wildfire spread rate, aggravating the subsequent erosion process like eucalyptus (Alarcón, 2019). This increase in wildfires consequently weakens the ecosystem forcing it to lose its ability to host local fauna and capture the carbon emissions produced by the nearby communities. One of the solutions is the implementation of firebreaks: barriers that block the fire spread, giving more time for local authorities to control the emergency. They can be constructed in two main ways: a physical one like a highway or special plants that act like a natural barrier (Weir et al., n.d.). An advantage of the second type of firebreak is countering the erosion problems. Manually implementing natural firebreaks is not efficient, as it represents high expenses, risk of injuries, and limited working hours. To increase the sowing efficiency, this project proposes the use of an Unmanned Aerial Vehicle (UAV) to distribute seed pods throughout Ilaló to create firebreaks.

Nowadays there are many advances used in the development of UAV technology intended for agricultural purposes such as land inspection and distributing seeds. For example, drones have been used to reforest mangroves in Myanmar and the United Arab Emirates with the objective to foster marine life as well as to slow down the costal erosion. UAV's have also been used with reforestation purposes in locations difficult to access or dangerous in many countries, such as the United States, Canada, Australia, or New Zealand (Mohan et al., 2021). Likewise, technology developments have allowed for design distribution systems of UAV's to disperse seeds along a programmed path and use multiple drones as a swarm to cover more ground (Burema et al., 2016).

The main objective of this project is to develop a semi-automatic seed deposit system connected to a multi-rotor UAV. The specific objectives are to select the necessary components to meet the technical requirements of the project; to perform calculations of power, mechanical strains, and aerodynamics necessary to obtain dimensions and preliminary designs of the aircraft and the seed dispenser; to design the components in a CAD software, in order to perform a CFD and stress simulations; to build a prototype with the decided components.

The following methodologies will be applied, which include, but are not limited to, literature analysis and theoretical calculations, and planning and constructing a functional prototype. The expected results are to ensure that the prototype works correctly, fulfilling technical requirements and the specifications requested by the client.

Client requirements

For the entire duration of the project there were meetings with the client. He is the one who requests the construction of the prototype, gives the initial guidelines of what the project should focus on, and what are the minimum specs that the prototype should.

In the case of this project the major specifications was the payload, flight time, and the design of the seed distribution system. The main goal of the UAV is that it has the capability to distribute the seed pods across hard to access terrain, so the aircraft has to have the ability to fly and return without having power supply problems. Also, the drone has to carry enough seed pods, so it becomes a viable option. Likewise, the seed distribution system has to deliver the pods in accordance with the speed of the drone so there is one seed on the ground every two meters. To accomplish this the system has to be designed so the seeds will not collide or jam the system.

The main requirements given by the client are the following:

- Ideal flight time: 20 min
- Autonomous seed distribution system
- Approximate weight of the seed pods is 15 g
- Modular design
- Altitude from free surface is 6 m

Design alternatives

Different design proposals will be analyzed based on relevant engineering criteria, to find the most suitable option for the design of the UAV with the Seed Distribution System. The methodology used to determine the best proposal is by applying a weighted selection

matrix, where different weights are assigned to each engineering criteria and every option is evaluated in a scale from 0 to 10. Finally, the option with the highest score will be the most suitable solution. First, the size of the UAV will be determined, then the general design of the machine, followed by a material analysis for the UAV frame and, lastly, different design options for the distribution system will be proposed.

UAV Size

To decide the UAV size, two options will be taken into consideration. The first one consists of a UAV with six rotors and 30 in propellers. The distance between opposite rotors is at least 2 m. This model can carry approximately 13 kilograms of payload, which represents 1300 seed pods, for 15 minutes using a 44 V battery with 16000 mAh.

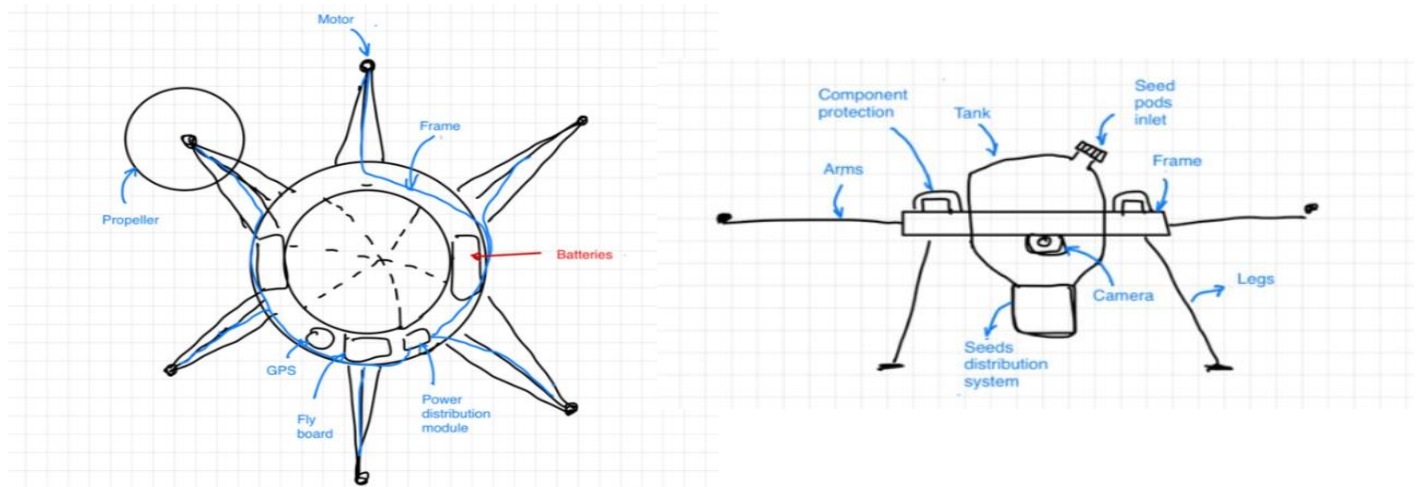


Figure 1: Hexacopter model.

The second option is a quadcopter with 22 in propellers. The distance between opposite propellers is 1.8 meters and can carry approximately 6 kg of payload, planting 300 seed pods per flight. It uses a 44 V battery with 16000 mAh, that allows it to fly for 15 minutes with a maximum payload.

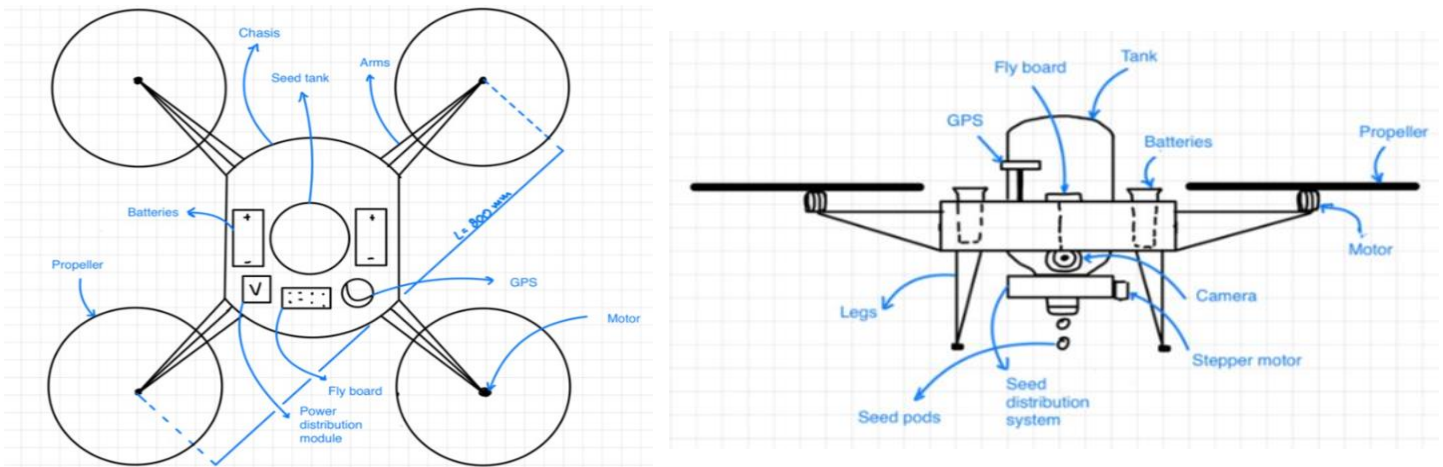


Figure 2: Quadcopter model.

The first criterion evaluated is the availability of the drone parts, as they need to be imported, this includes shipping time. Likewise, the price of each component needs to be considered, because of the limited budget available. On the other hand, there are cheaper suppliers, but their reliability is questionable, and the purchase risk is too high for the amount required. Finally, for the UAV to work properly, the existing parts need to be compatible with each other, so the assembly will not have any problems.

Table 1: UAV size selection table

Factor	Weight	Hexacopter		Quadcopter	
		Score	Weighted	Score	Weighted
Parts Availability	0.2	8	1.6	8	1.6
Delivery time	0.2	1	0.2	7	1.4
Price	0.15	9	1.35	5	0.75
Supplier Reliability	0.3	0	0	9	2.7
Assembly	0.15	8	1.2	8	1.2
Total	1	26	4.35	37	7.65

The most important criterion is the supplier reliability, as the amount intended to spend is high, so the less risk taken the better. Also, the availability of parts and the delivery time are important aspects to consider. The price and assembly criteria are not as constraining as the previous ones.

The highest score is for the quadcopter, as the parts found can keep up with the budget limitation and the supplier reliability is high enough to minimize the purchase risks. Also, the parts are available and can be delivered on time.

General design

For the general design of the UAV, four options are considered. Option 1 refers to the drone with the seed container in the middle of the drone.

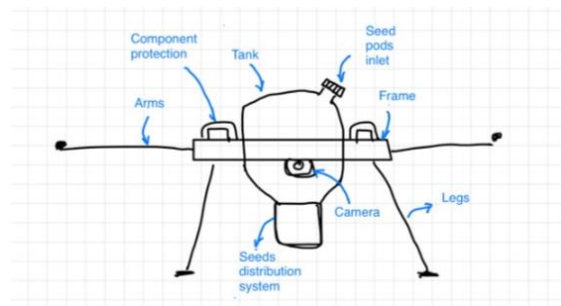


Figure 3: First design option

In the case of option 2, the seed container is located at the bottom of the UAV.

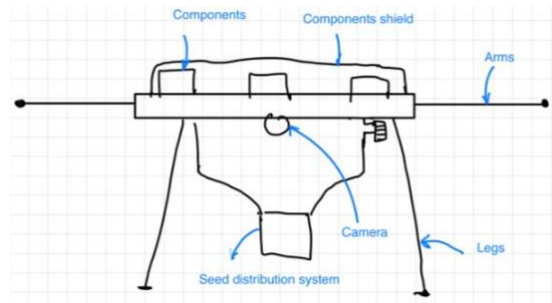


Figure 4: Second design option

For the option 3, the seed container is going to be at the top of the drone, and it is going to be connected to the seed distribution system by a pipe.

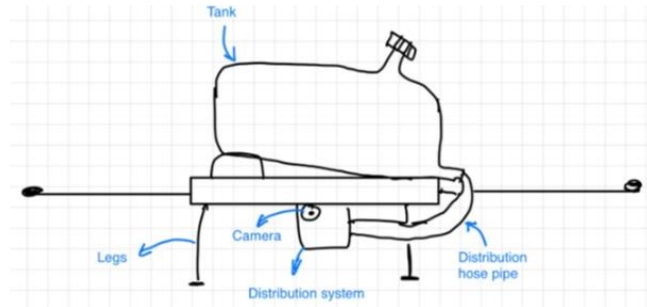


Figure 5: Third option design

Finally, in option 4 the container is also located at the top of the drone but is directly connected with the distribution system.

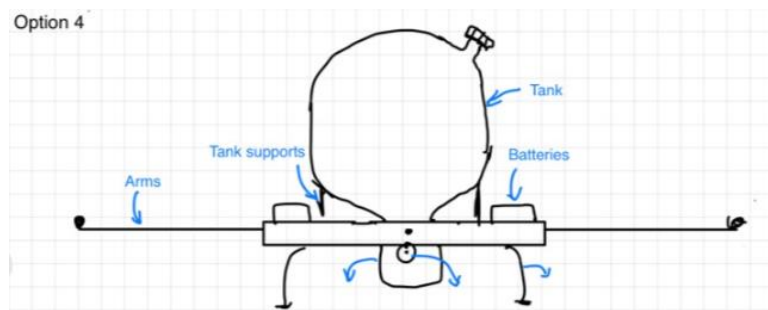


Figure 6: Fourth option design

To decide which general design is the best one, six criteria are being considered. The first one is the weight distribution; the best option is that the center of mass of the drone is as close to the center of the UAV as possible. Second is the ease of transportation, referring to how easy is to move the aircraft from one place to another, having as the main transportation method the bed of a pickup truck. Third is the container accessibility, where it is evaluated how hard it is to access to the main seed-container for doing tasks, like refilling the seeds, or cleaning it. Fourth is the frame weight, as it is needed to be as light as possible. Fifth the esthetics. Finally, is the distribution system method, which considers how difficult is to switch or modify the system in case that is needed.

Table 2: General design selection table

Criteria	Weight	Option 1		Option 2		Option 3		Option 4	
		Score	Weighted	Score	Weighted	Score	Weighted	Score	Weighted
Weight Distribution	0.3	10	3	8	2.4	3	0.9	4	1.2
Easy Transportation	0.2	7	1.4	5	1	7	1.4	7	1.4
Container Accessibility	0.15	9	1.35	5	0.75	9	1.35	10	1.5
Frame Weight	0.15	5	0.75	6	0.9	8	1.2	7	1.05
Esthetics	0.05	8	0.4	7	0.35	2	0.1	7	0.35
Distribution System	0.15	5	0.75	8	1.2	5	0.75	9	1.35
Total	1	44	7.65	39	6.6	34	5.7	44	6.85

In this case, the most important criteria is the weight distribution. The most ideal case is that the center of mass is in line with the propellers, so all the motors and other components can distribute the work equally. The esthetics are the less important parameter, because this vehicle will be used for heavy duty.

The highest weighted score was obtained by the first option, as it had the best weight distribution, and container accessibility.

Frame Materials

The frame material is one of the most critical components of the drone design. It must carry the weight of every system, be sturdy enough to not bend and affect the motors and be light so its weight will not suppose a problem. For these reasons the frame material is extremely important since its properties will determine many important parameters. Also, the drone frame is a relatively complex geometry, so it is important that the material is locally available and that it could be easily reshaped. Furthermore, price is an important constrain to consider since the budget of the project is limited.

The most common materials of drones are glass fiber, carbon fiber, aluminum alloy, PVC, covered balsa wood, and plywood. These are the materials that are considered and analyzed for the project. The score table is shown below:

Table 3: Score table for material selection.

Factor	Weight	Glass Fiber		Carbon Fiber		Aluminum Alloy		PVC		Covered Balsa Wood		Plywood	
		Score	Weighted	Score	Weighted	Score	Weighted	Score	Weighted	Score	Weighted	Score	Weighted
Weight	0.4	8	3.2	9	3.6	8	3.2	9	3.6	8	3.2	8	3.2
Ease of manufacture	0.1	7	0.7	5	0.5	8	0.8	6	0.6	2	0.2	9	0.9
Price	0.2	2	0.4	1	0.2	5	1	9	1.8	4	0.8	9	1.8
Mechanical Properties	0.3	9	2.7	10	3	5	1	2	0.6	7	2.1	3	0.9
Total	1	26	7	25	7.3	26	6	26	6.6	21	6.3	29	6.8

The four main criteria for the selection of the material are: weight, ease of manufacture, price, and mechanical properties. The criteria of ease of manufacture covers the ability of the material to be shaped into complex geometries, and how easy it is to be obtained locally. The weight criteria are an estimate based on the preliminary dimensions and the average density of each option. The price is scored using catalogs that may not have updated prices, or the selected supplier, so it is an estimate as well. The mechanical properties are also taken from papers and catalogs, but for the actual construction of the frame a stress strain analysis should be performed using the actual material the frame would be constructed in to obtain the real properties of the calculations.

After weighing every option using the criteria, plywood resulted as the ideal material for the construction of the frame. Its properties allow it to be light weight yet sturdy enough and it has a competitive price in the market. For the final construction the places where most stress is concentrated will be reinforced with thin aluminum plates to ensure resistance against crashed and avoid bending problems when the motors are in operation.

Seed distribution system

The seed distribution system is an entirely independent system apart from the UAV. It has its own battery, remote control, and calibration. The goal with this system is that it releases one seed every two meters, this condition must be related to the velocity of the drone. As the other systems, the weight is a significant criterion to consider. Also, the size must be in relation with the size of the drone. The price of the components is an important parameter as well. The design of the seed pods shape and size has not been definitively established, so the seed distribution system must be adaptable to changes. Furthermore, the system must be resistant to a certain degree to shocks or vibrations, so the durability of it is something important to consider.

The first design system is a rotary cylinder. In this system a cylinder has four divisions, in each one a single seed is deposited. The height of the cylinder is the same as the diameter of the seed pods, so only one can be in a section at the same time. There is a plate below the cylinder there is a hole so the seeds can come out. When the system starts rotating the seed is deployed and another one takes its place. The rotation is continuous and synchronized so the seeds are released periodically with the correct spacing.

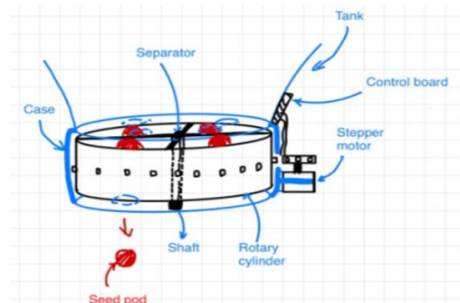


Figure 7: Rotatory cylinder

Another option is to implement a rotatory vertical plate with an open perimeter. The seed pods would enter from the container through an opening on the top of the device, the pods are located in the rotatory plate, and a stepper motor makes the plate rotate in a constant period in dependence of the seed drop rate. On the bottom of the device, there is an opening where the seed pod can exit the device and drop to the desired location.

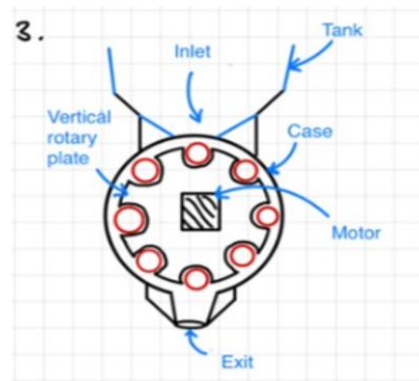


Figure 8: Rotatory vertical plate

The last scored system is a combination of a piston and the container in shape of a funnel. When a seed reaches the end of the funnel a piston pushes it laterally to the exterior. The piston is synchronized with the velocity of the drone, so the seed are released with the right spacing.

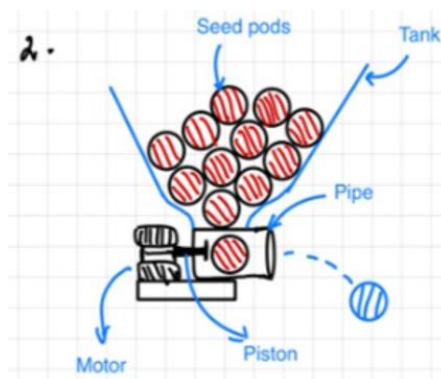


Figure 9: Piston-funnel

The score table for the three options is shown below:

Table 4: Score for the seed distribution system.

Factor	Weight	Rotary Cylinder		Carousel		Piston - Funnel	
		Score	Weighted	Score	Weighted	Score	Weighted
Weight	0.2	8	1.6	6	1.2	8	1.6
Size	0.1	8	0.8	7	0.7	8	0.8
Price	0.2	9	1.8	9	1.8	7	1.4
Adaptability	0.3	4	1.2	3	0.9	6	1.8
Durability	0.2	6	1.2	7	1.4	6	1.2
Total	1	35	6.6	32	6	35	6.8

After scoring each system using the selected criteria, the system that better adapts to the client needs is the rotary cylinder system. This one is simple enough, so the components don't need much maintenance or are too complicated to obtain or modify. The electronics of this system will be fed from an independent smaller battery than the one used by the aircraft, so this system will not affect the battery life of the other components. Nevertheless, due to the required payload the weight of the seed tank will not be negligible in comparison with the rest of the UAV.

Project management

Proper organization is fundamental to the success of any project. To guarantee the fulfillment of the objectives a task schedule in the form a Gantt diagram. The schedule was thought to distribute the main tasks for the planification, construction, and testing of the UAV along the agreed period with the client. The summarized version of the Gantt diagram is presented below:

Table 5: Summarized Gantt diagram.

Task	Dates
Project definition	16/01 - 23/01
Analysis of the feasibility of the project	24/01 - 30/01
Start of the design	31/01 - 13/02
Design	14/02 - 20/02
Main Calculations	21/02 - 20/03
Construction and Testing	21/03 - 30/04
Final Presentation	01/05 - 15/05

After establishing the schedule of activities, a budget was drafted to keep record of the expenses of each of the systems that make up the UAV. Below it shown a table summarizing those expenses, table XX located in annex XX presents the more detailed version of the budget.

Table 6: Summarized project budget.

System	Precio
Flight control	1800
Seed distribution system	100
Drone structure	200
Total	2100

Engineering Standards

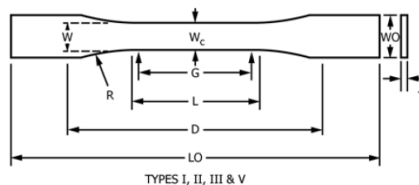
ASTM D638-14

This test method covers the determination of the tensile properties of unreinforced in the form of standard dumbbell shaped specimens. The test method is applicable for any thickness up to 14 [mm]. The test data by this method is useful in engineering design.

The testing procedure stated in this standard is important to obtain the mechanical properties of the 3D printed parts of the drone. The final properties of parts made by additive manufacturing are dependent of the calibration of the 3D printer and quality of the materials used. Therefore, it is necessary to perform tensile strength tests using the machine and raw material to have the real properties.

To perform this experiment, it is necessary to have a testing machine of the constant rate of crosshead movement type having a load indicator, crosshead extension indicator, modulus of elasticity measurements and low extension indicator. Because of the way the tests specimens are fabricated the modulus of elasticity and ultimate tensile strength are of the layers of the object.

The following figure presents the dimension of the test specimens. The type I is selected because it is assumed that the final 3D printed part is comparable to a rigid or semirigid polymer.



Dimensions (see drawings)	Specimen Dimensions for Thickness, T , mm (in.) ^A					Tolerances
	7 (0.28) or under		Over 7 to 14 (0.28 to 0.55), incl	4 (0.16) or under		
	Type I	Type II	Type III	Type IV ^B	Type V ^{C,D}	
W —Width of narrow section ^{E,F}	13 (0.50)	6 (0.25)	19 (0.75)	6 (0.25)	3.18 (0.125)	± 0.5 (± 0.02) ^{B,C}
L —Length of narrow section	57 (2.25)	57 (2.25)	57 (2.25)	33 (1.30)	9.53 (0.375)	± 0.5 (± 0.02) ^C
W_C —Width overall, min ^G	19 (0.75)	19 (0.75)	29 (1.13)	19 (0.75)	...	+ 6.4 (+ 0.25)
W_O —Width overall, min ^G	9.53 (0.375)	+ 3.18 (+ 0.125)
L_O —Length overall, min ^H	165 (6.5)	183 (7.2)	246 (9.7)	115 (4.5)	63.5 (2.5)	no max (no max)
G —Gage length ^I	50 (2.00)	50 (2.00)	50 (2.00)	...	7.62 (0.300)	± 0.25 (± 0.010) ^C
G —Gage length ^I	25 (1.00)	...	± 0.13 (± 0.005)
D —Distance between grips	115 (4.5)	135 (5.3)	115 (4.5)	65 (2.5) ^J	25.4 (1.0)	± 5 (± 0.2)
R —Radius of fillet	76 (3.00)	76 (3.00)	76 (3.00)	14 (0.56)	12.7 (0.5)	± 1 (± 0.04) ^C
R_O —Outer radius (Type IV)	25 (1.00)	...	± 1 (± 0.04)

Figure 10: Dimension for tensile strength tests specimens.

1939.1 Standard for Framework for Structuring Low Altitude Airspace for Unmanned Aerial Vehicle Operation

This standard defines the capabilities and infrastructure UAVs must comply with, to remain inside the international altitude air space regulations (IEE Standards Association).

Standard Specification for Design and Construction of a Small Unmanned Aircraft System.

This standard specifies the design, construction, and test requirements for small UAVs. It is intended for vehicles with a maximum takeoff weight of 25 kg or less (ASTM F38 Unmanned Aircraft Systems).

Resolution DGAC-DGAC-2020-0110-R

This resolution states the regulations applicable for the operation of remote-controlled aircrafts. It is applicable for UAVs between 0.25 and 150 kg. It is obligatory to register the aircraft to the proper authorities and purchase an insurance policy that can be between 3000 and 12000 US dollars depending on the maximum takeoff weight. The UAVs cannot be operated near aerodromes, State safety zones, heliports, airports among others. The minimum distance to operate from these zones is 9 kilometers. The maximum flight altitude is 122 meters above ground level between sunrise and sundown while there is proper weather conditions and a visual contact with the aircraft is guaranteed (DIRECCIÓN GENERAL DE AVIACIÓN CIVIL, 2020).

ASTM D7127-13

Standard Test Method for Measurement of Surface Roughness: the roughness measurement is necessary for the 3D printed pieces where the surface quality depends on an many factors, such as 3D printer calibrations, material, piece geometry, among others.

ASTM A1087-16

Standard Practice for Using Hand Calipers: the use of calipers is important to verify the size and distance of holes at the drone structure and arms. Also, the width of the components and shafts diameters.

Tolerance ISO system

Seeds distribution system shaft tolerance for fixed adjustment setting:
 $15h_{11}-15H_{11}$ $15h_{11}-15H_{11}$

MATERIAL SELECTION AND DESIGN

Methods

The design of the UAV and its sub systems was an iterative process. Many tests of the prototypes were performed to determine their validity and performance. The system that was most tested was the seed distribution system.

The final design of the tank is somewhat different from the initial concept shown in figure 7. The central seed container is taller than the one initially expected. Furthermore, the number of divisions is increased from 4 to 10. Also, the power transmission was moved from the side of the cylinder to the center of it. Through testing it was found to be easier and need less pieces than the initial concept.

To test this system some muck ups were created to make sure that the system will work properly before manufacturing the actual tank. By using this method, the final design of the seed distribution system should work properly. Another part that was mucked up were the seed pods. The actual capsules were not available at the time of the design of the seed distribution system, so a recreation of what the capsules was necessary to tests the system. Initially mud balls covered in plastic film was used. Nevertheless, the consistency of the balls wasn't enough to withstand the rotation of the cylinder, as a result the balls were crushed, and the system was jammed. With these tests it was concluded that the seed pods should be as spherical and smooth as possible. As a solution, the mud balls were covered in wax. With this the balls gained consistency and became smooth and round.

Material and component selection

Motors, propellers, and ESC

Because of the client requirements the most important components are the motors. They must have enough thrust to lift the entire UAV and the payload. Also, for maneuverability reasons the motors should be able to lift double the actual weight of the aircraft (González, 2021). It is expected that the weight of the UAV including all the systems and components is 12 kg and 6 kg of payload. This means that the minimum combined thrust of the quadcopter motors should be 36 kg.

Furthermore, because of the application that the aircraft will have not all commercially available motors are appropriate. This UAV is likely to get dirty, wet, or in general it will be exposed to many environmental factors that normal drone motors are not suitable for. Because of this, agricultural grade motors will be selected for this application. Normally these motors are used for fumigation or package delivery.

The selected motor is: SunnySky X6215S 170KV. This was selected because at 44.4 V it can lift 12 kg per motor without the risk of overheating. The combined thrust is 48 kg, which is more than enough to lift the aircraft and the payload combined.



Figure 11: Selected motor for the UAV

To achieve the maximum thrust it's necessary the appropriate propellers. The selected ones are Tarot T Series 2255 High Efficiency Carbon Fiber Propeller CW/CCW TL2846. The motor manufacturer recommends propellers size 22x6.6 in. Nevertheless, due to supplier problems and budget constrains the selected propellers are slightly smaller, they are 22x5.5 in in size. Also, the propellers must be bought with the wingspan in clockwise and counterclockwise directions. If only one type is assembled to the aircraft the UAV would spin instead of flying. The material of the propeller is also important. The drone could experience crashes, so the propellers need to be tough enough to resist the impact of a fall from the operation altitude. The selected propellers are made of carbon fiber, which gives security that they will resist an impact.



Figure 12: Selected propellers.

The Electronic Speed Controllers (ESC) are fundamental for the functioning of the UAV. They are responsible for translating the commands from the flight controller to the motors. Due to the size, voltage, and current draw of the motors a high voltage ESC is necessary. In addition, this component also must be shockproof, corrosion resistant, and with low heat generation. The selected ones are: Flycolor FlyDragon V4 80A 5-12S 32bit HV ESC for Agricultural Drones. This manufacturer gathers all the desired characteristics of the controller and are compatible with the rest of the components.



Figure 13: Selected ESC

Flight controller and telemetry

The flight controller is the brain and heart of the drone. Inside this component there are all the necessary sensors for a swift flight, such as: accelerometer, compass, magnetometer, gyroscope, among others. Also, this is where the remote-control antenna, GPS and telemetry will be connected. The selected flight controller is the: Pixhawk 5x Standard Set + M8N GPS (SKU20117). This brand is selected because of its widespread use in the industry and available information about it. Furthermore, it is compatible with Ardupilot, an open-source mission planner platform that allows to control, calibrate, and plan autopilot routes. In addition, it includes the GPS module for the autonomous flight option.

Another advantage that the Pixhawk 5x offers is the redundancy of its sensors. This means that it has many sensors of the same type. The benefit of this is that if one of those sensors were to fail, others would take its place and the aircraft would still be able to function properly.



Figure 14: Pixhawk 5x

Another important component for the proper use of the UAV is the telemetry. Because the Pixhawk 5x was selected as the flight controller, the telemetry radio of the same brand was selected: Sik Telemetry Radio V3-100mW 915MHz. The telemetry radio is used to monitor and change parameters remotely, even when the UAV is in operation. With this and the Ardupilot program it's possible to know the state of discharge of the batteries, location, altitude, inclination, warnings, and other important information.



Figure 15: Telemetry radios

Batteries

The batteries should have enough voltage and current to feed the flight controller, ESC, and motors. Also, the typical type of batteries used in drones are Lithium Polymer

(LiPo). This type of battery offers stable voltage supply, quick charge, and are relatively lightweight for their current grading.

For this application two 6S batteries of 16000 mAh connected in series are necessary. The connection will allow them to supply the 44.4 V that the drone needs, and they will discharge equally when the drone is turned on.



Figure 16: Selected battery.

Table 7: Summary of flight system components

Name	Link
SunnySky X6215S 170KV	https://www.rc-wing.com/sunnysky-x6215s-170kv-210kv-350kv-high-power-brushless-motor-for-drones.html
Flycolor FlyDragon V4 80A 5-12S 32bit HV ESC for Agricultural Drones	https://www.rc-wing.com/flycolor-flydragon-v4-80a-5-12s-32bit-hv-esc-for-agricultural-drones.html
Tarot T Series 2255 High Efficiency Carbon Fiber Propeller CW/CCW TL2846 (2pcs)	https://www.rc-wing.com/tarot-tl2846-2255-cf-propeller.html
Pixhawk 5x Standard Set + M8N GPS (SKU20117)	https://shop.holybro.com/pixhawk-5x_p1279.html
Sik Telemetry Radio V3-100mW 915MHz	https://shop.holybro.com/sik-telemetry-radio-v3_p1103.html
Battery 6s	https://rcbattery.com/liprior-16000mah-6s-12c-22-2v-lipo-battery-with-xt90-plug.html

Frame Materials

The frame material selection was based mainly on the availability of the materials in the local market and, most important, the weight they will add to the whole system. Likewise,

another important selection criterion was the cost of the materials. The UAV frame is composed of two plywood plates, aluminum arms and an aluminum landing station. This structure needs to be able to support the entire payload, the electronic components weight and the total thrust of the brushless motors.

The arm length is selected to be 45 cm, so the propellers have enough space to rotate without crossing over the frame plate. Likewise, the arm with needs to be able to hold the motor, with a diameter of 69 mm. Because of the market availability, the following aluminum profile is selected for the UAV arms.

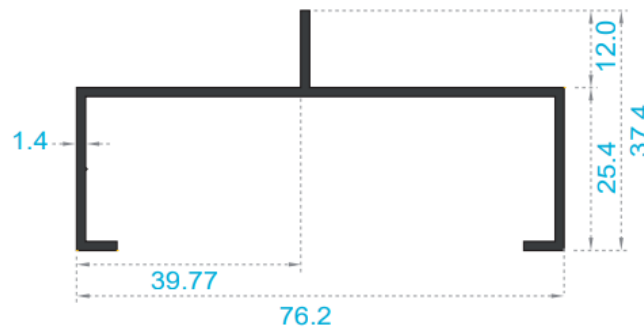


Figure 17: Aluminum profile for the UAV arms (Cedal, s.f.).

On an analog way the dimensions of the plate are determined in such a way that the electronic components and the sed container fit. Likewise, the plate needs to be able to endure the moment caused by the thrust of the motors. The minimum thickness of the plywood plate that has a factor of safety of 1.2 is 10.79 mm. The plate used for the frame has a 12 mm thickness, as it is the nearest thickness available above 10.79 mm (Pelíkan, s.f.).

The aluminum profile selected for the landing station is a square profile of 2.5 mm thickness. For a theoretical take off weight of 22 kg, the factor of safety for the UAV legs is 174.8.

Seed distribution container

The material selected for the seed distribution system is PETG. The selection criteria are based in the availability of the material and the flexibility of manufacture. The manufacture method is by 3D printing, which provides the option of swiftly iterating the final design. Besides, additive manufacturing gives the opportunity of producing more complex geometries that can better suit the system requirements.

Design for Manufacturing

The following table describes the parts we are going to manufacture throughout the construction of the UAV. Two main manufacturing technologies will be used. Numerical control, to perform drilling and milling operations; and additive manufacturing, to produce the seed distribution system parts with 3D printing.

Table 8: List of Parts and Manufacturing Technologies.

List of Parts					
Assembly	Part	Quantity	Description	Manufacturing technology	Manufacturing Process
Structure	Arms	4	UAV arms made of aluminum C profiles.	Numerical Control	Drilling
	Base plate	1	Plywood plate where the electronic components will be attached.	Numerical Control	Milling and drilling
	Cover plate	1	Plywood plate to cover the electronic components and assemble the arms.	Numerical Control	Milling and drilling

	Landing station	1	Aluminum landing structure.	Numerical Control	Drilling, welding
Distribution System	Container Body	1	The middle part of the seed carrier.	Additive Manufacturing	3D Printing
	Carrousel	1	Device to control the delivery rate of the seed pods.	Additive Manufacturing	3D Printing
	Motor holder	1	Holder for the stepper motor that moves the carrousel.	Additive Manufacturing	3D Printing
	Container top lid	1	Top lid of the seed container.	Additive Manufacturing	3D Printing
	Container bottom lid	1	Bottom lid of the seed container.	Additive Manufacturing	3D Printing

The manufacturing flow charts for every piece is detailed in the annexes section at the end of the document.

Engineering experiment

PETG stress strain tests

To obtain the mechanical properties of the 3D printed pieces it is used the ASTM D638-14 explained in the engineering standards section. Three test specimens were subjected to the test to obtain an average value for the mechanical properties.

The stress strain graphics for the tests specimens are shown below:

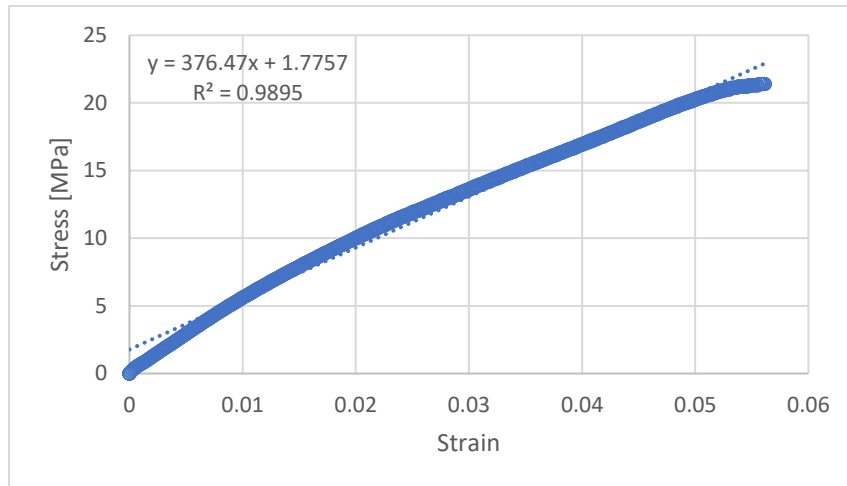


Figure 18: Stress strain graph for the first test specimen.

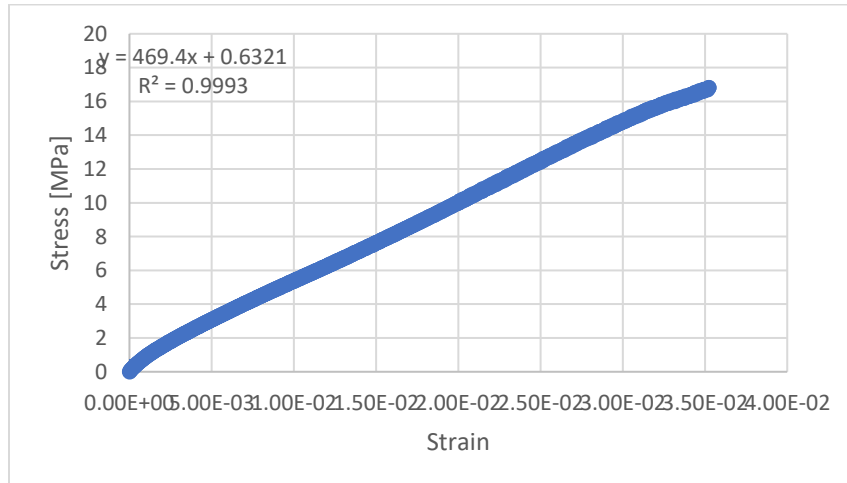


Figure 19: Stress strain graph for the second test specimen.

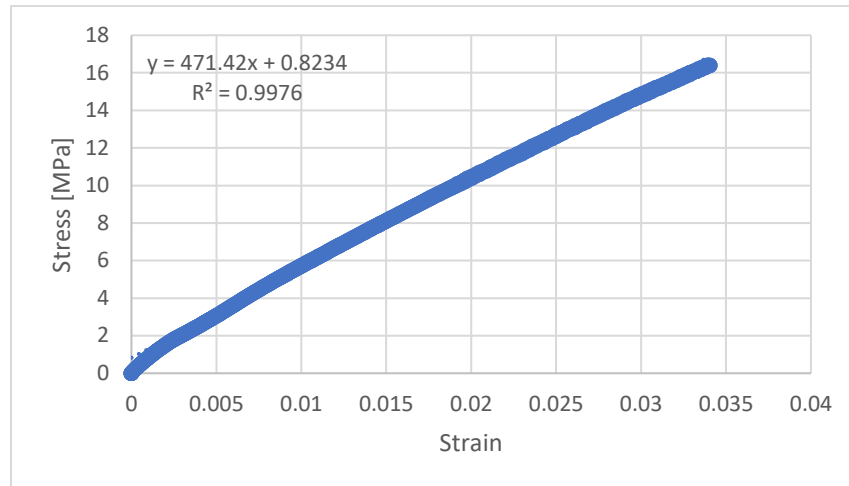


Figure 20: Stress strain graph for the fourth test specimen.

The three graphs provide important information to consider in the design of the pieces. The important information is summarized:

Table 9: Results of the mechanical properties of 3D printed pieces

Test Specimen	Maximun Force [N]	Maximun Stress [Mpa]	Modulus of Elasticity [MPa]
1	2060	21.4	376.47
2	1560	16.8	469.4
4	1570	16.4	471.42
Average	1730	18.2	439.10

The value of the maximum force and stress that the test specimens endured during the experiments are given by the program of the tensile strength testing machine. Meanwhile, the value of the modulus of elasticity is the slope of the linear function that describes the test for every specimen. The value used is the average of the results.

In addition, the three graphs shown before show that the PETG when 3D printed has brittle behavior. The graphs only show elastic region and not plastic one. With this we can

say that the 3D printing parts will not elongate, but simply break when the stress is greater than maximum allowable stress obtained experimentally.

These tests were important because the final properties of 3D printed parts are dependent on the 3D printer calibration and quality of the material. Because of this, the material properties must be obtained before performing any calculation. Also, the parts of the same system should be printed using the same printer, to ensure constant properties.

Thrust calculation through motor rotational velocity

A method used to calculate the thrust of the motors and propellers combined is to determine the rotational speed of the motor and use the following equation. (Staples, 2014)

$$F = 4.392399 \times 10^{-8} \cdot RPM_{prop} \frac{d^{3.5}}{\sqrt{pitch}} (4.23333 \times 10^{-4} \cdot RPM_{prop} \cdot pitch - V_0)$$

The values of RPM for the equation are obtained limiting the throttle of the motors in steps of 10%, starting from 10% throttle to 100% throttle. The measurement of the rotational velocity was made using a tachometer. The results of this experiment are shown below, including the calculation of the thrust:

Table 10: Experimental thrust calculation

THROTTLE [%]	RPM				F [N]
	1	2	3	AVG	
10	485.3	458.1	457.8	467.07	0.475119
20	1343.7	1355.5	1356.7	1351.97	3.980857
30	2238.3	2201.8	2201.2	2213.77	10.67354
40	3199.2	3199.5	3199.5	3199.40	22.29368
50	4016.1	4029.7	4019.4	4021.73	35.22664
60	4936.4	4958.5	4944.9	4946.60	53.29153
70	5841	5821.3	5818.5	5826.93	73.94771
80	6652.3	6665.4	6662.4	6660.03	96.60452
90	7358.1	7362.8	7363.6	7361.50	118.0259
100	7359.5	7362.2	7363.6	7361.77	118.0344

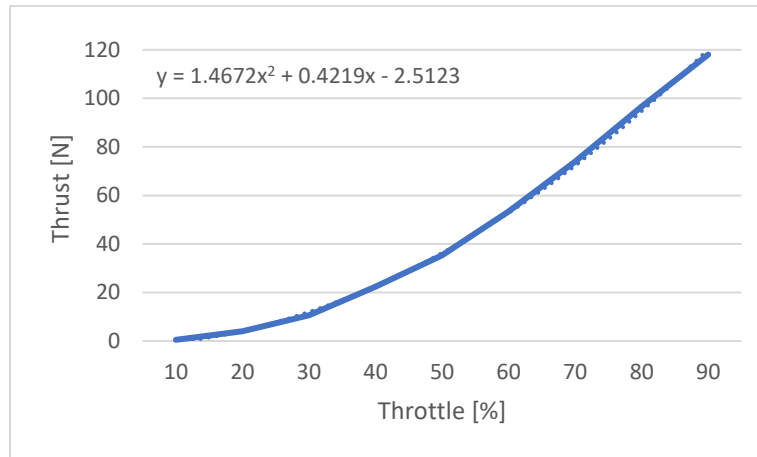


Figure 21: Thrust in function of throttle graph.

According to table 9 the maximum thrust of the motors using the selected propellers is 11.8 kg. This value is more enough to lift the UAV and payload combined. Figure 21 shows that the relationship between is nonlinear. The relationship between these two variables is more of an exponential or polynomial. When controlling the drone, the operator should be careful and pay attention of how much throttle is the remote-control supplying.

RESULTS AND DISCUSSION

Engineering analysis

Propeller lift calculation

For the analysis of the propeller thrust, Gabriel Staples empirical equation was used.

First, the nomenclature used to perform, these calculations are presented below:

F = thrust (N)

\dot{m} = mass flow rate (kg/s)

V_e = exit velocity of the airflow through the propeller (induced velocity, inflow velocity, or velocity induced by the propeller) (m/s)

V_{ac} = aircraft airspeed (m/s)

V_{pitch} = propeller pitch speed (m/s)

ρ = air density (kg/m³)

A = area through propeller, normal to airflow (area that the propeller sweeps) (m²)

P = pressure (Pa)

$$F = \frac{mdv}{dt} = ma$$

$$F = \frac{dm}{dt}v = \dot{m}v = \dot{m}V_e$$

In the case of a moving aircraft, the velocity of the air produce by the acceleration of the propeller is the most significant variable in the thrust generation. That is why the change in velocity is what matters.

$$F = \dot{m}\Delta V = \dot{m}(V_e - V_{ac})$$

The equation above is known as the theoretical dynamic thrust equation.

Since,

$$\dot{m} = \rho AV_e$$

Replacing the mass flow expression in the theoretical dynamic thrust equation the equation number 4 is obtained

$$F = \rho AV_e \Delta V = \rho AV_e^2 - \rho AV_e V_{ac}$$

$$A = \frac{\pi d^2}{4}$$

Know, replacing the equation number 5 in equation number 4

$$F = \rho \frac{\pi d^2}{4} V_e \Delta V = \rho \frac{\pi d^2}{4} V_e^2 - \rho \frac{\pi d^2}{4} V_e V_{ac}$$

$$F = \rho \frac{\pi d^2}{4} (V_e^2 - V_e V_{ac})$$

It is assumed that V_e is approximately equal to V_{pitch} . Since the pitch is known as the theoretical distance forward which a propeller moves. It can be expressed as following.

$$V_{pitch}(mph) = RPM_{prop} \cdot Pitch_{prop}(in) \cdot \frac{1ft}{12in} \cdot \frac{1mile}{5280ft} \cdot \frac{60min}{hr}$$

Replacing equation 7 in equation 6 and considering that the aircraft is not moving $V_{ac} = 0$ also it can be considered that the density of the air is $\rho = 1.2 \frac{kg}{m^3}$.

$$F = 1.2 \frac{\pi(0.0254 \cdot d^2)}{4} (RPM_{prop} \cdot Pitch \cdot 0.0254 \cdot \frac{1min}{60sec})^2 [N]$$

The factor 0.0254 is used to convert units into meters.

In order to make this equation applicable to real life some assumptions and empirical corrections must be applied.

Most of the thrust produce by the propeller occur in a distance between the 70% ~80% of the blade radius measure from the propeller hub ($0.7\sim 0.8 \cdot \text{Blade radius}$)

The number of propeller blades affect the way the air flows throughout. More blades mean mor air sustentation but also means more air blockage. That why this equation works better for a two bladed rotor.

The form of the blade is not considered to make calculations easier; the only important characteristics of the blade is its pitch and diameter.

Because of the inflow velocity is not constant across the rotor blades, it is necessary to include a correction factor that minimizes the error. It is important to notice that the bigger the radius of the propeller and the smaller the pitch, the thrust and efficiency of the propeller grow. To make this possible, a relation between radius and pitch must be find. Gabriel Staples empirically finds the following formula to correct the equation 8.

$$F = 1.2 \frac{\pi(0.0254 \cdot d^2)}{4} (RPM_{prop} \cdot Pitch \cdot 0.0254 \cdot \frac{1 \text{ min}}{60 \text{ sec}})^2 (k_1 \frac{d}{pitch})^{k_2} [N]$$

$$\text{Where } k_1 = \frac{1}{3.29546} \text{ and } k_2 = 1.5$$

Simplifying the equation 9 and including aircraft velocity.

$$F = 4.392399 \times 10^{-8} \cdot RPM_{prop} \frac{d^{3.5}}{\sqrt{pitch}} (4.23333 \times 10^{-4} \cdot RPM_{prop} \cdot pitch - V_0)$$

$$\text{Where } RPM_{prop} = \frac{rev}{min}; d = in; pitch = in; V_0 = \frac{m}{s}$$

Know replacing the variables in equation 10 with the data given in the datasheet from the motor and propellers.

$$RPM = 170 \frac{rpm}{V} \times 44.4 V = 7548 rpm$$

$$d = 22 in$$

$$pitch = 5.5 in$$

$$F_{static} = 4.392399 \times 10^{-8} \cdot 7548 \frac{22^{3.5}}{\sqrt{5.5}} (4.23333 \times 10^{-4} \cdot 7548 \cdot 5.5 - 0) [N]$$

$$F_{static} = 12652.638 [N]$$

For the dynamic case it is consider that the aircraft velocity is $3 \frac{m}{s}$

$$F_{dynamic} = 4.392399 \times 10^{-8} \cdot 7548 \frac{22^{3.5}}{\sqrt{5.5}} (4.23333 \times 10^{-4} \cdot 7548 \cdot 5.5 - 3) [N]$$

$$F_{dynamic} = 10491.860 [N]$$

To verify that the data obtained by the equation is correct it compares the thrust value found in the technical data sheet of the motor select and find the error between measurements. The thrust value given by the motor manufacturer at max throttle is $13600 gf \approx 133.37 [N]$. The percentual error obtained is:

$$error (\%) = \frac{|real\ value - theoretical\ value|}{theoretical\ value} \cdot 100\%$$

$$error (\%) = \frac{|12652 - 13600|}{13600} \cdot 100\% = 6.97 \%$$

The value above shows that the empirical equation used works perfectly for this situation.

Seed distribution system calculations

Bolts joining seed tank with UAV frame

Fastener Stiffness

To begin the analysis of the bolts that join the tank where the seed will be located, it was first determined the necessary length of the bolts. To achieve this the following schematic is useful:

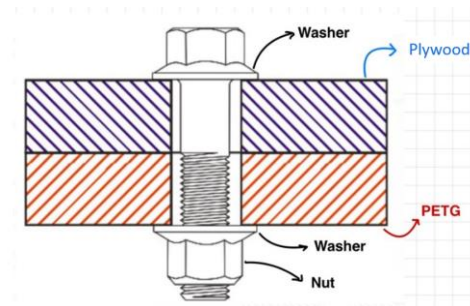


Figure 22: Tank bolted joint schematic.

To determine the necessary bolt length, it is important to define some parameters:

- L_{wood} : plywood plate thickness [mm]
- $L_{\text{dist,sys}}$: seed distribution system thickness [mm]
- d : bolt nominal diameter [mm]
- p : bolt thread pitch [mm]
- t : washer thickness [mm]
- H : nut height [mm]
- l : thickness of all material squeezed between face of bolt and face of nut [mm]
- A_t : tensile strength area [mm²]
- E_{wood} : plywood modulus of elasticity [MPa]
- E_{PETG} : PETG modulus of elasticity [MPa]
- E_{bolt} : bolt material modulus of elasticity [MPa]
- S_p : minimum proof strength [MPa]

- N: number of bolts (6)

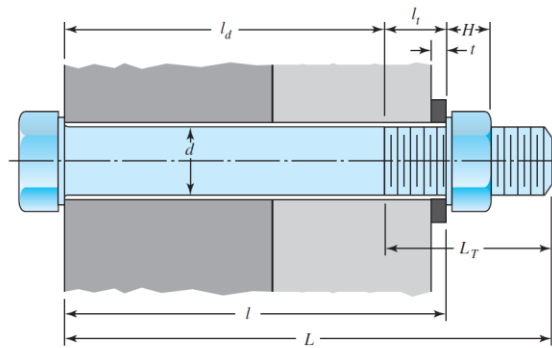


Figure 23: important dimensional parameters for bolts.

The nominal diameter of the bolt will be 3 [mm]. The calculation of the bolt length is:

$$L = \text{Thickness Al} + \text{thickness PETG} + H + 2(t) + 2(p)$$

$$L = 2 + 10 + 8.4 + 2(2.3) + 2(1.25)$$

$$L = 30.1[\text{mm}]$$

With this information we can determine the bolt that is needed. The selected one is: M3x1.25x30. For this application the bolt has a fine pitch spacing.

Knowing the total length, it is possible to calculate the other dimensional parameters of the bolt:

- Total threaded length of the bolt. Because the L of the selected bolt is less than 125 [mm] and d is less than 48 [mm], the value of L_t is calculated with the following equation:

$$L_t = 2d + 6$$

$$L_t = 12 [\text{mm}]$$

- Unthreaded length:

$$l_d = L - L_t$$

$$l_d = 18.1 [mm]$$

- Threaded length of the bolt inside the joint:

$$l_t = l - l_d$$

$$l_t = 3.9 [mm]$$

- Nominal diameter:

$$A_d = \frac{\pi d^2}{4}$$

$$A_d = 7.069 [mm^2]$$

- Tensile strength area. This value is obtained from table 8.1 of Shigley's Mechanical Engineering Design (Budynas & Nisbett, 2014):

$$A_t = 5.03 [mm^2]$$

Once calculated and determined the dimensional parameters, the fastener stiffness is obtained, the value of E in the equation is the elastic modulus of steel:

$$k_b = \frac{A_d A_t E}{A_d l_t + A_t l_d}$$

$$k_b = 62051 [N]$$

Member stiffness

After calculating the bolt stiffness, it is necessary to calculate the members stiffness. For this the two material layers must be divided in frustums. The division of the layers is the following:

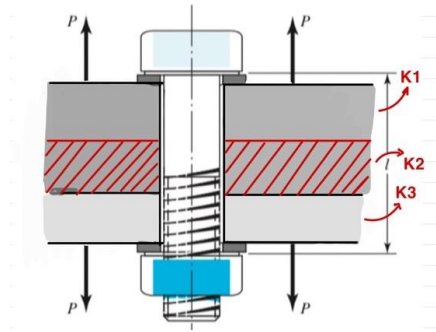


Figure 24: Frustum division of the material layers.

The geometry has to be divided into three frustums because the thickness of the layers is unequal. The top and bottom layer must be of the same thickness, and the middle one the difference. Since the top plywood layer is 12 [mm] and the bottom PETG layer is 10 [mm], the three frustums will be needed for the calculation. The bottom one are 10 [mm] in thickness, and the middle one is 2 [mm]. The stiffness of the frustum is represented by k_1 , k_2 , and k_3 . For the equation D is equal to $1.5d$, and E is equal to the elastic modulus of the material.

The calculation of the frustum is the following:

$$k_1 = \frac{0.5774\pi E_{wood}d}{\ln \frac{(1.155t_1 + D - d)(D + d)}{(1.155t_1 + D + d)(D - d)}}$$

$$k_1 = 14144 [N]$$

$$k_2 = \frac{0.5774\pi E_{wood}d}{\ln \frac{(1.155t_2 + D - d)(D + d)}{(1.155t_2 + D + d)(D - d)}}$$

$$k_2 = 26239 [N]$$

$$k_3 = \frac{0.5774\pi E_{PETG}d}{\ln \frac{(1.155t_3 + D - d)(D + d)}{(1.155t_3 + D + d)(D - d)}}$$

$$k_3 = 1941 [N]$$

The equivalent stiffness equals:

$$k_m = \left(\frac{1}{k_1} + \frac{1}{k_2} + \frac{1}{k_3} \right)^{-1}$$

$$k_m = 1602 [N]$$

Tension joints

After calculating the bolt and equivalent members stiffness, it is possible to obtain the stiffness constant of the joint:

$$C = \frac{k_b}{k_b + k_m}$$

$$C = 0,9748$$

To determine the tension factors of the joint, some important parameters are introduced:

S_p : minimum proof strength

F_p : proof load

F_i : preload

P : total force

N : number of bolts

The values for each of these parameters are the following:

- Minimum proof strength. This value is obtained from table 8.11 of Shigley's Mechanical Engineering Design (Budynas & Nisbett, 2014):

$$S_p = 225 [MPa]$$

- Proof load:

$$F_p = A_t S_p$$

$$F_p = 1132[N]$$

- Preload:

$$F_i = 0.75F_p$$

$$F_i = 848.8[N]$$

- Total force. It is expected that the drone could carry a maximum of 6 [kg] of payload inside the tank, so the design force is the most critical case. This value will be per bolt, meaning the total force divided by 6:

$$P = mg$$

$$P = 58.8[N]$$

Maximum allowable forces

For joints in tension there are three methods to obtain the safety factor: yielding safety factor, load safety factor, and separation safety factor. Yielding safety factor guards against static stress exceeding the proof strength. Load safety factor is applied only to the load P as a guard against overloading. Meanwhile, separation safety factor guards against the joint separating. To obtain the maximum loads in each case the safety factors take a value of 1.2. If the max load obtained with each one is greater than P, then the joint will hold. The equations are multiplied by N because the total force is important for the analysis.

- Yielding safety factor:

$$P_p = \frac{\left(\frac{S_p A_t}{\eta_p} - F_i \right)}{C} (N)$$

$$P_p = 580.5[N]$$

- Load safety factor maximum load:

$$P_L = \frac{S_p A_t - F_i}{\eta_L} (N)$$

$$P_L = 1451[kN]$$

- Separation safety factor

$$P_o = \frac{F_i}{\eta_o(1 - C)} (N)$$

$$P_o = 168584[kN]$$

Each of the maximum loads are much greater than P, assuming a small value for the safety factor. Because of this, it is safe to say that the selected bolts will fulfill their purpose with no issues.

Seed Pod Container Size

For the frame design, it is important to determine the minimum size the seed pod container needs to be, to carry a determined number of seed pods. First, it is necessary to define the size and weight of each pod. Through experimental methods, the pod diameter is determined to be around 1 [in] and its weight is approximately 15 [g].

With the pod parameters, the first step is to determine the volume of one pod, assuming the pod has a spherical shape.

$$V_{pod} = \frac{4}{3} \cdot \pi \cdot \left(\frac{d_{pod}}{2}\right)^3$$

$$V_{pod} = 8580 [mm^3]$$

The first design iteration is assuming the drone will take off with a 6 kg payload, which represents 400 seed pods. With the number of pods and the unit volume, the minimal container volume is determined.

$$V_{min} = N_{pod} \cdot V_{pod}$$

$$V_{min} = 3432 [cm^3]$$

For ease of manufacture, the container design will be a cylinder. To fit the frame, the diameter of the cylinder is selected to be 15 [cm]. The height of the container is determined as follows.

$$L_{cont} = \frac{4 \cdot V_{min}}{\pi \cdot d_{cont}^2}$$

$$L_{cont} = 19.42 [cm]$$

Seed Distribution Carousel Speed

The seed pods need to be released approximately every 2 meters. For size reasons, the carousel is designed to carry 10 seed pods at the time. The following figure is a preliminary design of the carousel rotor.

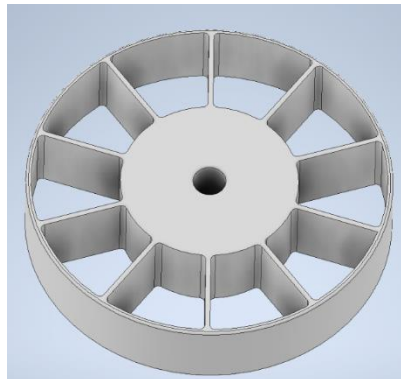


Figure 25: Design of the carousel rotor.

Since the UAV velocity is 3 m/s, while distributing the seed pods. The rotation speed of the carousel is calculated as follows.

One seed needs to be released every two meters. For the release, the carousel needs to rotate 36 degrees. The UAV moves at 3 m/s, which is why the rotor needs to have an angular speed of 36° every 2/3 of a second.

$$\omega = \frac{36}{2/3} = 54 \left[\frac{deg}{s} \right]$$

Container axial loading

The container needs to support 6 kg of seed pods. It is necessary to guarantee that the container will not axially fail. The following diagram shows the axial loading that the container is supporting.

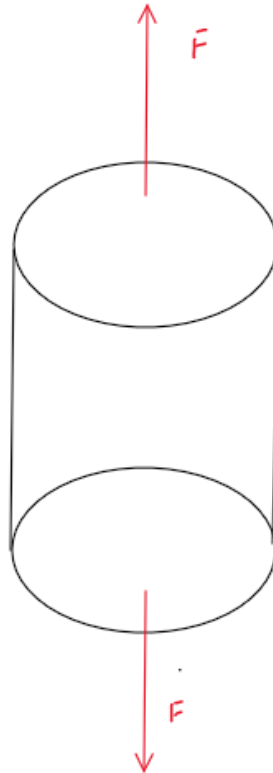


Figure 26: Container axial loading.

The external diameter of the container is 152 mm, and the internal diameter is 146 mm. The cross-sectional area of the cylinder is calculated as follows.

$$A = \frac{\pi \cdot (d_{ext}^2 - d_{int}^2)}{4}$$

The force applied is simply the mass of the seed pods times the gravitational constant.

The axial stress is calculated as follows.

$$\sigma = \frac{F}{A}$$

Finally, the safety factor is calculated using the ultimate tensile strength, as the container material is brittle. The safety factor is calculated to be 10.28.

Container bottom force analysis

The bottom of the container of the seed distribution is made of PETG and has a thickness of about 8[mm]. The principal force that is going to act on it is a distributed load made by all the weight of the seeds.

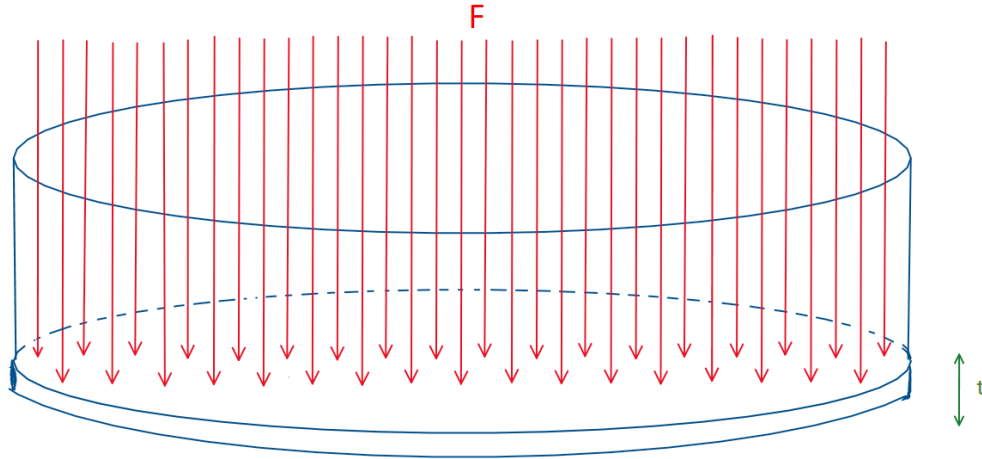


Figure 27: Distributed load on the bottom of the tank.

The bottom of the tank can be analyzed as a ‘clamped’ circular plate. Data:

- $F=60$ [N]
- $R = 73$ [mm]
- $E = 439.1$ [Pa]
- $\nu = 0.43$
- $t = 8$ [mm]
- $S_{ut} = 18.2$ [Pa]

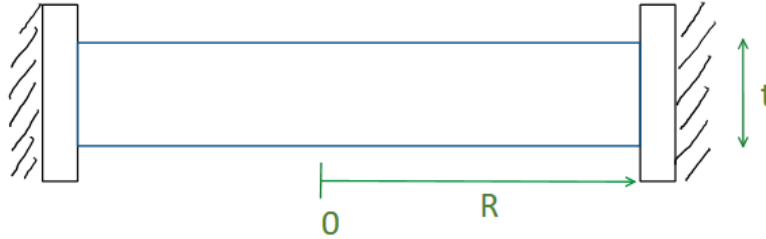


Figure 28: Clamped circular plate representation.

The distributed load is making a pressure in the bottom of this tank, so:

$$q = \frac{F}{A}$$

$$q = 3.395 \cdot 10^{-3} [Pa]$$

For the deformation on 'y' and the stressed suffered by this plate, the formulas were extracted from literature. (Hearn, 1997)

$$y_{max} = \frac{3}{16} \cdot \frac{qR^4(1-r^2)}{Et^3}$$

$$y_{max} = 0.073 [mm]$$

$$\sigma_{r_{max}} = \frac{3qR^2}{4t^2}$$

$$\sigma_{r_{max}} = 0.2238 [Pa]$$

$$\sigma_{z_{max}} = \frac{3qR^2}{8t^2} \cdot (1 + \nu)$$

$$\sigma_{z_{max}} = 0.16 [Pa]$$

The zone that is going to suffer more deflection is right in the middle of the plate, so if an infinitesimal element is taken, the stresses that this is going to suffer are:

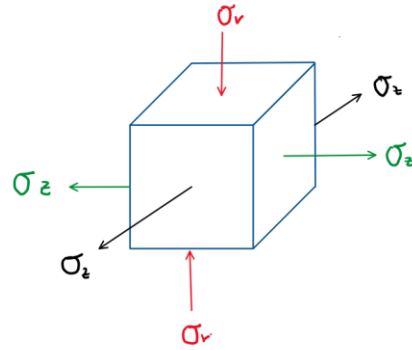


Figure 29: Infinitesimal Element 3D

As these are combined stresses, they can be analyzed using the 3D Von Mises stress theory: (Budynas & Nisbett, 2014)

$$\sigma' = \left[\frac{(\sigma_1 - \sigma_2)^2 + (\sigma_2 - \sigma_3)^2 + (\sigma_3 - \sigma_1)^2}{2} \right]^{1/2}$$

Where:

$$\sigma_1 = \sigma_3 = \sigma_z$$

$$\sigma_2 = \sigma_r$$

$$\sigma'_{3D} = \left[\frac{(\sigma_z - \sigma_r)^2 + (\sigma_r - \sigma_z)^2}{2} \right]^{1/2}$$

$$\sigma'_{3D} = 0.2571 [Pa]$$

This can also be analyzed as a 2D element. Where the equation will result in

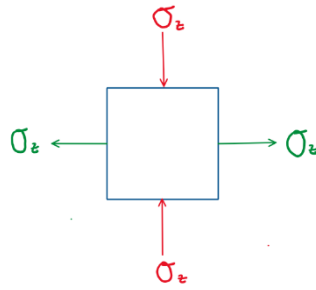


Figure 30: Infinitesimal Element 2D

$$\sigma'_{2D} = (\sigma_z^2 - \sigma_z\sigma_r + \sigma_r^2)^{1/2}$$

$$\sigma'_{2D} = 0.1997[Pa]$$

Finally having the Von misses Stress, a safety factor can be obtained comparing it with the ultimate tensile strength of the PETG.

$$\eta_{2D} = \frac{S_{ut}}{\sigma'_{2D}}$$

$$\eta_{2D} = 91.13$$

$$\eta_{3D} = \frac{S_{ut}}{\sigma'_{3D}}$$

$$\eta_{3D} = 66.15$$

Stepper motor torque

For the distribution system, a stepper motor will be used to rotate the carrousel. The carrousel has space for 10 seed pods at the same time. To calculate the torque needed for the system, the torque needed to move just one seed pod and multiply this value times 10. To calculate the torque, the weight of the carrousel is neglected. The next figure represents a diagram of the problem.

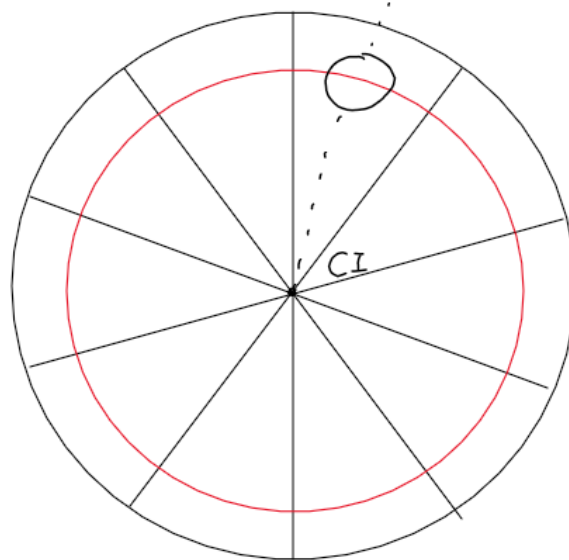


Figure 31: Carrousel diagram.

To calculate the torque needed for one seed, the work and energy principle for a rigid body. The moment of inertia of the sphere is calculated with reference to the carrousel axis, by using the parallel axis theorem.

$$I_{CI} = \frac{2}{5} \cdot m_b \cdot r_{esf}^2 + r_{CI}^2 \cdot m_b$$

Where:

I_{CI} : moment of inertia with reference to the instantaneous center.

m_b : seed pod mass.

r_{esf} : seed pod radius.

r_{CI} : distance between the seed pod and the instantaneous center (57 [mm]).

Finally, the moment that works on the movement of the seed pod is calculated with the following equation.

$$M \cdot (\theta_2 - \theta_1) = \frac{1}{2} I_{CI} \cdot \omega^2$$

Where:

M : Torque needed to move one seed pod.

θ_1 : Initial angular position of the seed pod.

θ_2 : Final angular position of the seed pod.

ω : Angular velocity the seed pod moves.

Assuming the initial angular position is zero and that the seed pod needs to move 1/10 of a circumference ($\theta_2 = 36^\circ$) every 2/3 of a second, the needed torque to move one seed pod is $4.72 \cdot 10^{-4}$ [Nm].

Finally, the torque needed to move ten seed pods at a time is the following.

$$T = 4.72 \cdot 10^{-3} \text{ [Nm]}$$

Dynamic analysis of the seed pod

To calculate the dynamics of the seed pod distribution, assumptions need to be made to properly analyze the parabolic motion. The assumptions are the following.

- Air resistance is negligible.
- The UAV moves at a constant speed.
- There is no vertical impulse when the pod is released.
- The relative velocity between the UAV and the pod is zero when the pod is released.
- The seed pod is considered as a particle.

The following figure describes the parabolic motion of the seed pod.

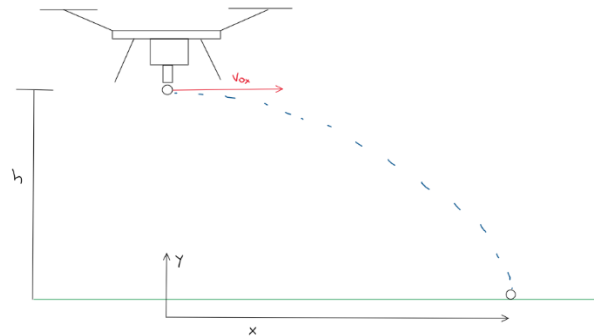


Figure 32: Seed pod motion diagram.

Where:

- h : height at which the pod is released (6m).
- V_{ox} : initial horizontal velocity (3 m/s).
- x : horizontal distance the pod travels before reaching the ground.
- V_y : vertical velocity the pod has when it reaches the ground.
- g : gravitational acceleration.
- t : time for the seed to reach the ground.
- h_0 : ground level.

First, to determine the final vertical velocity of the seed pod, the following equation will be used.

$$V_y^2 = -2 \cdot g \cdot (h_0 - h)$$

The final velocity is calculated as follows.

$$V_y = \sqrt{-2 \cdot 9.81 \cdot (0 - 6)}$$

$$V_y = 10.85 \left[\frac{m}{s} \right]$$

With the final velocity, the motion time is determined using the parabolic motion equations.

$$V_y = V_{oy} - g \cdot t$$

$$t = \frac{V_{oy} - V_y}{g}$$

$$t = \frac{0 - (-10.85)}{9.81}$$

$$t = 1.11 \text{ [s]}$$

Finally, the horizontal distance traveled by the seed pod from the release moment to the moment it touches the ground is calculated as follows.

$$x = V_{ox} \cdot t$$

$$x = 3 \cdot 1.11$$

$$x = 3.33 \text{ [m]}$$

UAV frame calculations

Drone arm analysis

It was decided that an aluminum C profile with a fin is going to be used, the dimensions are provided from a CEDAL catalog. All the calculations are made by the program EEs, the code can be found at the end of the document.

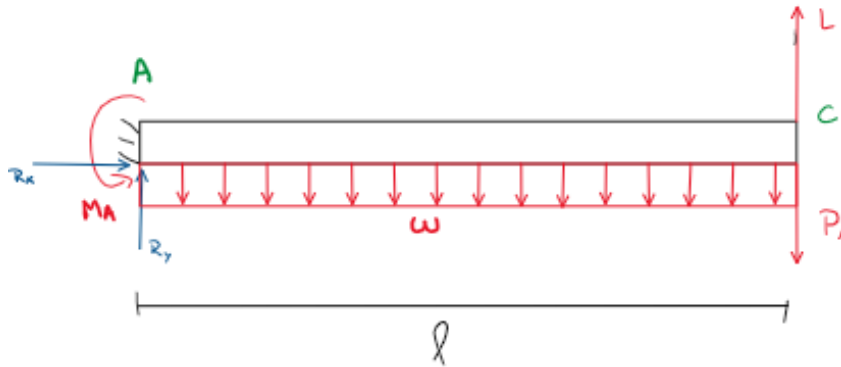


Figure 33: Beam Free body diagram (Maximum force)

Data and calculations

- Thickness = 1.4 mm
- Width = 76.2 mm
- Height = 25.4 mm
- $L = 5.25$ mm
- $L_{fin} = 12$ [mm]
- $g = 9.81$ [m/s²]
- $L = 124.08$ [N] *This Value is extracted from the Lift calculations.
- $m_{motor} = 360$ [g]
- Length = 0.4 [m]
- $m_{meter} = 0.554$ [kg/m]
- Mass

$$m = m_{meter} * Length$$

$$m = 0.2216 \text{ [kg]}$$

- Frame Weight (W)

$$W = m \frac{g}{l}$$

$$W = 5.435 \left[\frac{N}{m} \right]$$

- Motor weight (W_m)

$$W_m = 0.36 \cdot 9.81$$

$$W_m = 3.532 [N]$$

Location of the C profile Centroid

For the drone arms, an aluminum C profile with fin will be used. The following figure presents the profile dimensions.

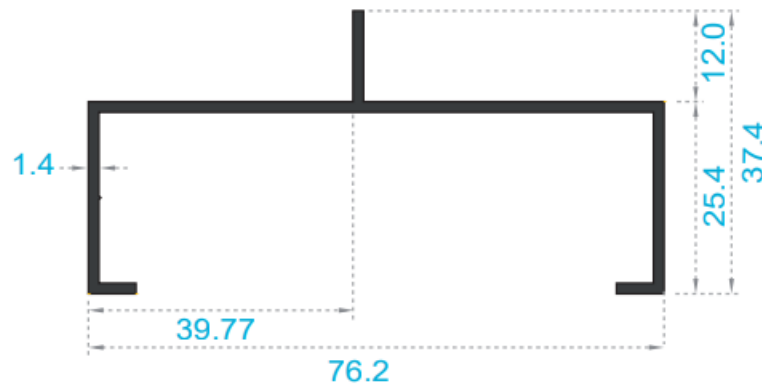


Figure 34: C profile dimensions.

As the manufacturer does not provide the moment of inertia of the profile, the centroid of the sectional area needs to be determined. The superposition principle is used. The vertical distance of the centroid from the top surface of the profile is 6.025 mm, the horizontal distance from the left surface is 37.9 mm.

Second moment of inertia

To determine the moment of inertia of the profile, the moments of inertia of each section is calculated separately and added up to determine the moment of inertia of the entire profile. The parallel axis theorem will be used. The second moment of inertia is $1.505 \cdot 10^{-8} [m^4]$.

Moment summation on A

$$\sum M = 0$$

$$M_A - W \cdot \frac{l^2}{2} + L \cdot l - W_m \cdot l = 0$$

$$M_A = W \cdot \frac{l^2}{2} - L \cdot l + W_m \cdot l$$

Reactions in Point A

$$\sum F_y = 0$$

$$R_y - W \cdot l + L - W_M = 0$$

Analysis at the maximum force

For this the motors are going to be lifting 12 kg, so the lift force value is going to be:

$$L = 124.08[N]$$

Moment summation:

$$M_{A,Max} = -47.78[Nm]$$

Reactions in A:

$$R_{y,Max} = -118.4[N]$$

There are no reactions on the x axis.

Shear force and bending moment diagram

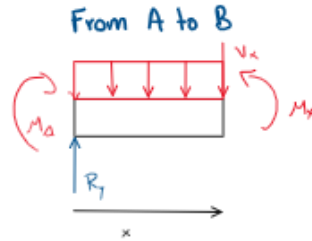


Figure 35: Shear forces and Moment diagram (Maximum Force)

From A to B

Shear:

$$-V_x - W \cdot x + R_{y,Max} = 0$$

$$V_x = 118.4 - 5.435x$$

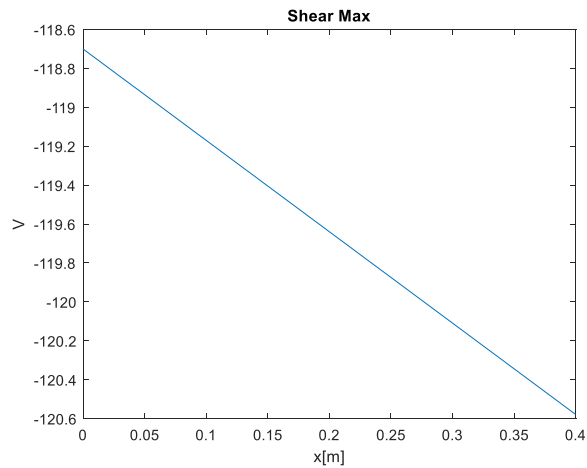


Figure 36: Maximum Shear Force Diagram

Moment:

$$M_x + W \frac{x^2}{2} - R_{y,Max}x - M_{A,Max} = 0$$

$$M_x = -118.4x - 2.71x^2 + 47.84$$

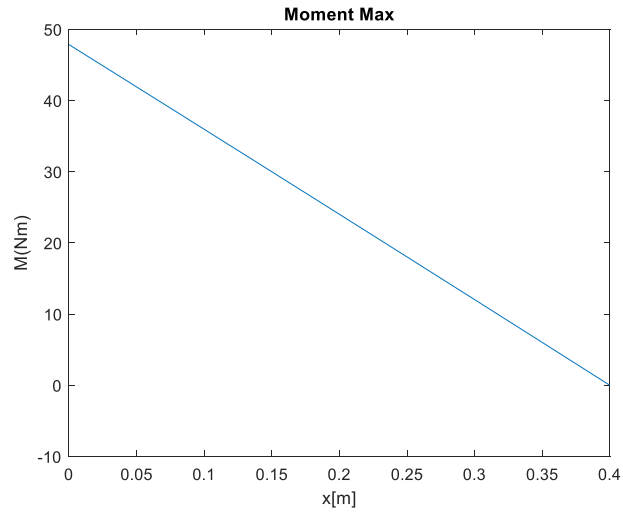


Figure 37: Maximum Moment Diagram

Analysis at the minimum force

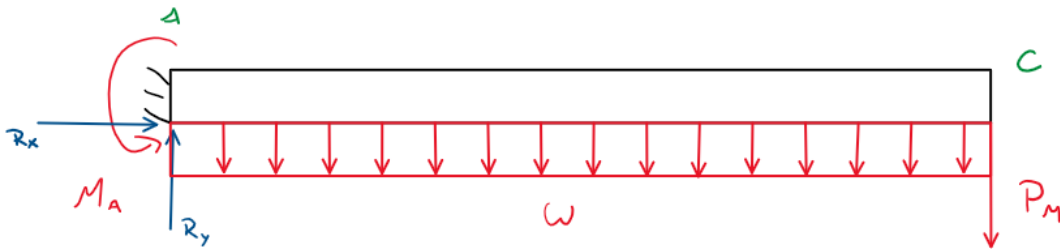


Figure 38: Beam Free body diagram (Minimum force)

For this the motors will be off

$$L=0[\text{N}].$$

Moment:

$$M_{A,min} = 1.847[\text{Nm}]$$

Reactions:

$$R_{y,min} = 5.705[N]$$

Shear force and bending moment diagram when minimum force is applied

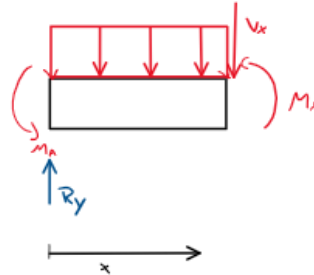


Figure 39: Shear forces and Moment diagram (Minimum Force)

Shear:

$$-V_x - W_x + R_y = 0$$

$$V_x = 5.705 - 5.435x$$

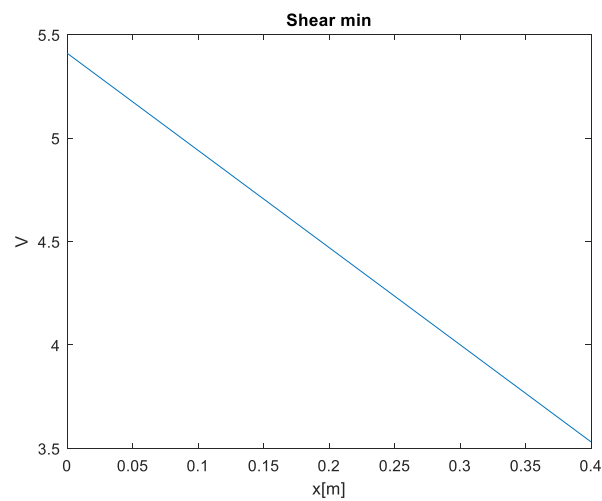


Figure 40: Minimum Shear Force Diagram

Moment:

$$M_x + W \frac{x^2}{2} - R_y x + M_A = 0$$

$$M_x = 5.705x - 2.71x^2 - 1.847$$

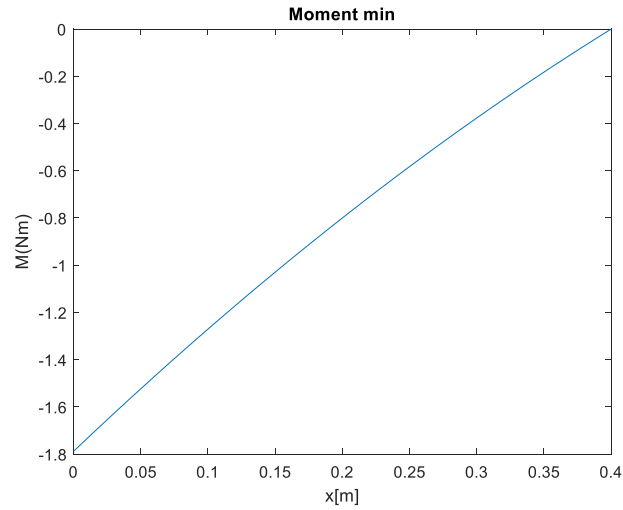


Figure 41: Minimum Moment Diagram

Fatigue stress analysis at the arm of the UAV

$$\sigma = \frac{M \cdot C}{I}$$

$$\sigma_{Max} = \frac{K_F M_{Max} \cdot D}{2I}$$

$$\sigma_{min} = \frac{K_F M_{min} \cdot D}{2I}$$

The ultimate tensile strength of aluminum is the following.

- $S_{ut} = 324$ [MPa] (Budynas & Nisbett, 2014).

Following “Shigley Mechanical Engineering Design” it says that for an $S_{ut} < 1400$ [MPa], the Endurance limit will be:

- $S_e = 1/2 S_{ut} = 162$ [MPa] (Budynas & Nisbett, 2014)

The rest of the concentration factors are also calculated following the theory of the same source.

$$S_e = k_a k_b k_c K_d k_e k_f S'_e$$

$$k_a = a S_{ut}^b$$

- $a = 4.51$ [MPa]
- $b = -0.265$

$$k_b = 1.24 d_e^{-0.107},$$

- $D_e = 0.808 \cdot (\text{height} \cdot \text{width})^{\frac{1}{2}}$ (Nonrotating, non-circular axis)

$$k_c = 1 \text{ (Bending)}$$

$$k_d = 1 \text{ (Temperature 20[C])}$$

$$k_e = 0.868 \text{ (95\% Reliability)}$$

$$k_f = 1$$

Stress Concentration

The arm will have 5 mm holes in the top surface for assembly purposes. The static stress concentration factor is determined using the figure A15.2 (Budynas & Nisbett, 2014).

$$\frac{d_{hole}}{thickness} = \frac{5}{1.4} = 3.57$$

$$\frac{d_{hole}}{width} = \frac{5}{76.2} = 0.0656$$

$$k_T = 1.7$$

The fatigue stress concentration factor is determined using the following equation.

$$K_F = 1 + q \cdot (K_T - 1)$$

The notch sensitivity, q , is determined with the figure 6.20 (Budynas & Nisbett, 2014).

$$q = 0.75$$

The stress concentration factor is the following.

$$K_F = 1.525$$

Average stress and Amplitude Stress

$$\sigma_m = \frac{\sigma_{max} + \sigma_{min}}{2}$$

$$\sigma_a = \frac{|\sigma_{max} - \sigma_{min}|}{2}$$

Gerber Failure Criteria

The Gerber Failure criteria is used to determine the safety factor due to fatigue.

$$n_f = \frac{1}{2} \left(\frac{S_{ut}}{\sigma_m} \right)^2 \cdot \frac{\sigma_a}{S_e} \cdot \left[-1 + \sqrt{1 + \left(2 \cdot \sigma_m \cdot \frac{S_e}{S_{ut} \cdot \sigma_a} \right)^2} \right]$$

With this formula and the program EEs it is shown that the safety factor is around 3.688. The profile used is the smallest available on the manufacturers catalog, which is why the factor of safety can't be lowered.

First cycle failure safety factor

It is important to determine if the arm will not fail during the first cycle. The following equation will be used to determine the safety factor.

$$\sigma_a + \sigma_m = \frac{S_y}{n_s}$$

- Length between both materials

$$l = h + \left(\frac{d}{2}\right) = 4.95 \text{ [mm]}$$

Once all these lengths were determinate, the previous formulas used for joint analysis can be applied. For the material constant

$$k_m = \frac{(k_{m2} * k_{m1})}{(k_{m2} + k_{m1})} = \frac{(1567 * 3659)}{(1567 + 3659)} = 1097 \text{ [kN/m]}$$

The bolt constant is:

$$k_b = 405414 \text{ [kN/m]}$$

Stiffness constant:

$$C = 0.27$$

Knowing that the max load is 124.08 [N]:

$$F_b = C * \frac{P}{4} = 1490 \text{ [N]}$$

$$\sigma_b = \frac{F_b}{A_t} = 169.7 \text{ [MPa]}$$

$$\eta = \frac{S_p}{\sigma_b} = 1.326$$

Load safety factor:

$$F_i = 1482 \text{ [N]}$$

$$\eta_L = \frac{S_p A_t - F_i}{F_b}$$

$$\eta_L = 59$$

Separation safety factor

$$\eta_o = \frac{F_i}{(1 - C) \frac{P}{3}}$$

$$\eta_o = 65.42$$

As it was expected the calculates safety factors are similar to the ones found in previous joint analysis.

Stress analysis on the upper plate

Two square plates are going to be used as the main structural components. The UAV arms are going to be attached to the corners of the upper plate and spacers will connect the upper plate to the lower plate. Both plates have a hole in the middle for the seed pod container. Because of the symmetry of the plate, the analysis can be modeled as a 1-dimensional beam from the edge of the hole to the corner of the plate. The following figure shows the model used in the analysis.

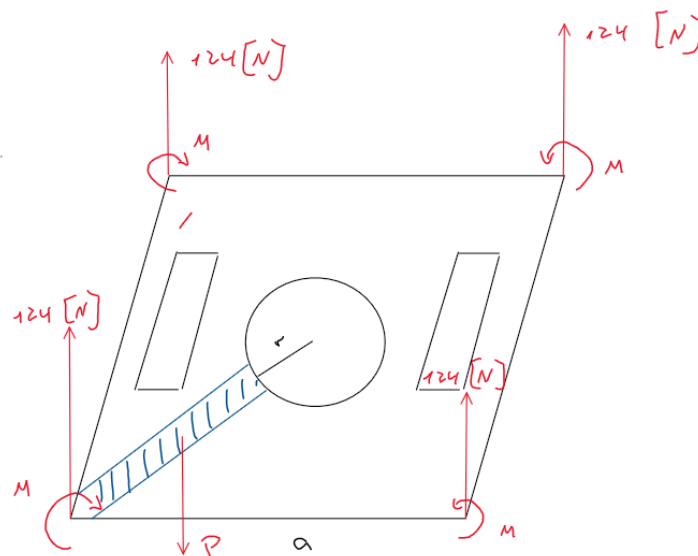


Figure 43: Plate model.

The beam is fixed at the end where the hole is and at the corner the propeller force and the arm moment are applied. The one-dimensional model is shown in the following figure.

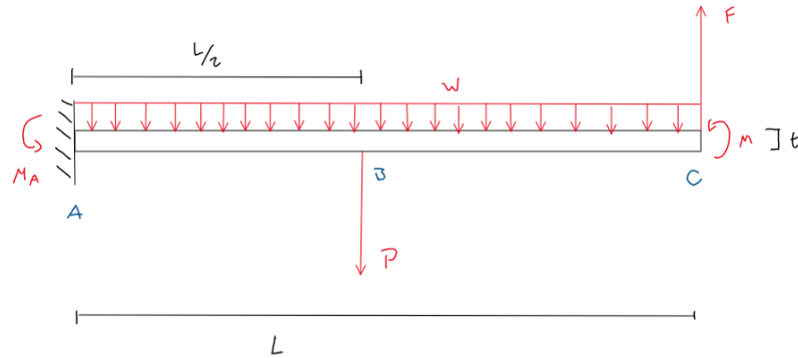


Figure 44: One-dimensional beam model.

The beam has a distributed force that represents the weight of the plate and a vertical force in the middle that represents the rest of the UAV weight distributed through the spacers joining with the other plate. It is assumed that the weight of the UAV is around 13 kg divided in four spacers connected in the middle of the plate. The model analyzed is a beam with a width of 15 cm. The length is calculated as a function of the length of the plate side.

$$L = \frac{1}{2} \cdot \sqrt{2 \cdot a^2} - r$$

The distributed force on top of the beam is calculated with the transversal area of the beam multiplied by the density and the gravitational constant.

$$w = \rho \cdot \text{width} \cdot t \cdot g$$

The applied moment is calculated by multiplying the length of the UAV arm times the force of the propellers in the case they are on or the motor weight in case the drone is not flying.

Analysis with maximum propeller thrust

With a maximum thrust, the upward vertical force has a magnitude of 124 [N]. A static analysis is performed on the modeled beam to calculate the location and the magnitude of the maximum bending moment and calculate the safety factor.

Moment summation on A:

$$\sum M_A = 0$$

$$M_A + M - P \cdot \frac{L}{2} - w \cdot \frac{L^2}{2} + F \cdot L = 0$$

$$M_A = \frac{L}{2} \cdot (P + w \cdot L) - F \cdot L - M$$

Force summation:

$$\sum F_y = 0$$

$$R_A = P + w \cdot L - F$$

Shear and Moment diagram

To determine the location and magnitude of the maximum bending moment, the shear and force diagrams for the beam will be determined.

Section AB:

The equation for the section AB of the beam is calculated from the following figure.

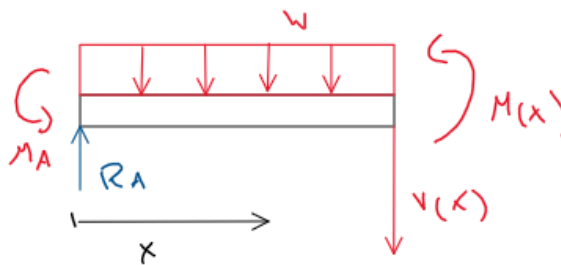


Figure 45: AB beam section.

The equations are the following.

$$V(x) = R_A - w \cdot x$$

$$M(x) = -w \cdot \frac{x^2}{2} + R_A \cdot x - M_A$$

Section BC:

Likewise, the equations for section BC are derived from the following figure.

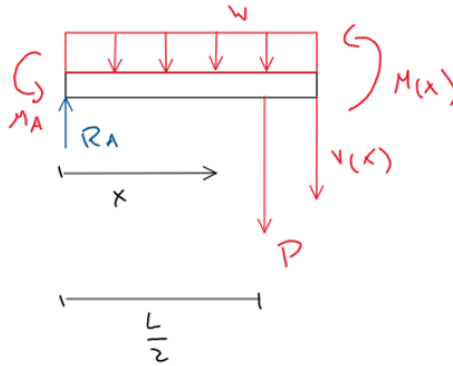


Figure 46: Beam section BC.

The equations are the following.

$$V(x) = R_A - w \cdot x - P$$

$$M(x) = -w \cdot \frac{x^2}{2} + R_A \cdot x - M_A - P \cdot \left(x - \frac{L}{2}\right)$$

With the previous analysis, the magnitude of the maximum moment is determined, with which the maximum bending stress is calculated. The following figure shows the shear force diagram in relation to the beam length.

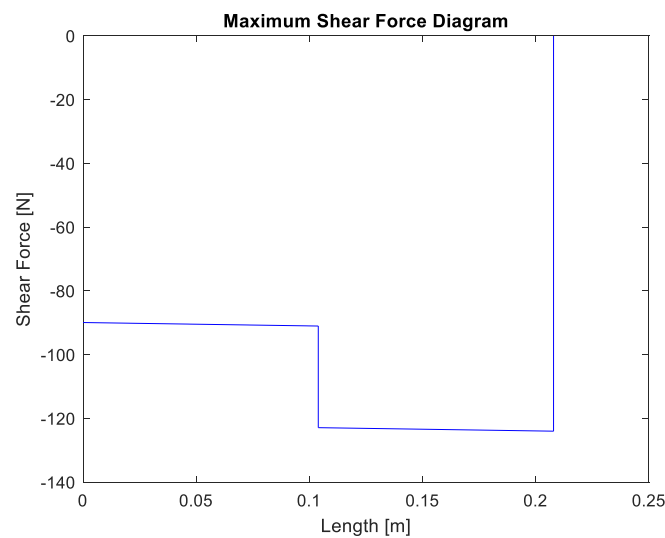


Figure 47: Shear force diagram for maximum thrust.

The maximum shear force is in section BC of the beam. The moment diagram is shown in the following figure.

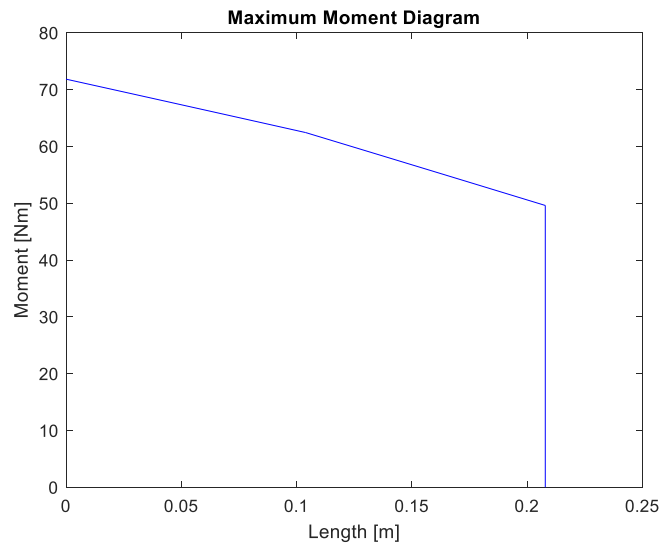


Figure 48: Moment diagram for maximum thrust.

The maximum moment is at the fixed end of the beam, with a magnitude of 71.74 [Nm].

Landed analysis

The analysis when the motors are turned off and the UAV is on land is determined with the following diagram.

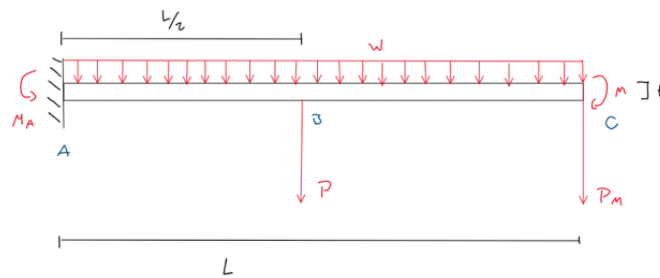


Figure 49: Landed analysis model.

The motor weights 0.36 kg. The analysis is made analog to the previous case, with the following equations as a result.

$$M_A = M + P \cdot \frac{L}{2} + w \cdot \frac{L^2}{2} + P_M \cdot L$$

$$R_A = P + P_M + w \cdot L$$

Shear force and moment diagram:

Since section AB and BC are the same as in the preceding case, the equations remain the same. However, the magnitudes vary. The shear force diagram is the following.

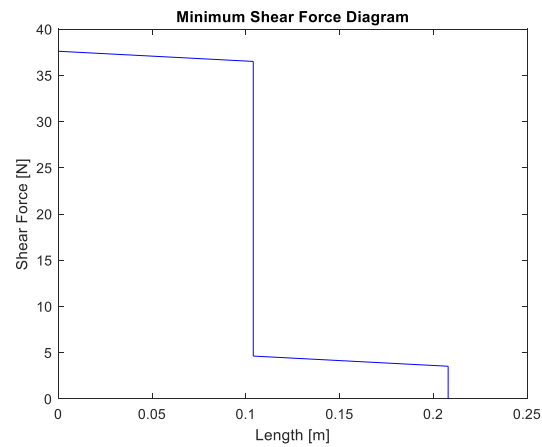


Figure 50: Shear force diagram with landed UAV.

Likewise, the moment diagram is shown in the next figure.

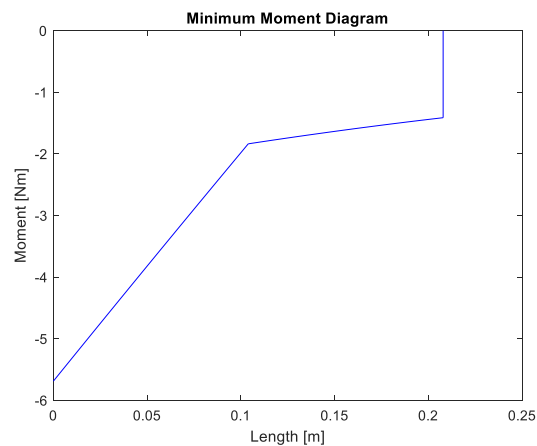


Figure 51: Moment diagram with landed UAV.

Analog to the preceding case, the minimum moment is at the fixed end of the beam, with a magnitude of -5.689 [Nm].

Fatigue stress analysis

The stress analysis is made for two materials. The first material is plywood and the second is aluminum. The aluminum ultimate tensile strength is 324 [MPa], while the plywood ultimate tensile strength is 27.6 [MPa]. For either case, the endurance limit is calculated as follows.

$$S_e' = 1/2 S_{ut}$$

$$S_e = k_a k_b k_c K_d k_e k_f S_e'$$

$$k_a = a S_{ut}^b$$

- $a = 4.51$ [MPa]
- $b = -0.265$

$$k_b = 1.24 d_e^{-0.107},$$

- $d_e = 0.808 \cdot (\text{height} \cdot \text{width})^{\frac{1}{2}}$ (Nonrotating, non-circular axis)

$$k_c = 1 \text{ (Bending)}$$

$$k_d = 1 \text{ (Temperature } 20[\text{C}] \text{)}$$

$$k_e = 0.868 \text{ (95\% Reliability)}$$

$$k_f = 1$$

The analysis is made in two locations of the beam. In the maximum bending moment location and near the corner, where there are holes for the arm assembly, that act as a stress concentrator. The minimum and maximum stress is calculated as follows.

$$\sigma_{Max} = \frac{K_F M_{Max} \cdot t}{2I}$$

$$\sigma_{min} = \frac{K_F M_{min} \cdot t}{2I}$$

In the first location, KF is 1 while in the second location it is determined to be 1.36.

The average and amplitude stress are calculated with the following equations.

$$\sigma_m = \frac{\sigma_{max} + \sigma_{min}}{2}$$

$$\sigma_a = \frac{|\sigma_{max} - \sigma_{min}|}{2}$$

$$r = \frac{\sigma_a}{\sigma_m}$$

For plywood, the fatigue failure criteria for brittle materials is used to determine the factor of safety.

$$S_a = \frac{r \cdot S_{ut} + S_e}{2} \left[-1 + \sqrt{1 + \frac{4 \cdot r \cdot S_{ut} \cdot S_e}{(r \cdot S_{ut} + S_e)^2}} \right]$$

$$\eta_f = \frac{S_a}{\sigma_a}$$

For aluminum, the Gerber failure criteria is used.

$$\eta_f = \frac{1}{2} \left(\frac{S_{ut}}{\sigma_m} \right)^2 \cdot \frac{\sigma_a}{S_e} \left[-1 + \sqrt{1 + \left(\frac{2 \cdot \sigma_m \cdot S_e}{S_{ut} \cdot \sigma_a} \right)^2} \right]$$

Also, for ductile materials is important to determine the safety factor for a first cycle failure.

$$\sigma_a + \sigma_m = \frac{S_y}{\eta_p}$$

The analysis is made by varying the plate thickness values and calculating the safety factors at both locations. This way, the minimum thickness can be determined for a safety factor of at least 1.2. It is important to keep the thickness as low as possible, to lower the total UAV weight. The following figure shows the safety factors at both locations and the plate mass in dependence of the plate thickness for plywood.

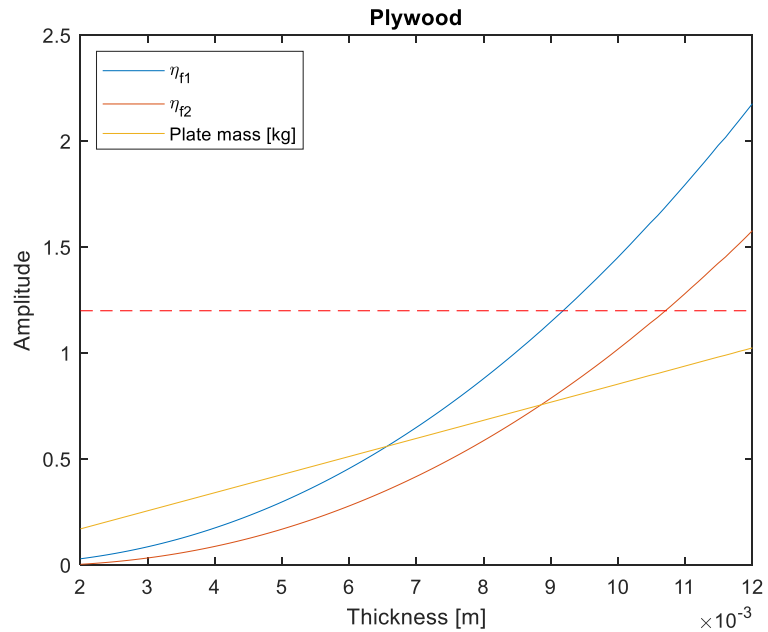


Figure 52: Safety factors for a plywood plate.

For the plywood plate, the minimum thickness is 10.79[mm], with a weight of 0.9 [kg].

Likewise, the following figure shows the safety factors for an aluminum plate.

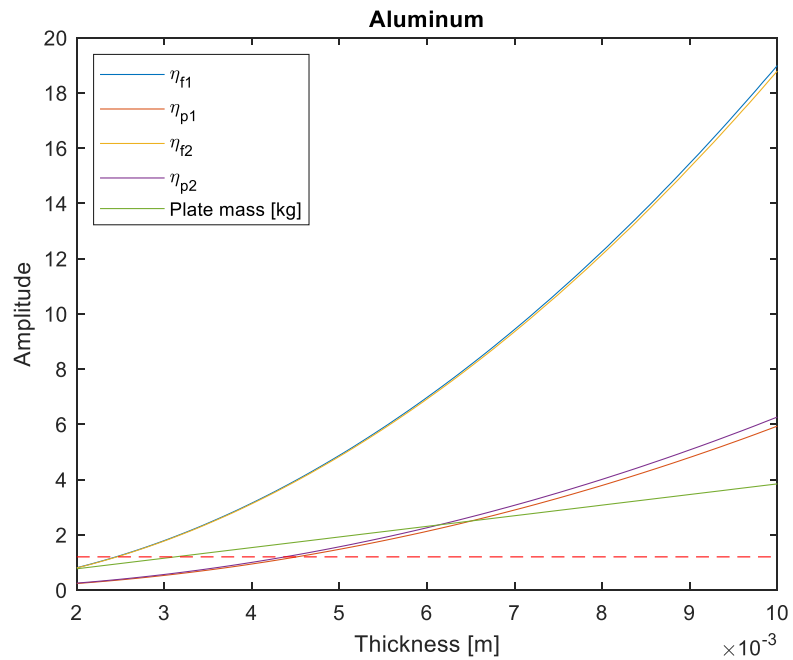


Figure 53: Safety factors for an aluminum plate.

The minimum thickness for an aluminum plate is 4.5 [mm] with a weight of 1.7 [kg]. An aluminum plate is much heavier than an acrylic plate. This analysis is an estimate of the safety factors for the structural upper plate of the UAV. However, the model used is a conservative one, which is why these thickness values can be lower and need to be confirmed by a static simulation.

Results and discussion

After evaluating the requirements of the client, establishing goals for the project, organizing the schedule and initial budget, selecting the main components for the flight system, performing all the necessary calculations, and acquiring all the construction materials in accordance with the calculations, a functional prototype of the seed distribution system and UAV was presented to the client.

The seed distribution system fulfills the client requirements. The system is controlled by an Arduino, so it is easily programable and controlled. The main tank can be expanded with extensions to accommodate more seed pods if needed. Furthermore, a combination of a separator and distributor of the capsules allow the system to deliver the seeds with minimum risk of damaging the pods or jamming the system. This system is connected to a battery apart from the other components of the aircraft, which means that it will not affect in a significant way the battery life of the flight system. Furthermore, the use a wireless relay makes it possible to turn the system on and off at any time of the flight by a ground operator, giving the user more control of the area where the seeds will be distributed.

The designed seed distribution system only works with spherical, smooth, and approximately 1 in in size seed pods. If the size or shape of the seed pods changes, the bottom part of the seed tank would have to be replaced to accommodate the new seed capsules. The system was tested using glass marbles as seed pods. These spheres were the most similar

object to the recommended seed pods. With the dimensions of the tank as it is (refer to annex XX), the tank can hold up to 150 seed pods and discharge them in approximately 100 seconds.



Figure 54: complete set of designed pieces of the seed distribution system.

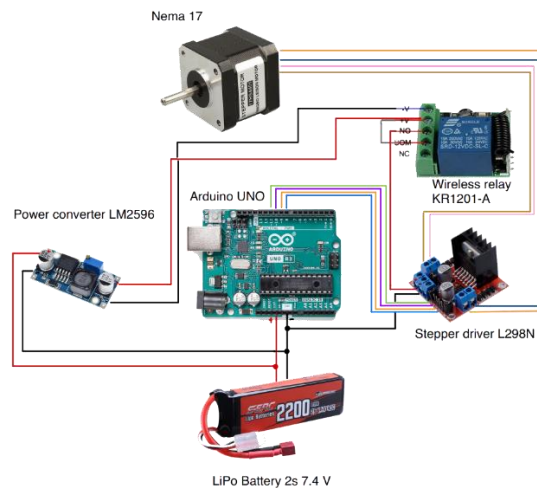


Figure 55: designed control circuit of the seed distribution system.

The final design of the UAV also fulfills the client requirements. The design of the structure to be easily repaired. The structural components are made of common cheap materials that are locally available. The final design is mechanically resistant and thought to withstand the heavy duty the UAV will be subjected to.

The final prototype was tested on the field. The final weight of the UAV including the seed distribution system is 13.5 kg. This result is heavier than what was initially expected, nonetheless, that change in weight will not suppose a problem for the operation of the aircraft. The maximum altitude the vehicle rose from the earth was approximately 10 m, which is more than the client requested. With the calculations and simulations it safe to estimate that the UAV will be able to carry the desired payload. During the conducted tests it was not possible to trial the seed distribution system in conjunction with the UAV because of the difficult maneuverability the size of the drone supposes.



Figure 56: final design of the UAV.

This prototype is the first of many possible iterations of this machine. For future work it is recommended to add a camera and First Person View (FPV) capabilities, lower the weight of the structure, since more weight means less payload and flight time. Also, changing the power distribution module (PDM) to the most recent one. To make sure the UAV is ready for real missions it should be tested more under a controlled environment by an experienced pilot. Finally, the integration of the seed pods with the seed distribution system has room for improvement.

Safety Through Design

One of the crucial steps in the development of the project is the risk analysis that needs to be considered to avoid waste of resources and time. It is also important to perform this analysis to plan the possible solutions to possible drawbacks that can arise during the development of the project. In the following section two of the highest impact risks will be described.

- Delay in delivery of components (C-001): since most of the components will be imported from the United States, there is a risk that these will not arrive on time and the prototype cannot be manufactured. To reduce the risk, it is necessary to verify that the supplier is trustworthy and order the components in anticipation.
- ESC Calibration Failure (T-006): the electronic speed controller (ESC) is one of the most sensitive components of the UAV system, it is responsible of the maneuverability in the air. If the calibration is not suitable the propulsion system will not function properly. To prevent failure, it is required to follow step by step the calibration process detailed in the ESC datasheet and buy an extra ESC as replacement.

These are the risk factors that can cause the biggest drawbacks during the project. However, there are more risks that need to be considered while moving forward with the prototype. For a detailed risk assessment please refer to the appendix section.

Maintenance and Operating Manual

To access the maintenance and the operating manual please refer to the appendix section.

REFERENCES

- Abudarag, Sakhr, Rashid Yagoub, Hassan Elfatih, and Zoran Filipovic. 2017. "Computational Analysis of Unmanned Aerial Vehicle (UAV)." *AIP Conference Proceedings* 1798. doi: 10.1063/1.4972593.
- Alarcón, Isabel. 2019. "El Ilaló No Cuenta Con Una Ordenanza Para Protegerlo Del Avance de La Urbanización."
- ASTM F38 Unmanned Aircraft Systems. (s.f.). Standard Specification for Design and Construction of a Small Unmanned Aircraft System (sUAS). ASTM F38 Unmanned Aircraft Systems.
- Bin Desa, Hazry, Muhamad Firdaus Bin Muhamad Dali, Mohd Zahiruddin Bin Dzulkipli, and Zul Azfar Bin Ahman. 2013. "Flying Apparatus for Aerial Agricultural Application." United States Patent and Trademark Office 1(19):9.
- Bhatnagar, Saheba, Laurence Gill, Shane Regan, Stephen Waldren, and Bidisha Ghosh. 2021. "A Nested Drone-Satellite Approach to Monitoring the Ecological Conditions of Wetlands." *ISPRS Journal of Photogrammetry and Remote Sensing* 174(January):151–65. doi: 10.1016/j.isprsjprs.2021.01.012.
- Blackstone, Michael S. 2005. "AERIAL REFORESTATION SYSTEM." 1(12):0–7.
- Burema, Harm, Salvador Bahia, and Anatholy Filin. 2016. "Aerial Farm Robot System for Crop Dusting, Planting, Fertilizing and Other Field Jobs." 2(12).
- Budynas, R., & Nisbett, K. (2014). *Shigley's Mechanical Engineering Design*. New York: McGraw Hill Education.
- Cedal. (s.f.). *Perfilería de Aluminio: Canales con Aleta*. Obtenido de CEDAL: http://www.cedal.com.ec/uploads/product/05_cedal-canales-con-aletas.pdf
- DIRECCIÓN GENERAL DE AVIACIÓN CIVIL. (2020). Resolución Nro. DGAC-DGAC-2020-0110-R. Quito: DIRECCIÓN GENERAL DE AVIACIÓN CIVIL.
- González, M. (21 de December de 2021). *Motores para Drones: Selecciona el Mejor Motor para tu Cuadricóptero*. Obtenido de Wondershare Filmora: <https://filmora.wondershare.es/drones/drone-motors.html>
- Hearn, E. (1997). Chapter 7 - Circular Plates and Diaphragms. En E. Hearn, *Mechanics of Materials 2* (págs. Pages 193-219). London: Butterworth-Heinemann. doi:<https://doi.org/10.1016/B978-075063266-9/50008-1>.
- IEE Standards Association. (s.f.). 1399.1 – Standard for a Framework for Structuring Low Altitude Airspace for Unmanned Aerial Vehicle (UAV) Operations. IEE Standards Association.

Pelíkan. (s.f.). Catálogo Plywood. Obtenido de Pelíkan:
<https://www.pelikano.com/catalogos/>

Staples, G. (12 de April de 2014). Propeller Static & Dynamic Thrust Calculation. Obtenido de Electricrcaircraftguy:
<https://www.electricrcaircraftguy.com/2014/04/propeller-static-dynamic-thrust-equation-background.html>

Fortes, Erico Pinheiro. 2017. “Seed Plant Drone for Reforestation.” *The Graduate Review* 2(1):13–26.

Lysych, Mikhail, Leonid Bukhtoyarov, and Denis Druchinin. 2021. “Design and Research Sowing Devices for Aerial Sowing of Forest Seeds with Uavs.” *Inventions* 6(4). doi: 10.3390/inventions6040083.

Khan, M. I., M. A. Salam, M. R. Afsar, M. N. Huda, and T. Mahmud. 2016. “Design, Fabrication and Performance Analysis of an Unmanned Aerial Vehicle.” *AIP Conference Proceedings* 1754. doi: 10.1063/1.4958448.

Purnomo, Dwi M. J., Matthew Bonner, Samaneh Moafi, and Guillermo Rein. 2021. “Using Cellular Automata to Simulate Field-Scale Flaming and Smouldering Wildfires in Tropical Peatlands.” *Proceedings of the Combustion Institute* 38(3):5119–27. doi: 10.1016/j.proci.2020.08.052.

Felismina, Raimundo, Miguel Silva, Artur Mateus, and Cândida Malça. 2017. “Study on the Aerodynamic Behavior of a UAV with an Applied Seeder for Agricultural Practices.” *AIP Conference Proceedings* 1836(June). doi: 10.1063/1.4981989.

Mohan, Midhun, Gabriella Richardson, Gopika Gopan, Matthew Mehdi Aghai, Shaurya Bajaj, G. A. Pabodh. Galgamuwa, Mikko Vastaranta, Pavithra S. Pitump. Arachchige, Lot Amorós, Ana Paula Dalla Corte, Sergio De-miguel, Rodrigo Vieira Leite, Mahlatse Kganyago, Eben North Broadbent, Willie Doaemo, Mohammed Abdullah Bin Shorab, and Adrian Cardil. 2021. “Uav-supported Forest Regeneration: Current Trends, Challenges and Implications.” *Remote Sensing* 13(13):1–31. doi: 10.3390/rs13132596.

Marzuki, Omar Faruqi, Ellie Yi, L. I. H. Teo, Azmin Shakrine, and Mohd Rafie. 2021. “The Mechanism of Drone Seeding Technology : A Review.” *The Malaysian Forester* 84(2):349–58.

Sarker, Md Samad, Shoyon Panday, Md Rasel, Md Abdus Salam, Kh Md Faisal, and Tanzimul Hasan Farabi. 2017. “Detail Design of Empennage of an Unmanned Aerial Vehicle.” *AIP Conference Proceedings* 1919. doi: 10.1063/1.5018551.

Horton, Christopher V., and Samuel R. Vorpahl. 2017. “Agricultural Drone For Use In Livestock Feeding.” 1(19):1–16.

Yamunathangam, D., J. Shanmathi, R. Caviya, and G. Saranya. 2020. “Payload Manipulation for Seed Sowing Unmanned Aerial Vehicle through Interface with Pixhawk Flight Controller.” *Proceedings of the 4th International Conference on Inventive Systems and Control, ICISC 2020 (Icisc):931–34*. doi: 10.1109/ICISC47916.2020.9171148.

Weir, John R., Terrence G. Bidwell, Russell Stevens, and John Mustain. n.d. "Firebreaks for Prescribed Burning." Oklahoma Cooperative Extension Service.

Mohan, Midhun, Gabriella Richardson, Gopika Gopan, Matthew Mehdi Aghai, Shaurya Bajaj, G. A. Pabodh. Galgamuwa, Mikko Vastaranta, Pavithra S. Pitump. Arachchige, Lot Amorós, Ana Paula Dalla Corte, Sergio De-miguel, Rodrigo Vieira Leite, Mahlatse Kganyago, Eben North Broadbent, Willie Doaemo, Mohammed Abdullah Bin Shorab, and Adrian Cardil. 2021. "Uav-supported Forest Regeneration: Current Trends, Challenges and Implications." *Remote Sensing* 13(13):1–30. doi: 10.3390/rs13132596.

Wang, Jian, Rui Jia, Jing Liang, Chen She, and Yi Peng Xu. 2021. "Evaluation of a Small Drone Performance Using Fuel Cell and Battery; Constraint and Mission Analyzes." *Energy Reports* 7:9108–21. doi: 10.1016/j.egy.2021.11.225.

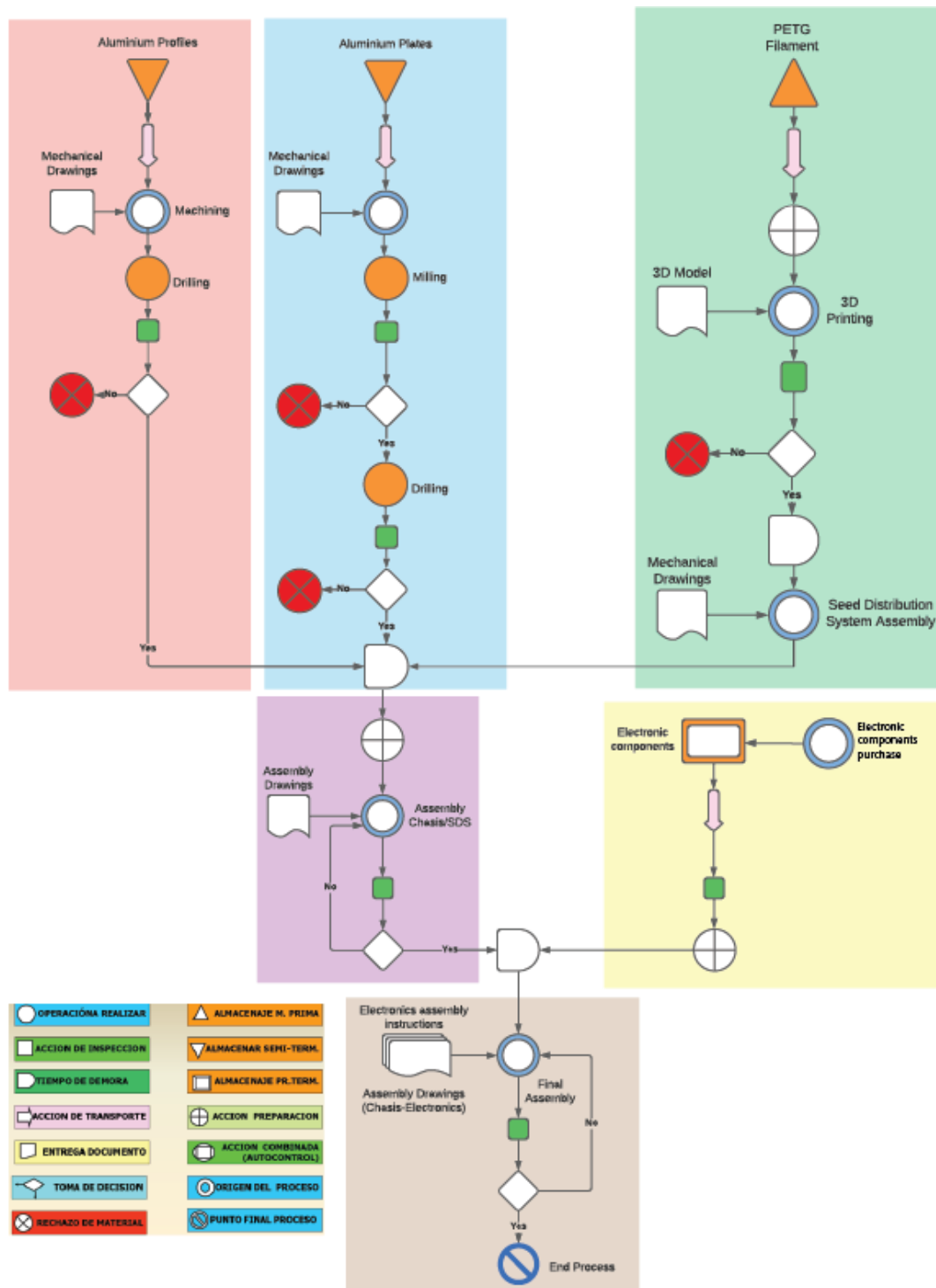
Guilmartin, John F. 2020. "Unmanned Aerial Vehicle | Definition, History, Types, & Facts | Britannica." Retrieved February 2, 2022 (<https://www.britannica.com/technology/unmanned-aerial-vehicle>).

Curipoma, Santiago. 2015. "PONTIFICIA UNIVERSIDAD CATÓLICA DEL ECUADOR FACULTAD DE CIENCIAS EXACTAS Y NATURALES ESCUELA DE CIENCIAS BIOLÓGICAS." Pontificia Universidad Católica del Ecuador.

Narayanan, Ram Gopal Lakshmi, and Oliver C. Ibe. 2015. "Joint Network for Disaster Relief and Search and Rescue Network Operations." *Wireless Public Safety Networks 1: Overview and Challenges* 163–93. doi: 10.1016/B978-1-78548-022-5.50006-6.

APENDIXES

Manufacture flow diagram



Risk Analysis

Table 11: Risk Assessment.

Code	Description	Priority	Responsible	Solution	Status	Observations
T-001	Obstruction of the seed distribution system	15	Mateo González	Build strong projectiles	Ongoing	
T-002	Poor weight distribution	8	Mateo González	Place the heaviest load in the center of the structure	Completed	
T-003	General drone short circuit	20	Mateo González	Protect the Electric Circuit	Completed	Check the connections before plug in the batteries
T-004	Frame manufacturing difficulties	9	Mateo González	Choose easy fabrication materials, outsource manufacture process	Completed	
T-005	Motor Failure	10	Gabriel Gómez	Research multiple options and select the best suited one and buy an extra motor as replacement	Completed	Higher investment
T-006	ESC Calibration Failure	20	Gabriel Gómez	Follow step by step the calibration process detailed in the ESC datasheet and buy an extra ESC as replacement	Completed	Control the calibration process and detail every step in the user's manual
T-007	Incompatible components	15	Gabriel Gómez	Research the components available in the market and follow the supplier's recommendations	Completed	May have a higher cost to follow the supplier's recommendations
T-008	Frame Mechanical Failure	10	Gabriel Gómez	Perform stress calculations with a safety factor of 2 and corroborate the results with simulations	Completed	More weight and higher costs
T-009	Aerodynamic Failure	15	Mateo Ormaza	Perform aerodynamic lift, drag calculations, and prove the	Completed	

				results with CFD simulations		
C-001	Delay in delivery of components	25	Mateo Ormaza	verify that the supplier is trustworthy and order in anticipation	Completed	
L-001	Incapability to fly the drone because of the Ecuadorian aviation regulatory frame	10	Nicolas Herrera	Perform deep research and acquire all the necessary permits for the flight of the drone.	Ongoing	It might be beneficial to speak to a lawyer about the matter
E-001	The client does not hand out the agreed budget	4	Nicolas Herrera	Deliver a complete list of components to the client with enough time for him to analyze and validate.	Completed	
O-001	Lack of experience in UAV flight	15	Nicolas Herrera	Find an expert in drone flight and let that person have control	Ongoing	
S-001	Accidents while building or operating the drone	15	Mateo Ormaza	Have all necessary precautions while building and managing the drone	Ongoing	Have the drone in a secure location to avoid accidents
RM-001	Mishandling of any component	15	Nicolas Herrera	Carefully read the manuals and datasheets of every component	Completed	

UAV SEED DISTRIBUTOR INSTRUCTION MANUAL

Universidad San Francisco de Quito

Nicolás Herrera, Mateo González, Gabriel Gómez, Mateo Ormaza Quito, Ecuador

UAV SEED DISTRIBUTOR INSTRUCTION MANUAL

i *Read this manual thoroughly to ensure correct use of the device. Save this for future reference in use.*

Universidad San Francisco de Quito

Nicolás Herrera, Mateo González, Gabriel Gómez, Mateo Ormaza
Quito, Ecuador

SAFETY PRECAUTIONS

Precautions in this instruction manual are defined as follows.

1. Before turning on the drone, check that all components are connected correctly
2. Only fly the drone in open areas.
- ▲ CAUTION!** 3. The operator must be at a safe distance and wear proper protective equipment to avoid accidents.
4. Do not stand between the propellers while the drone is armed.
- ▲ CAUTION!** 5. **!! Do not touch for any reason the propellers while they are in movement !!**
6. To charge the batteries use the appropriate charger to avoid damage.

To prevent the UAV from crashing it is recommended to hire a professional drone pilot

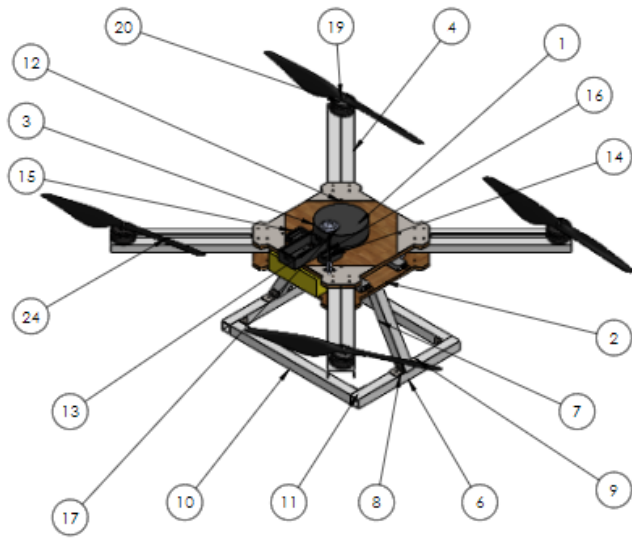
Contents

List of components and names of units.....	5
Motors	5
ELECTRONIC SPEED CONTROLLER (ESC)	7
FLIGHT CONTROLLER (PIXHAWK 5x).....	8
TELEMETRIE RADIO V3	9
PROPELLER 22 X 5.5.....	9
FUTABA RADIO CONTROL.....	10
BATTERIES (Liperior 16000 mAh 6s)	11
SEED DISTRIBUTOR	12
Electric installation.....	14
Software installation	15
Armed of the drone.....	16
Controls.....	19
SEED DISTRIBUTION SYSTEM ACTIVATION	20
Led/Buzzer meanings	20
Mission Planning	22
REFERENCES	24

Figure 1: drone parts.....	5
Figure 2: drawing of the brushless motor and its accessories. (SunnySkyUSA, 2022).....	6
Figure 3: ESC drawings. (Flycolor, 2022).....	7
Figure 4: Pixhawk 5x wiring sample guide. (Holybro, 2022).....	8
Figure 5: product description. (Holybro, SiK Telemetry Radio V3 Quick Start Guide Overview , 2018).....	9
Figure 6: drone propellers (CW and CCW).....	9
Figure 7: Futaba radio control switches assignments. (Futaba, 2012).....	10
Figure 8: Futaba radio controller receiver connections. (Futaba, 2012).....	11
Figure 9: 16000 mAh 6s battery.....	11
Figure 10: seed distributor parts.....	12
Figure 11: Overall drone orientation.....	13
Figure 12: electric connections for the drone.....	14
Figure 13: seed distributor system scheme.....	15
Figure 14: Mission Planner interface.....	16
Figure 15: second step to set up the flight board.....	17
Figure 16: uploading mandatory Firmware.....	17
Figure 17: finally step for fly board connection.....	18
Figure 18: basic drone dynamics (Gopalakrishnan, 2017).....	19
Figure 19: Led menings.....	22
Figure 20: mission planning interface.....	23

LIST OF COMPONENTS AND NAMES OF UNITS

i The following components are included in the package



ITEM NO.	PART NUMBER	DESCRIPTION	QTY.
1	Top UAV frame plate		1
2	Bottom UAV frame plate		1
3	Container		1
4	UAV arm		4
5	Spacer		4
6	Leg base		2
7	Leg		2
8	Leg support 2		4
9	Leg support		4
10	Leg Base 2		2
11	Support base		4
12	Steel plate		4
13	Pixhawk 5x		1
14	RC receiver		1
15	Telemetry Radio		1
16	GPS MOD_L_SKELET_STEP		1
17	GPS M8N_STEP		1
18	Power Distribution Board		1
19	Prop.step		4
20	Cratop.step		4
21	Caja circuito control stepper		1
22	Battery		2
23	Flycolor_ESC_80A_HobbyWing		4
24	Propeller 2255		4
25	Power Module		1

Figure 1: drone parts

Motors

i Four SunnySky X6215S 170KV High Power Brushless motor units are included with their correspondent accessories

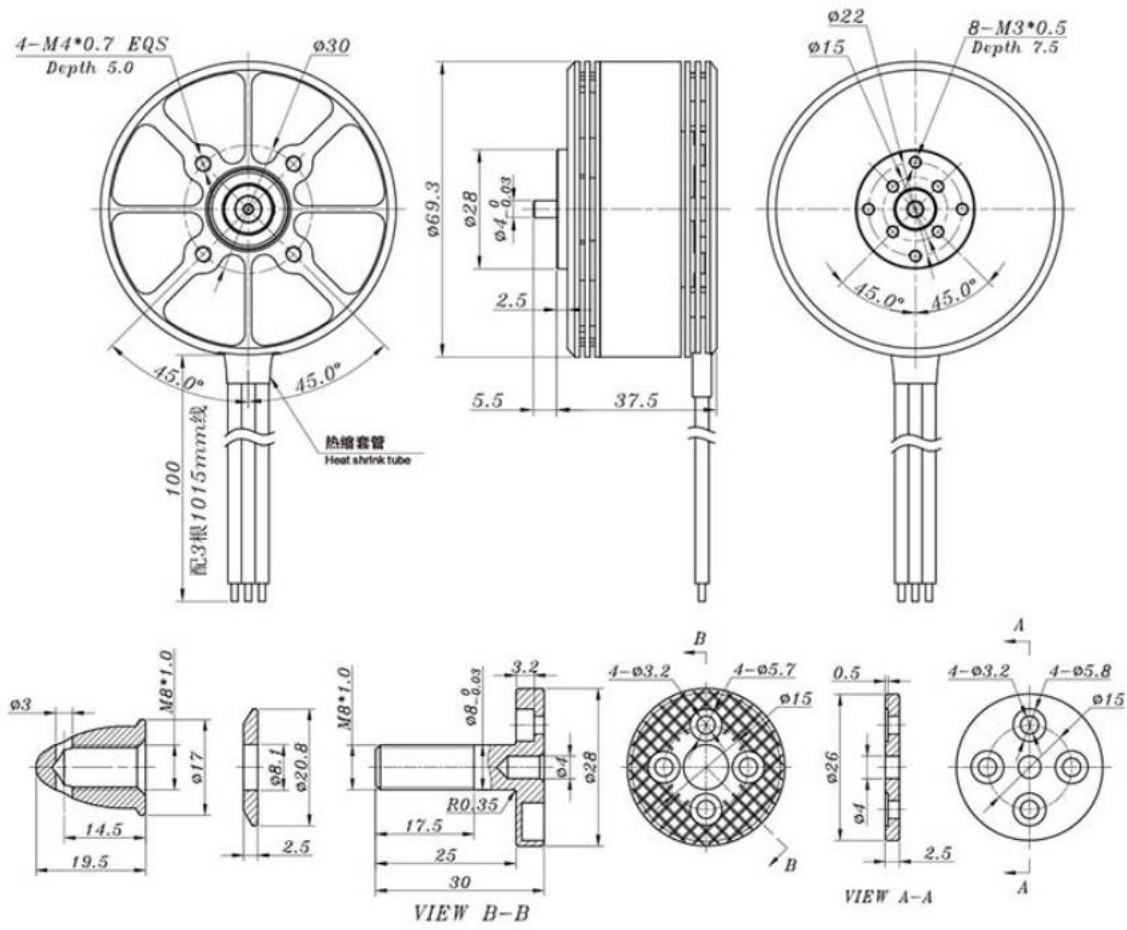


Figure 2: drawing of the brushless motor and its accessories. (SunnySkyUSA, 2022)

ELECTRONIC SPEED CONTROLLER (ESC)

i Four ESC are included.

NOTE: the plug-ins between the motor an ESC are not included

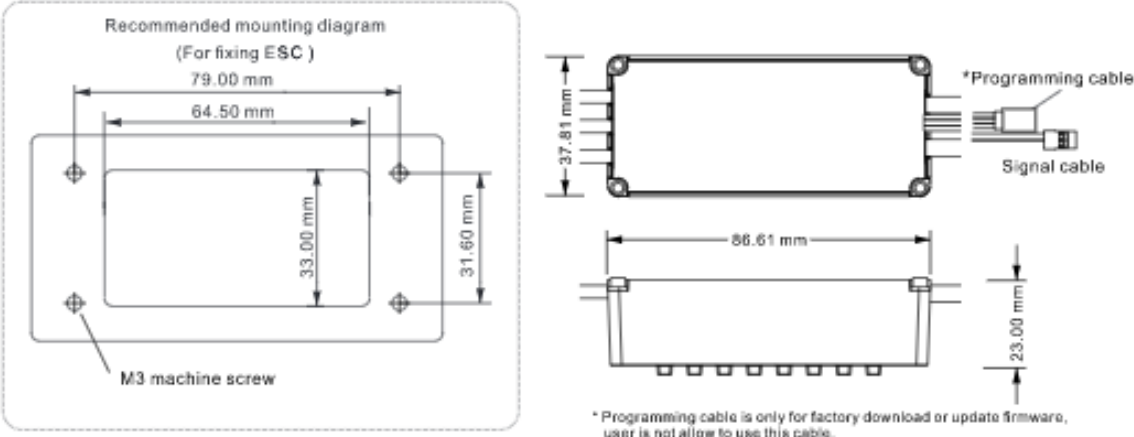


Figure 3: ESC drawings. (Flycolor, 2022)

TELEMETRIE RADIO V3

i SiK telemetry radio allows user to connect and monitor the flight of the UAV from the distance.

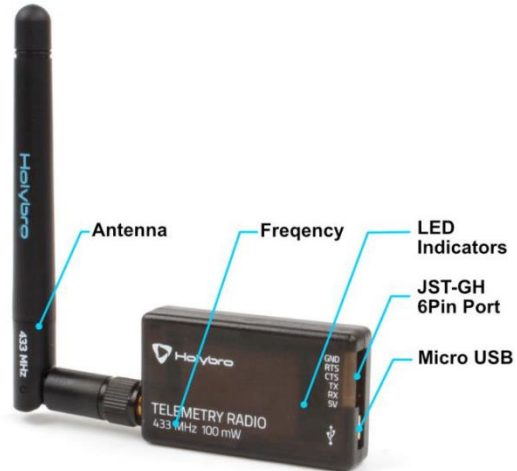


Figure 5: product description. (Holybro, SiK Telemetry Radio V3 Quick Start Guide Overview , 2018)

PROPELLER 22 X 5.5

i The package includes 2 pairs of propellers. A pair refers to a CW and CCW propellers. The propellers have a dimension of 22 in wingspan and 5.5 in pitch. The material is carbon fiber.



Figure 6: drone propellers (CW and CCW)

FUTABA RADIO CONTROL

i The radio control includes the radio receive. The following images shows the default switches assignments and connections

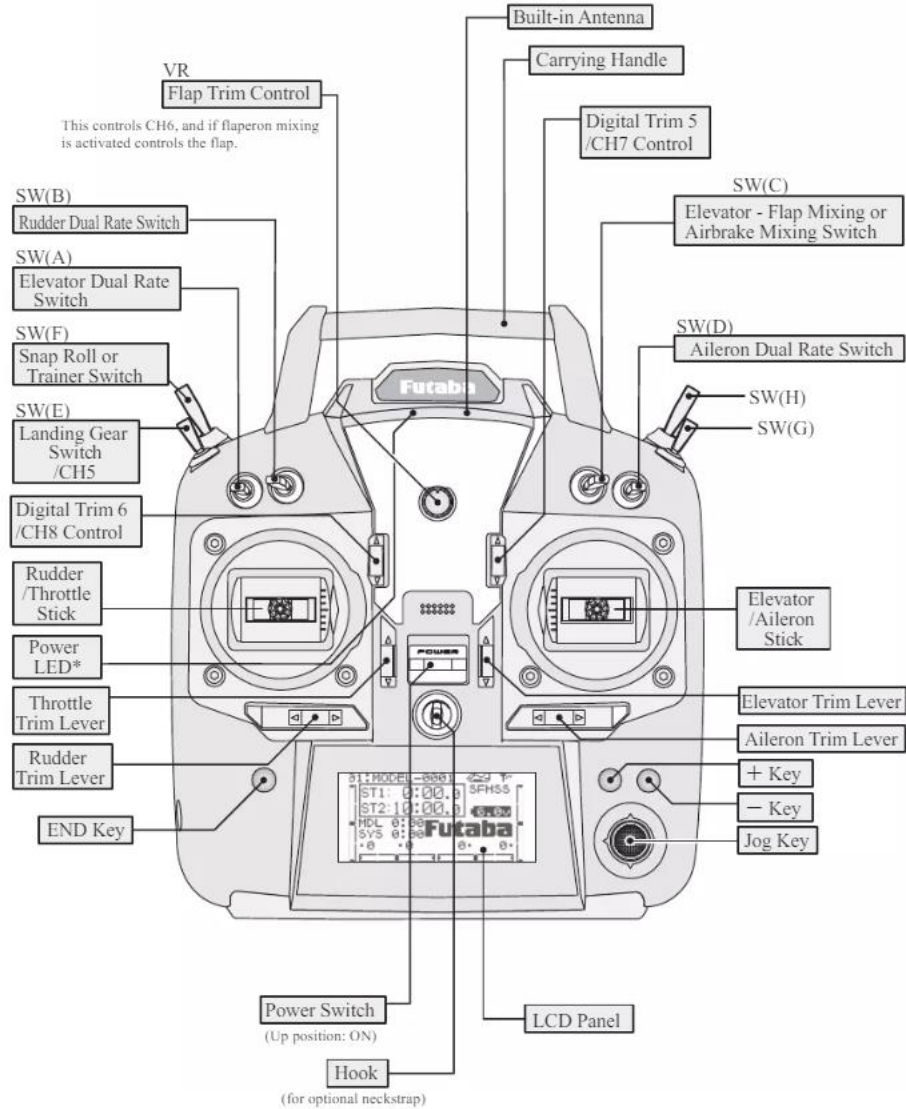


Figure 7: Futaba radio control switches assignments. (Futaba, 2012)

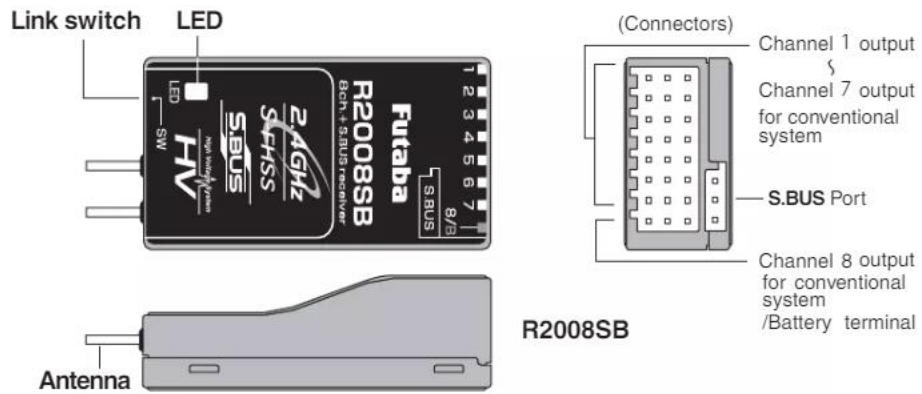


Figure 8: Futaba radio controller receiver connections. (Futaba, 2012)

BATTERIES (Liperior 16000 mAh 6s)

i NOTE: The necessary batteries are two LiPo 6S 1600 mAh connected in series. Two of them are necessary because the motors need 44.4 V. Each battery will supply 22.2 V.



Figure 9: 16000 mAh 6s battery

SEED DISTRIBUTOR

i NOTE: The distribution system is considered as an independent component. It has its own electrical circuit and an external power.

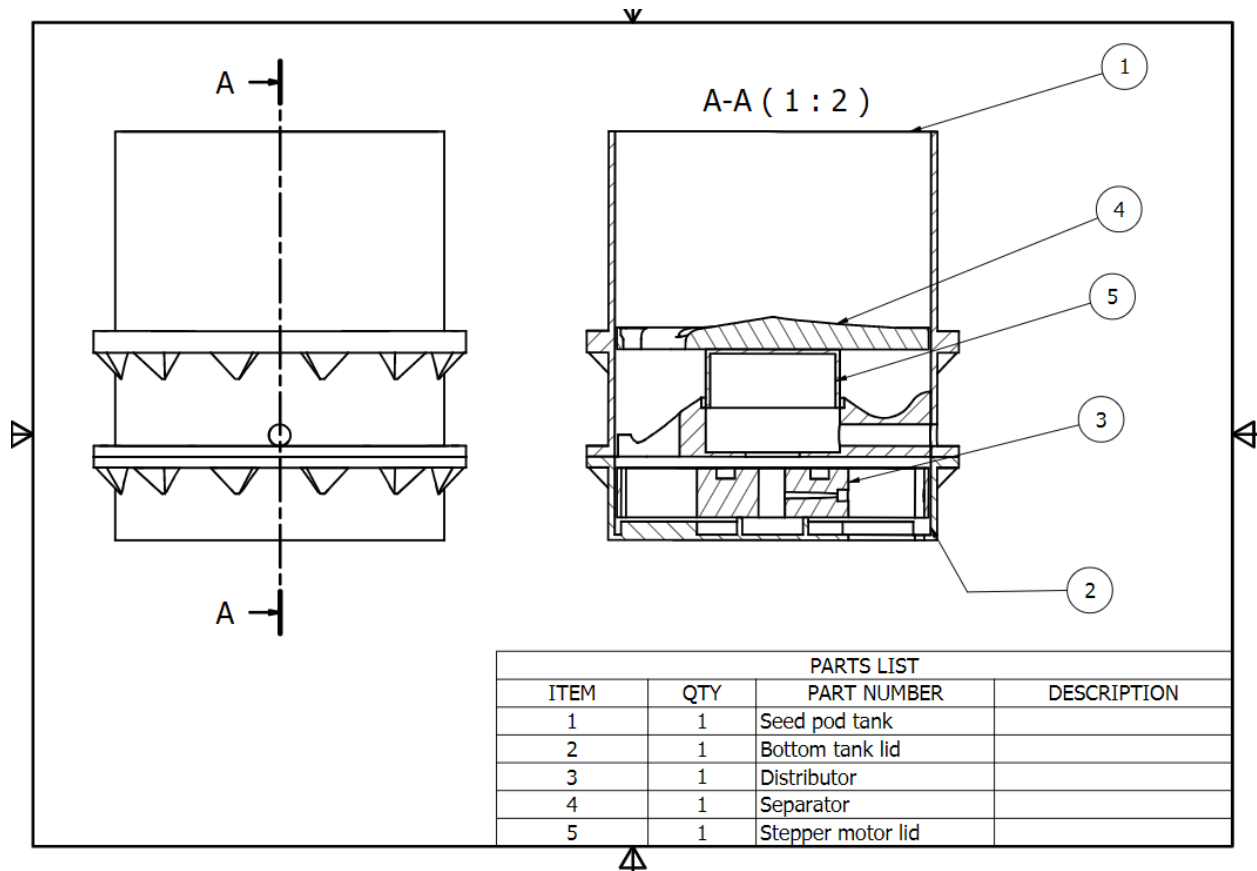


Figure 10: seed distributor parts

Installation and initiation

The following image shows the orientation of the drone. Specifically, the orientation that the flight board (Pixhawk 5x) and the GPS must have, as well shows the orientation that the propellers should have.

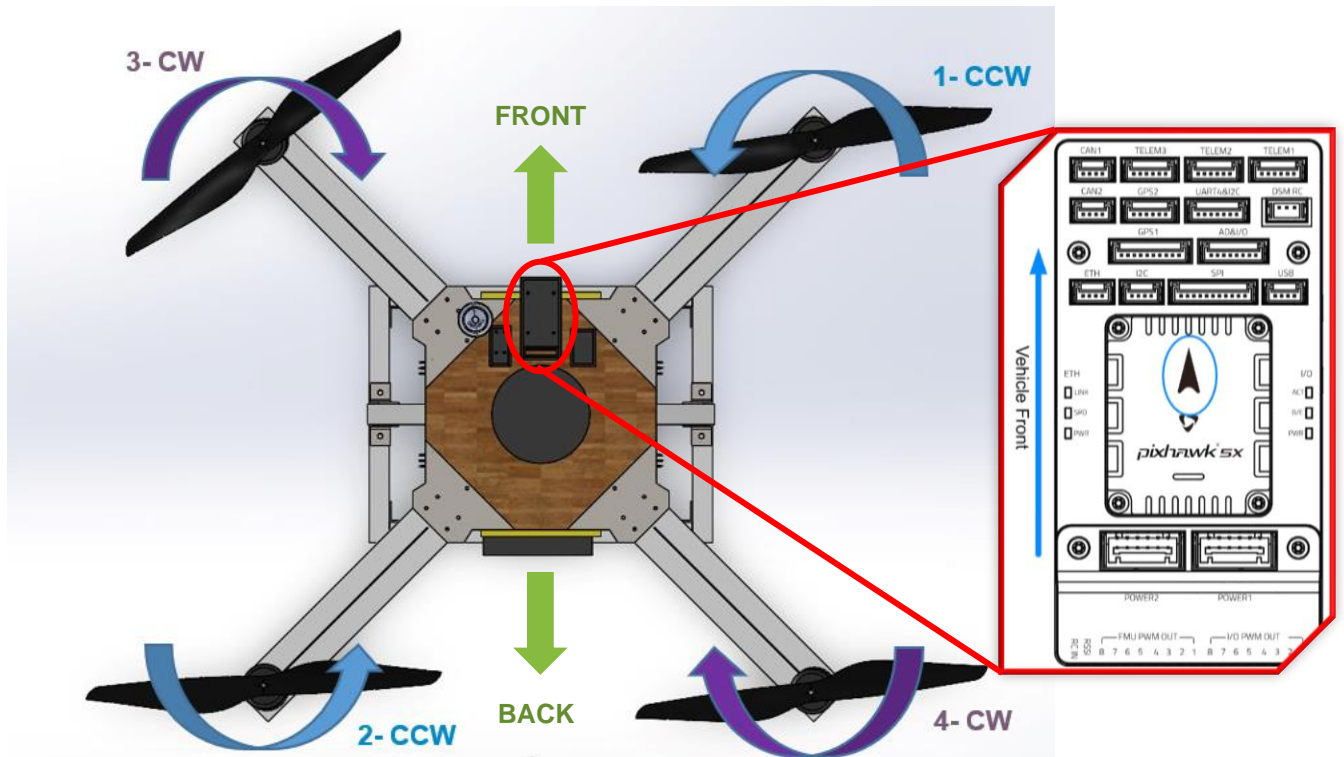


Figure 11: Overall drone orientation

Electric installation

The following image shows how the electric installation for the motors, ESC, Pixhawk and all the accessories should be connected.

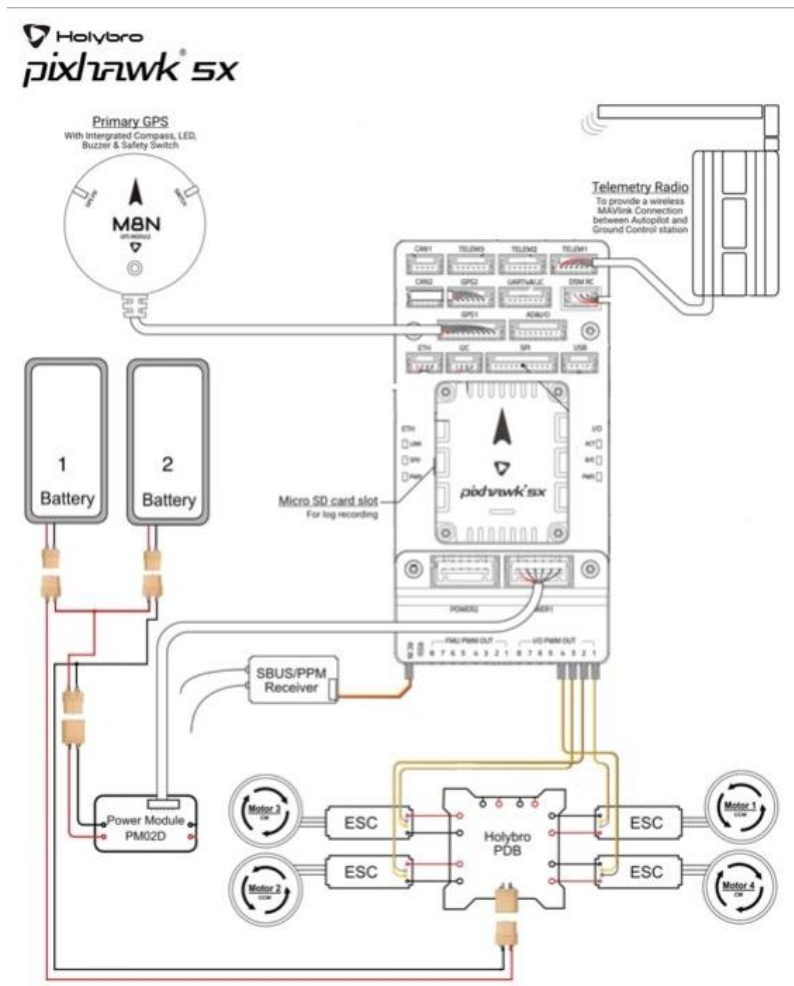


Figure 12: electric connections for the drone

i NOTE: To turn on the drone, it is necessary to follow the next steps to ensure that the operation of the aircraft is optimal.

1. Connect the battery located at the back of the drone first
2. Connect the second battery (front battery) y second place.

At the time both batteries are connected a beep in all the motors, as well as sounds and lights in the GPS should be heard. If this does not happen, check the connections at the ESC, Motors and Pixhawk.

i ATTENTION!!: If any connection needs to be changed, disconnect both batteries first.

For the seed distribution system, the following electrical scheme is presented

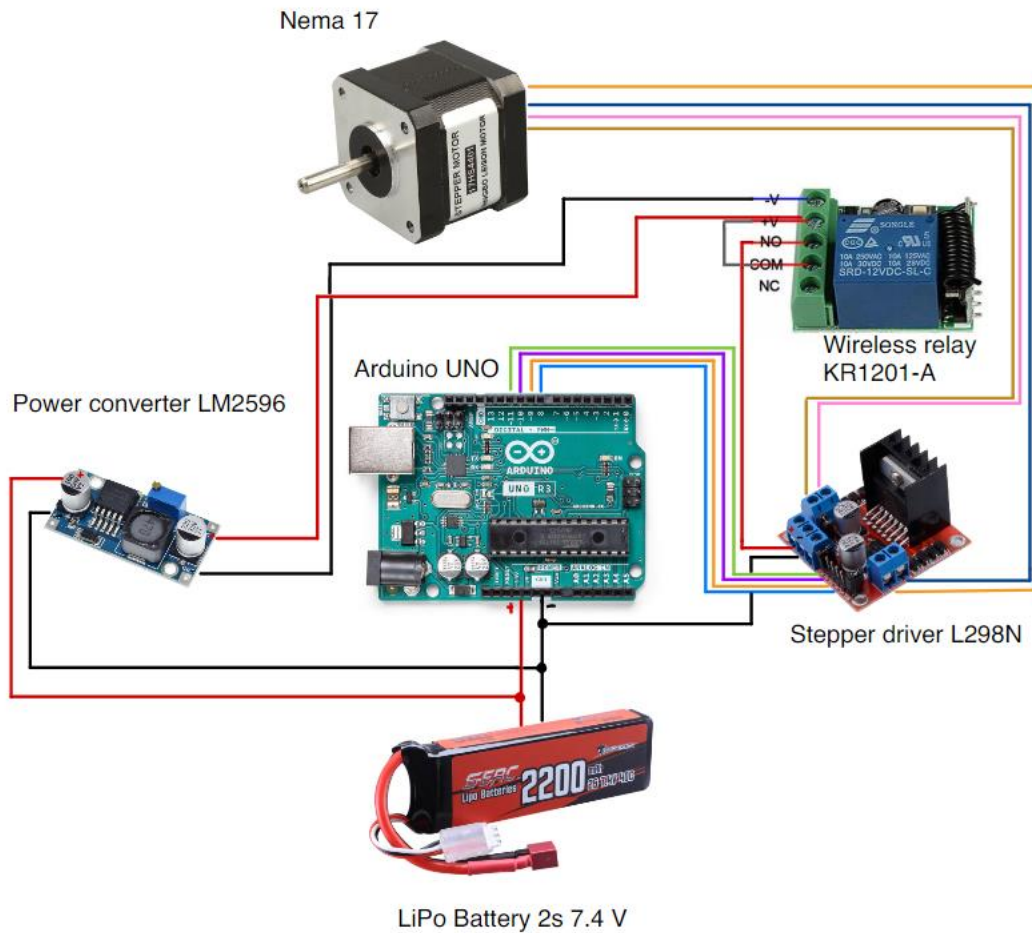


Figure 13: seed distributor system scheme

Software installation

To be able to control the flight board, the installation of a program compatible with the Pixhawk is required. the recommended program to use is called Mission Planner. This program allows the user to calibrate the ESC, the radio control, and the motors. It also allows to generate automatic flight routes. In addition, it allows, through the use of telemetry, to monitor parameters such as battery consumption, speeds (in all axes), inclination angles (in all axes), altitude, among others.

i NOTE: Mission Planner is an interface program power by Ardupilot. Any other software that is compatible and includes Ardupilot can be used.

i NOTE: to download the software consult the official site of Ardupilot.



Figure 14: Mission Planner interface

Armed of the drone

i In order to activate the drone, it is necessary to follow the following steps.

1. Connect the Pixhawk via cable or telemetry to the computer.
2. At the top of the screen go to the "Set up" tab and choose the option to install Firmware. Select "all option", at the bottom of the white bar, then in model tab select the flight board model and in firmware tab select the latest updated version of "arducopter.apj". finally click on "upload firmware".

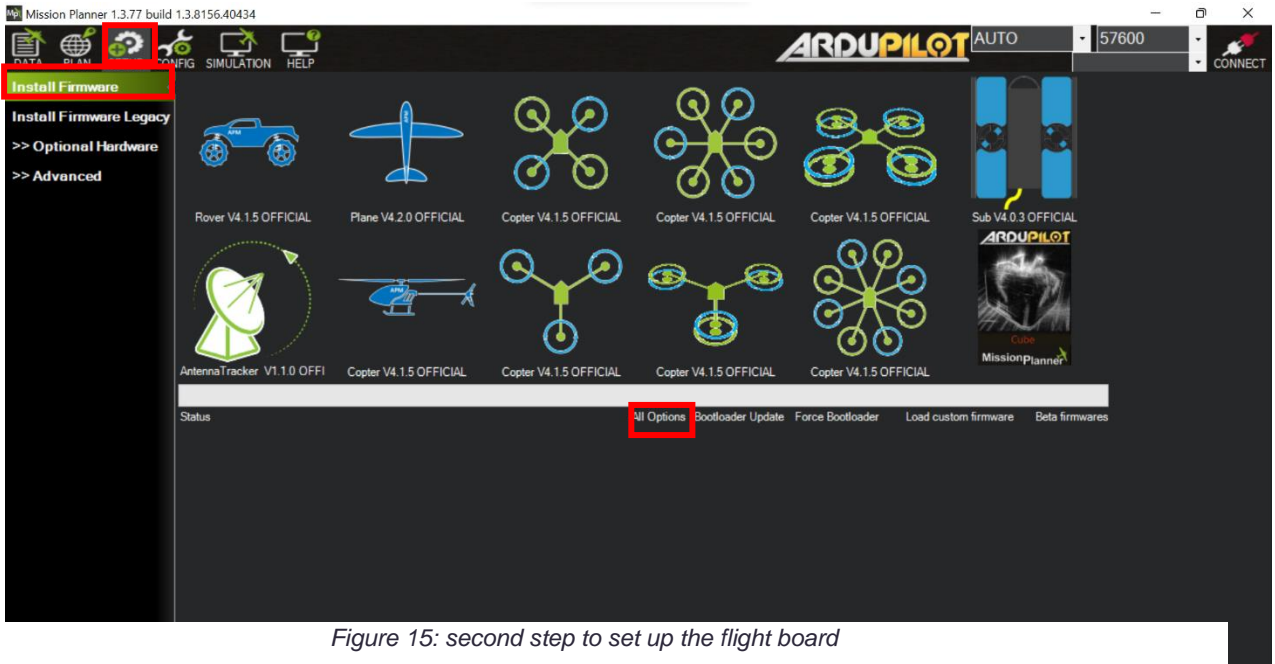


Figure 15: second step to set up the flight board

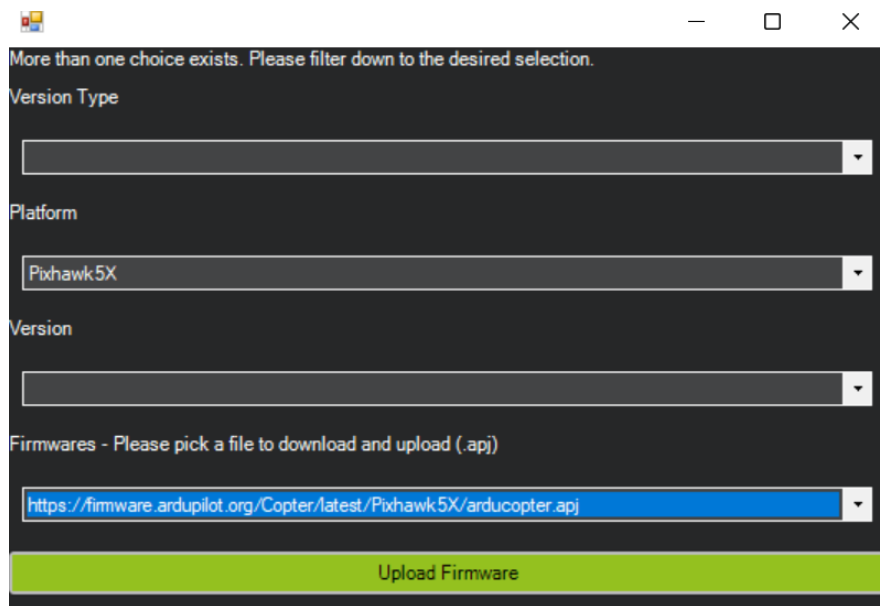


Figure 16: uploading mandatory Firmware

3. Finally click in the upper left corner on the "Connect" tab.

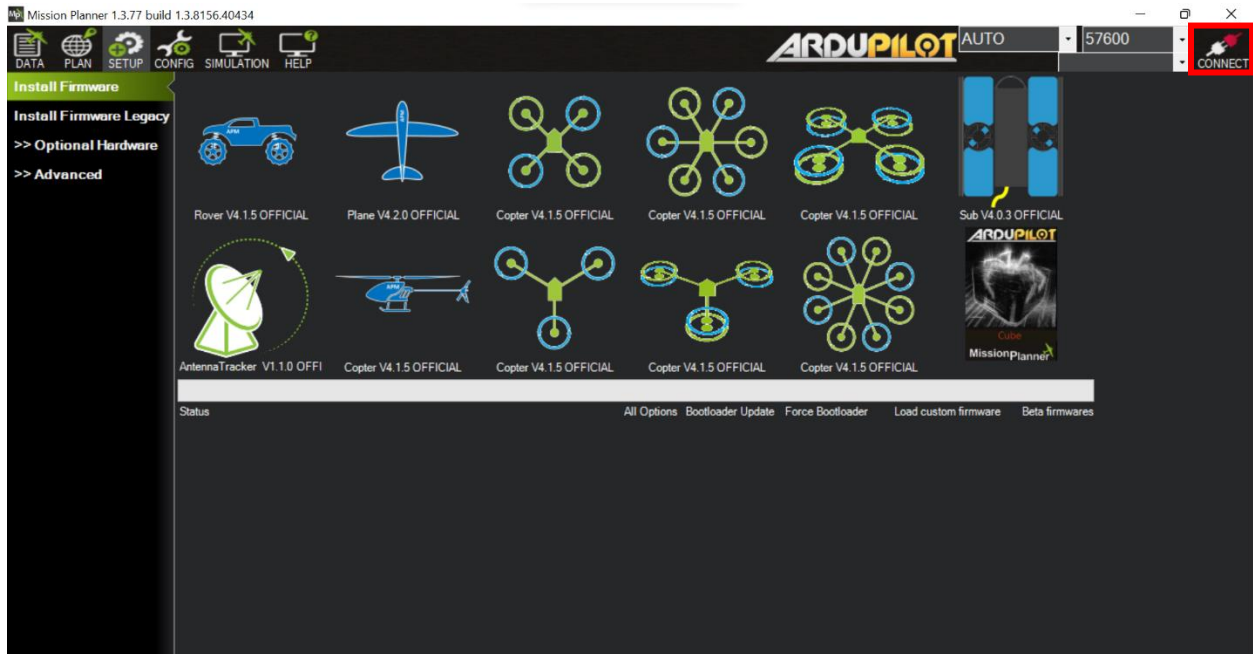


Figure 17: finally step for fly board connection.

i **NOTE:** The maintenance guide specifies in greater detail how to carry out the relevant calibration for the operation of all the components of the Drone. In the same way if it is needed further calibration, consult the official page of Ardupilot and Mission Planner.

CONTROLS

i The image below shows the basic dynamic movements to control a quadcopter in the air.

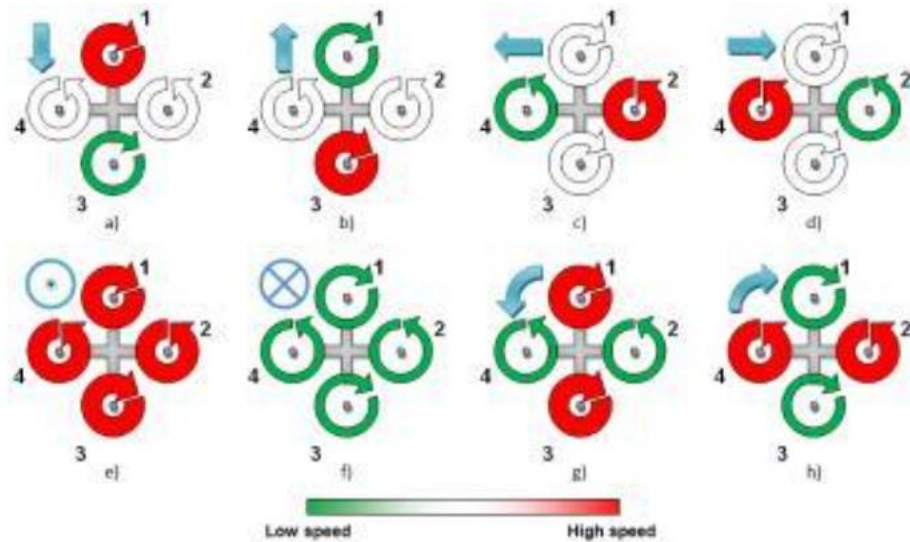
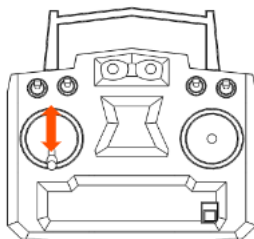


Figure 18: basic drone dynamics (Gopalakrishnan, 2017)

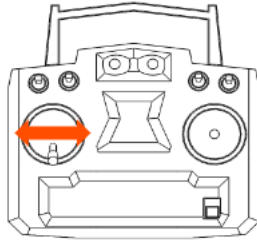
- a) and b) represent the dynamic movement called **pitch**.
- c) and d) represent the dynamic movement called **roll**.
- g) and h) represent the dynamic movement called **yaw**.
- e) represents the **downward** movement.
- f) represents the **upward** movement.

i The commands to perform the roll, pitch, yaw, up and down movements of the aircraft with the radio control are shown below. It is important to mention that regardless of the sensitivity of the control and the skill of the pilot, the stable handling of the drone can be difficult.

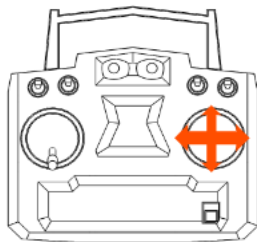
1. up/takeoff – down/land



2. Yaw



3. Roll / Pitch



Switch G (upper right part of the control) has 3 positions 3, 4 and 5:

3) LAND position

4) AUTO position

5) STABILIZE position



SEED DISTRIBUTION SYSTEM ACTIVATION

To activate the seed distribution system a secondary control must be activated. The secondary control count with only one button. One press to activate, to deactivate the system press the button again.

i *NOTE: The wireless relay has a 50 meters range*

LED/BUZZER MEANINGS

1. Flashing red and blue: Initializing gyroscopes. Hold the vehicle still and level while it initializes the sensors.

2. Flashing blue: Disarmed, no GPS lock found. Autopilot, loiter and return-to-launch modes require GPS lock.
3. Solid blue: Armed with no GPS lock
4. Flashing green: Disarmed (ready to arm), GPS lock acquired. Quick double tone when disarming from the armed state.
5. Fast Flashing green: Same as above but GPS is using SBAS (so should have better position estimate).
6. Solid green - with single long tone at time of arming: Armed, GPS lock acquired. Ready to fly!
7. Double flashing yellow: Failing pre-arm checks (system refuses to arm).
8. Single Flashing yellow: Radio failsafe activated
9. Flashing yellow - with quick beeping tone: Battery failsafe activated
10. Flashing yellow and blue - with high-high-high-low tone sequence (dah-dah-dah-doh): GPS glitch or GPS failsafe activated
11. Flashing red and yellow - with rising tone: EKF or Inertial Nav failure
12. Flashing Red, Blue and Green: Copter ESC Calibration mode entered. See Electronic Speed Controller (ESC) Calibration

13. SOS tone sequence: SD Card missing (or other SD error like bad format etc.)

Reference: <https://ardupilot.org/copter/docs/common-leds-pixhawk.html>

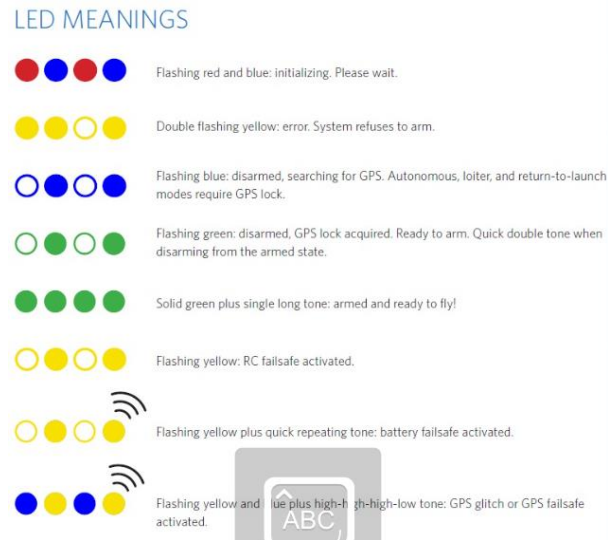


Figure 19: Led meanings

i Note: These signals were extracted directly from the official page of Ardupilot

Mission Planning

i To create and run mission it is necessary to switch the vehicle to AUTO mode.

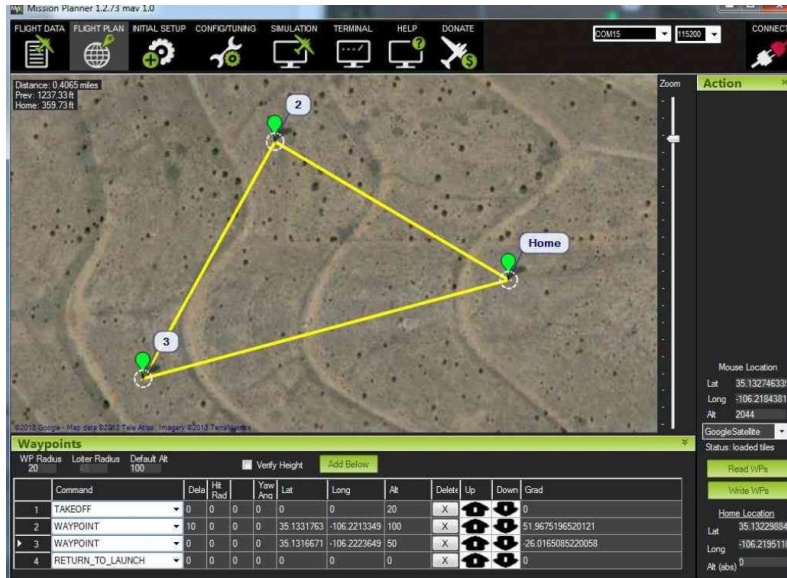


Figure 20: mission planning interface

1. Set a home point by clicking on the map screen
2. Once the starting point is chosen, a path is created by clicking where you want to generate a point (predefined patterns can be created by right clicking on the map and selecting the desired pattern)
3. The table below the map shows parameters such as height and distance which can be modified depending on what is needed
4. These paths can be saved and can be opened at any time or exported to another computer with ease.

i For more information consult the official page of ardupilot

REFERENCES

- Flycolor. (2022). *Multi-RotorBrushlessESC*. Retrieved from Flycolor: en.flycolor.net/index.php?s=member&c=api&m=file&id=1583
- Futaba. (2012). *Futaba 8J manual*. Retrieved from Manual.ec: <https://www.manual.ec/futaba/8j/manual?p=93>
- Gopalakrishnan, E. (2017). *QUADCOPTER FLIGHT MECHANICS MODEL AND CONTROL ALGORITHMS*. Retrieved from QUADCOPTER FLIGHT MECHANICS MODEL AND CONTROL ALGORITHMS: https://wiki.control.fel.cvut.cz/mediawiki/images/5/5e/Dp_2017_gopalakrishnan_eswarmurthi.pdf
- Holybro. (2018). *Sik Telemetry Radio V3 Quick Start Guide Overview* . Retrieved from Holybro: www.holybro.com/manual/Holybro_Sik_Radio_V3_Quick_Start_Guide.pdf
- Holybro. (2022). *Pixhawk 5X*. Retrieved from Holybro: <http://www.holybro.com/product/pixhawk-5x/>
- SunnySkyUSA. (2022). *SunnySky XS High Power X6215S Brushless Motors*. Retrieved from sunnyskyusa: <https://sunnyskyusa.com/products/x6215s>
- Team, A. D. (2021). *LEDs Meaning*. Retrieved from ArduPilot: <https://ardupilot.org/copter/docs/common-leds-pixhawk.html>

UAV SEED DISTRIBUTOR MAINTENANCE MANUAL

Universidad San Francisco de Quito

Nicolás Herrera, Mateo González, Gabriel Gómez, Mateo Ormaza Quito, Ecuador

UAV SEED DISTRIBUTOR MAINTENANCE MANUAL

i *Read this manual thoroughly to ensure correct maintenance of the device. Save this for future reference in use.*

Universidad San Francisco de Quito

Nicolás Herrera, Mateo González, Gabriel Gómez, Mateo Ormaza
Quito, Ecuador

SAFETY PRECAUTIONS

Precautions before any procedure in this maintenance manual are defined as follows.

1. Before turning on the drone, check that all components are connected correctly

▲ CAUTION! 2. **MAKE SURE THE DRONE IS WITHOUT PROPELLERS.**

3. Make sure to connect and disconnect the batteries in the correct order.

To prevent the UAV from irreparable damage it is recommended to contact the provider for any reparation.

Contact Information:

-
- *Gabriel Gómez:*
 - *Mateo González:*
 - *Nicolás Herrera:*
 - *Mateo Ormaza:*
-

Contents

CALIBRATION	5
ELECTRONIC SPEED CONTROLLER (ESC) CALIBRATION	5
PC AIDED CALIBRATION.....	6
Accelerometer Calibration.....	6
Compass Calibration.....	8
Radio Control Calibration.....	10
Motor Test.....	11
CLEANING	13
Motors.....	13
Electronics	13
Structure	14
WARNINGS	14

Figure Index

Figure 1: Radio Controller Example (Throttle up).....	5
Figure 2: GPS module. (Indicator LED).....	5
Figure 3: GPS module. (Safety Switch/LED).....	5
Figure 4: Radio Controller Example (Throttle down).	6
Figure 5: Mission Planer - Initial Setup.....	6
Figure 6: Mission Planer - Accelerometer Calibration key.....	7
Figure 7: Mission Planer - Calibrate Accelerator key.	7
Figure 8: Examples of Drone sides.	7
Figure 9: Mission Planer - Calibrate Level key.....	8
Figure 10: Mission Planner - Simple Accelerometer Calibration key.....	8
Figure 11: Mission Planner - Compass Key.....	9
Figure 12: Mission Planner - Compasses Recognition.....	9
Figure 13: Mission Planner - Start Compass Calibration Key.....	9
Figure 14: Mission Planner - Radio Control Key.....	10
Figure 15: Mission Planner - Calibrate Radio Key.....	10
Figure 16: Mission Planner - Radio Sticks Values.....	11
Figure 17: Mission Planner - Radio Switches Values.....	11
Figure 18: Mission Planner - Optional Hardware Key.....	11
Figure 19: Mission Planner - Motor Test Key.....	12
Figure 20: Mission Planner - Throttle and time test modification.....	12
Figure 21: Mission Planner - Test Motors (Separately).....	12
Figure 22: Mission Planner - Test all motors Key.....	13

CALIBRATION

ELECTRONIC SPEED CONTROLLER (ESC) CALIBRATION

i The ESC's must be properly mounted and connected to their motors.

i **THERE MUST BE NOT PROPELLERS ON THE DRONE BEFORE STARTING WITH THIS PROCEDURE.**

1. Disconnect the batteries (USB in case it is powering the Pixhawk 5x).
2. Turn on the radio controller and set the throttle to its maximum.



Figure 1: Radio Controller Example (Throttle up).

3. Connect the batteries.
4. The GPS light indicator should be displaying the colors red, blue, and yellow in a circular pattern.



Figure 2: GPS module. (Indicator LED)

5. Disconnect the batteries and reconnect the batteries.
6. Arm the Drone (Press the safety switch until the red light stops blinking).



Figure 3: GPS module. (Safety Switch/LED)

7. The drone will beep up to 3 times in a row. After this a long beep is going to be heard.

- Take the throttle all the way down



Figure 4: Radio Controller Example (Throttle down).

- The drone will beep twice, one long time and one short. This will mean your ESC's have been calibrated.
- Disconnect the batteries.

PC AIDED CALIBRATION

- i** For the next calibration steps, it is necessary to have the software "Mission Planner".
- i** **THERE MUST BE NOT PROPELLERS ON THE DRONE BEFORE STARTING WITH THIS PROCEDURE.**
- i** Plug in the Pixhawk to the computer and connect it to the mission planner.

Accelerometer Calibration

- Go into the 'Initial Setup' on the Mission Planner.

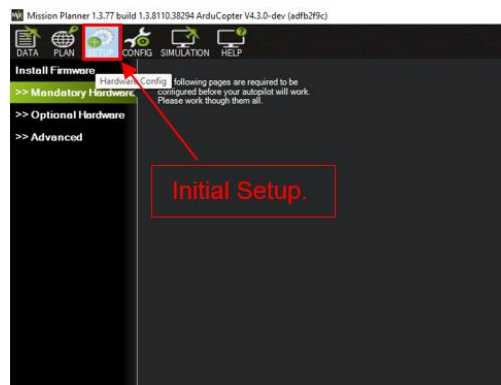


Figure 5: Mission Planer - Initial Setup.

- Go to Accelerometer Calibration (Located at the left of the mission planner).

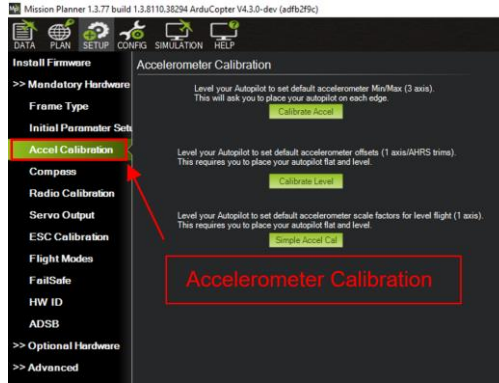


Figure 6: Mission Planer - Accelerometer Calibration key.

3. Before continuing, make sure your drone is leveled and flat.
4. Click on 'Calibrate accelerator'

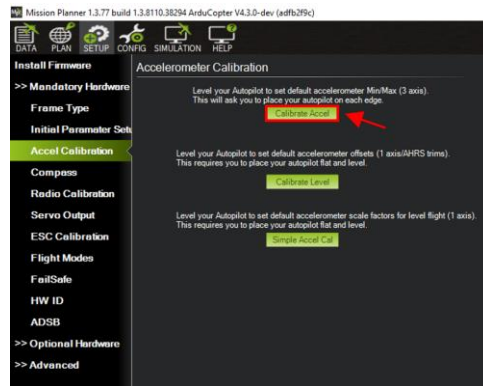


Figure 7: Mission Planer - Calibrate Accelerator key.

5. The program will ask you to place the drone in different positions.
 - a. Level.
 - b. Left Side.
 - c. Right Side.
 - d. Nose Down.
 - e. Nose up.
 - f. Back side.

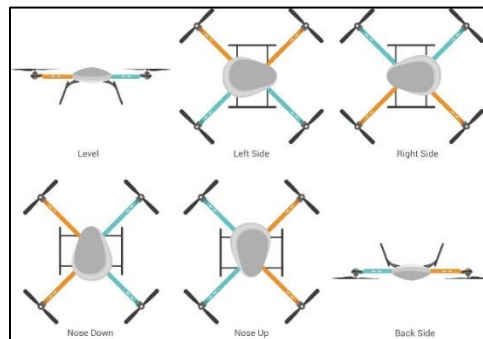


Figure 8: Examples of Drone sides.

i Make sure you place the drone as close as leveled in every axis.

i The positions will always be in relation to the point of the arrow on the Pixhawk as 'nose/front'.

- When completed place your Drone on level again.
- Press the 'Calibrate level' button.

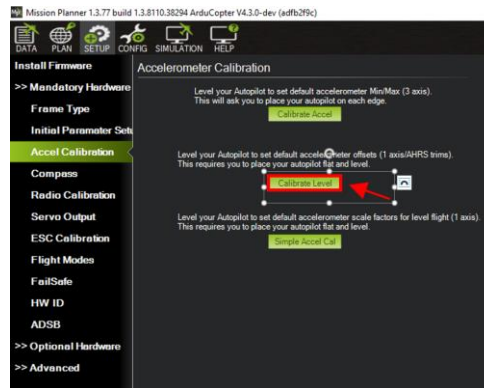


Figure 9: Mission Planner - Calibrate Level key.

- When completed press the 'Simple Accelerometer Calibration' key.

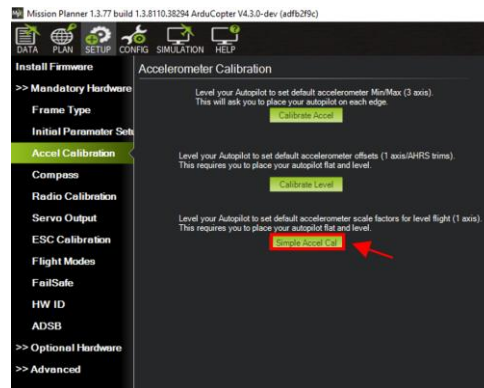


Figure 10: Mission Planner - Simple Accelerometer Calibration key

- Reboot the drone (disconnect all batteries and connect them again).

Compass Calibration

i Before starting this process, the GPS and the Pixhawk must be placed in the drone, and their arrows should be pointing to the same direction.

- Inside the 'Setup' menu go to 'Mandatory Hardware'
- Click into 'Compass' at the left side of the Mission Planner.

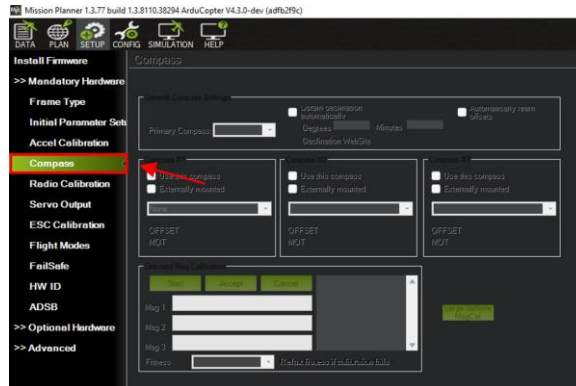


Figure 11: Mission Planner - Compass Key

- There you will see the two compasses, one from the Pixhawk and one from the mission planner.

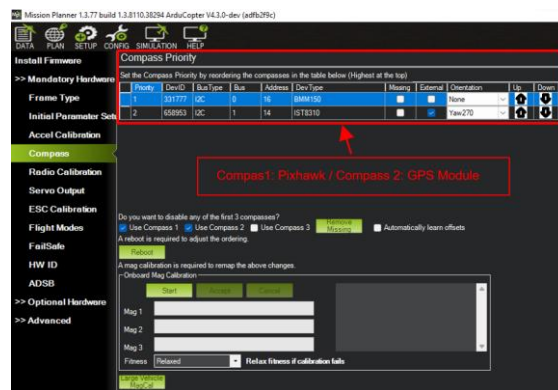


Figure 12: Mission Planner - Compasses Recognition.

- Click on 'Start' into the Onboard Mag Calibration.

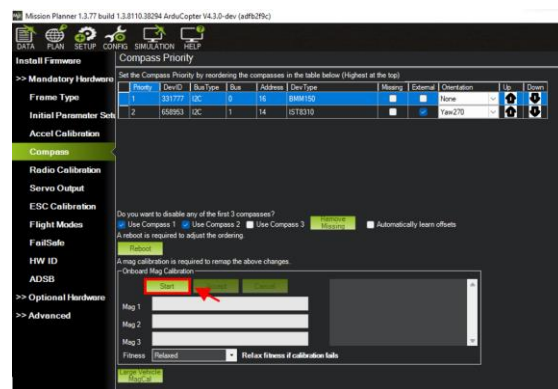


Figure 13: Mission Planner - Start Compass Calibration Key

- Start turning the drone around all the axis until the two bars ('Mag 1' and 'Mag 2') are completely full.
- The phrase 'calibration successful' should appear for both magnetometers.
- Reboot the system.

i If one or both magnetometers do not calibrate the bar will start fulling itself again. If this happens constantly, make sure both arrows are pointing to the same direction all time.

i In the worst cases one magnetometer can be removed (Remove Missing).

Radio Control Calibration

i Before starting this process make sure that the Transmitter and the receiver are on.

1. Inside the 'Setup' menu go to 'Mandatory Hardware'
2. Click into 'Radio Calibration' at the left side of the mission planner.

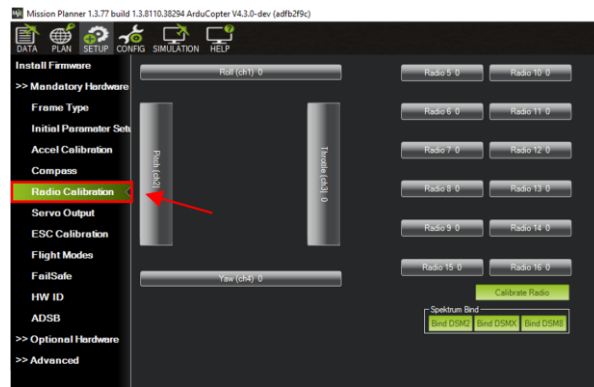


Figure 14: Mission Planner - Radio Control Key

3. Click on 'Calibrate Radio'.



Figure 15: Mission Planner - Calibrate Radio Key

4. Move all the sticks to their maximum and minimum



Figure 16: Mission Planner - Radio Sticks Values.

5. Move all the switches to all their possible positions.



Figure 17: Mission Planner - Radio Switches Values.

6. Make sure the throttle is in its minimum and all the rest sticks at the middle range.
7. Click done and reboot the system.

Motor Test

1. Inside the 'Setup' menu go to 'Optional Hardware'

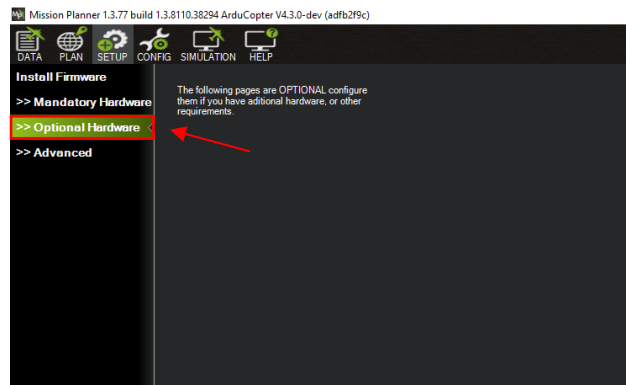


Figure 18: Mission Planner - Optional Hardware Key

2. Click into 'Motor Testing' at the left side of the mission planner.

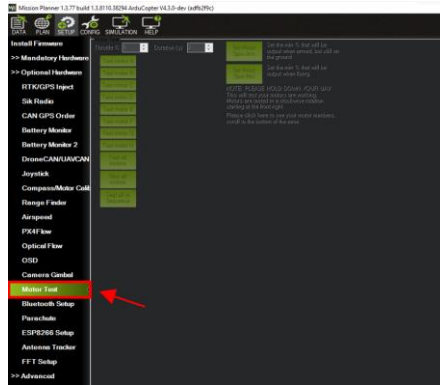


Figure 19: Mission Planner - Motor Test Key

3. Set the percentage of power and the time that you want to provide for the test.



Figure 20: Mission Planner - Throttle and time test modification

4. Test each motor separately and make sure all are turning the way they are supposed to.



Figure 21: Mission Planner - Test Motors (Separately)

i If they are not, refer to Electrical Installations in the instruction manual and change the polarities of the ESC/motor connection. For doing this the two cables of the extremes should change positions.

- When it is proved that all the motors are rotating to the correct side. Test all the motors at the same time and make sure them all are spinning at the same speed.



Figure 22: Mission Planner - Test all motors Key

i In the case they are not spinning at the same speed the ESC calibration should be made again.

CLEANING

i Before starting the cleaning process, make sure NO batteries are connected.

Motors

i Remove the propellers from the motors.

i Disconnect the motors from the ESC's.

i Detach the motors from the arms by removing the screws under them.

- With the help of a compressed air gun start blowing all the dirt from the motor.
- If there are solids at the sides after using the compressed air, remove them with the help of a thin blade.
- Repeat these steps until the motors are totally clean.

i If after repeating these process a couple of time, the motor is still not spinning normally. Please contact your provider.

Electronics

- Remove the lids of each component box.
- With the help of a compressed air gun blow all the electronics and connections.

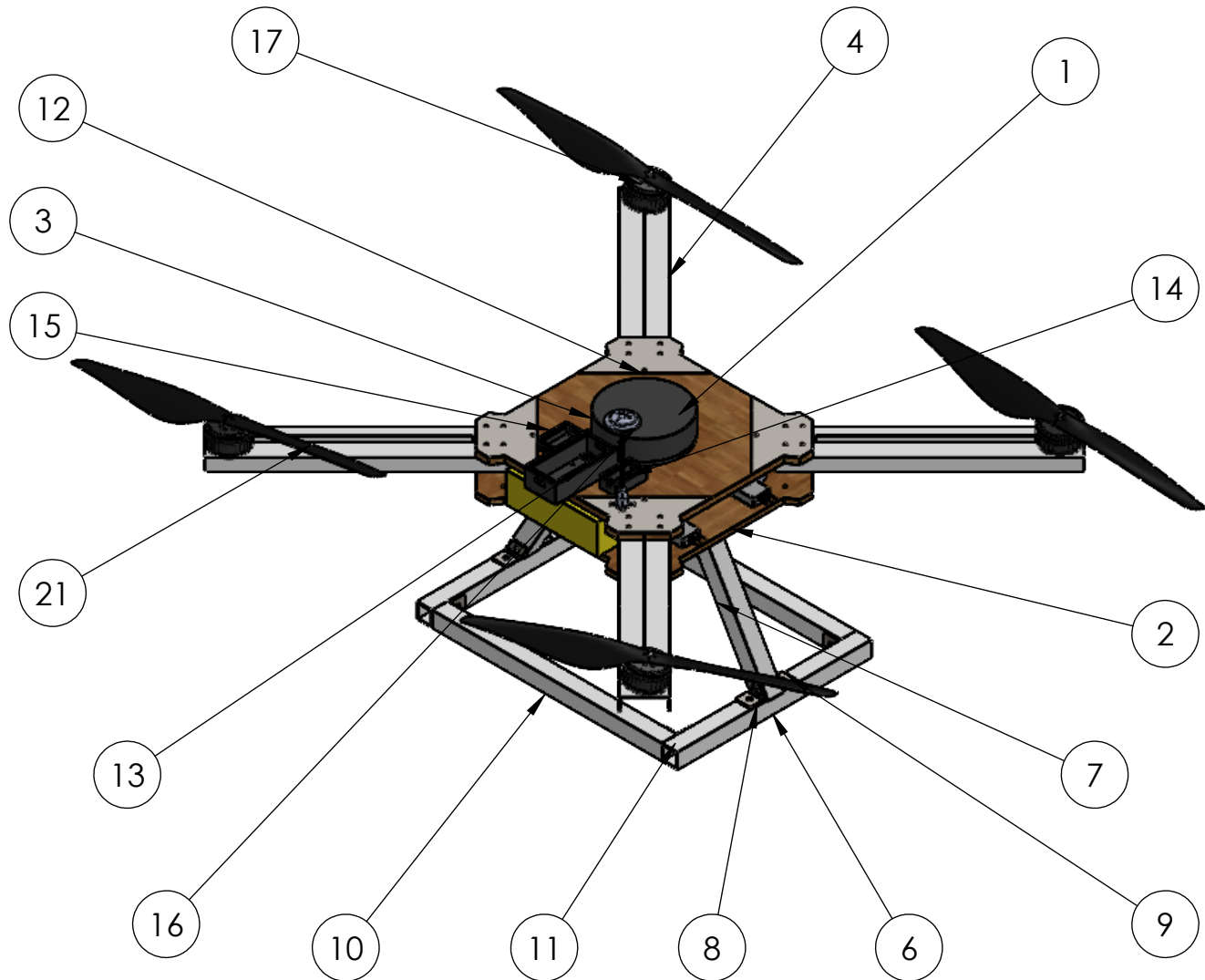
i Make sure there are no solid particles in the connection slots.

Structure

- i** *For the rest of the structure also use the compressed air gun.*
- i** *After blowing the most of dirt away, use a wipe with water and clean the structure.*

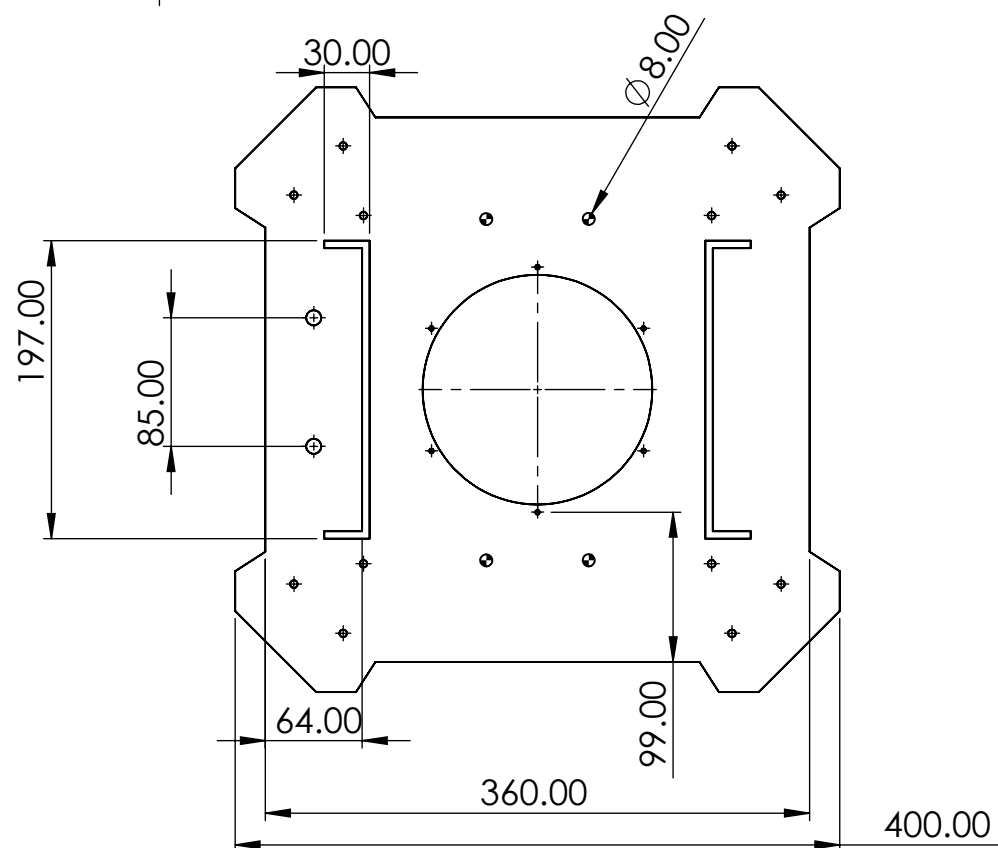
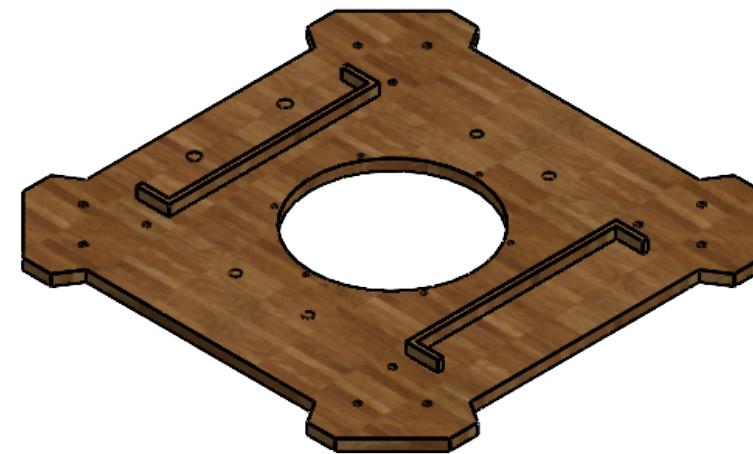
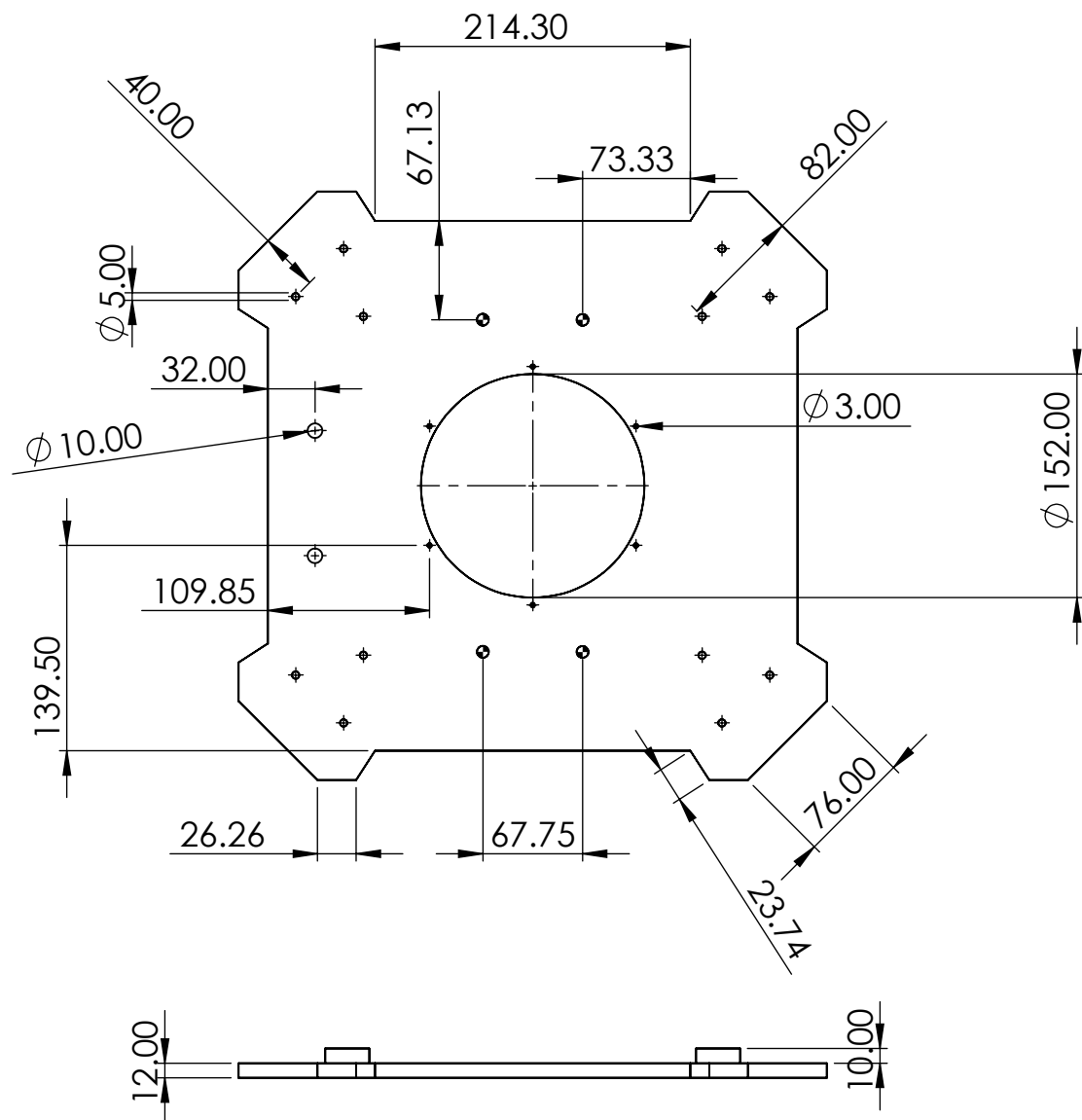
WARNINGS

- i** *If there are any damaged parts, contact your provider.*
- i** *Do not attempt to disassemble the structure.*
- i** *If any electronic does not respond as it should please contact the provider.*
- i** *In case of fire, caused by the electronics/batteries. Do not attempt to reconnect the drone again and contact the provider.*

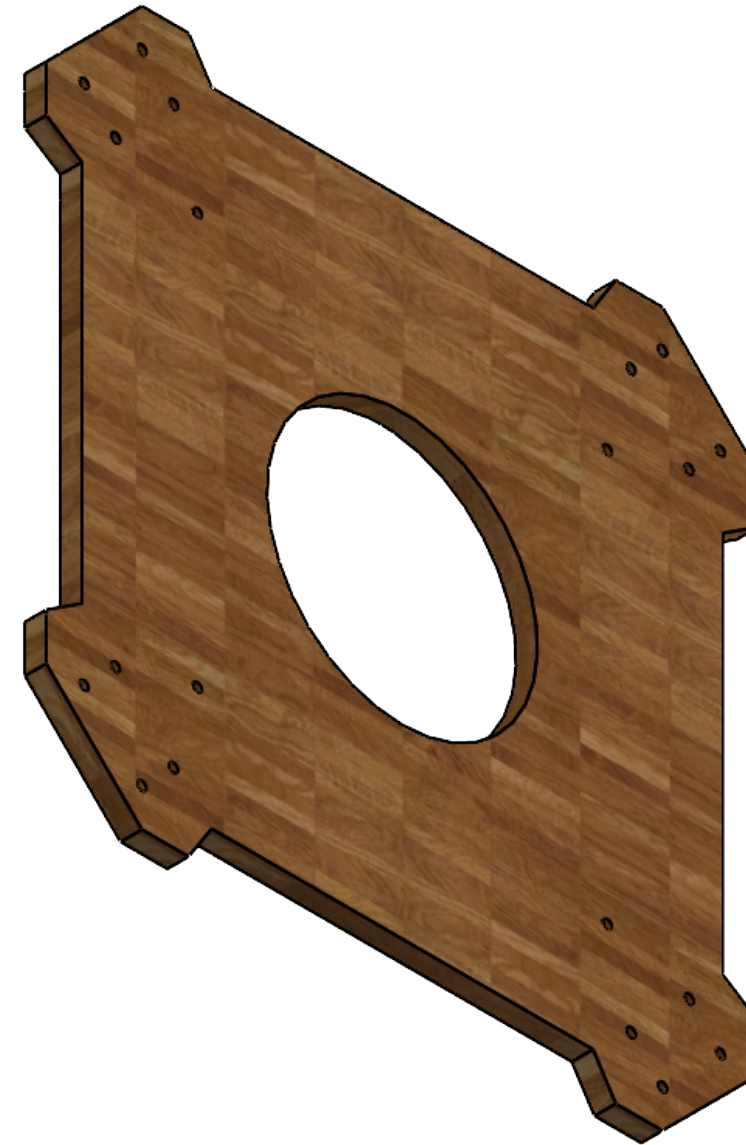
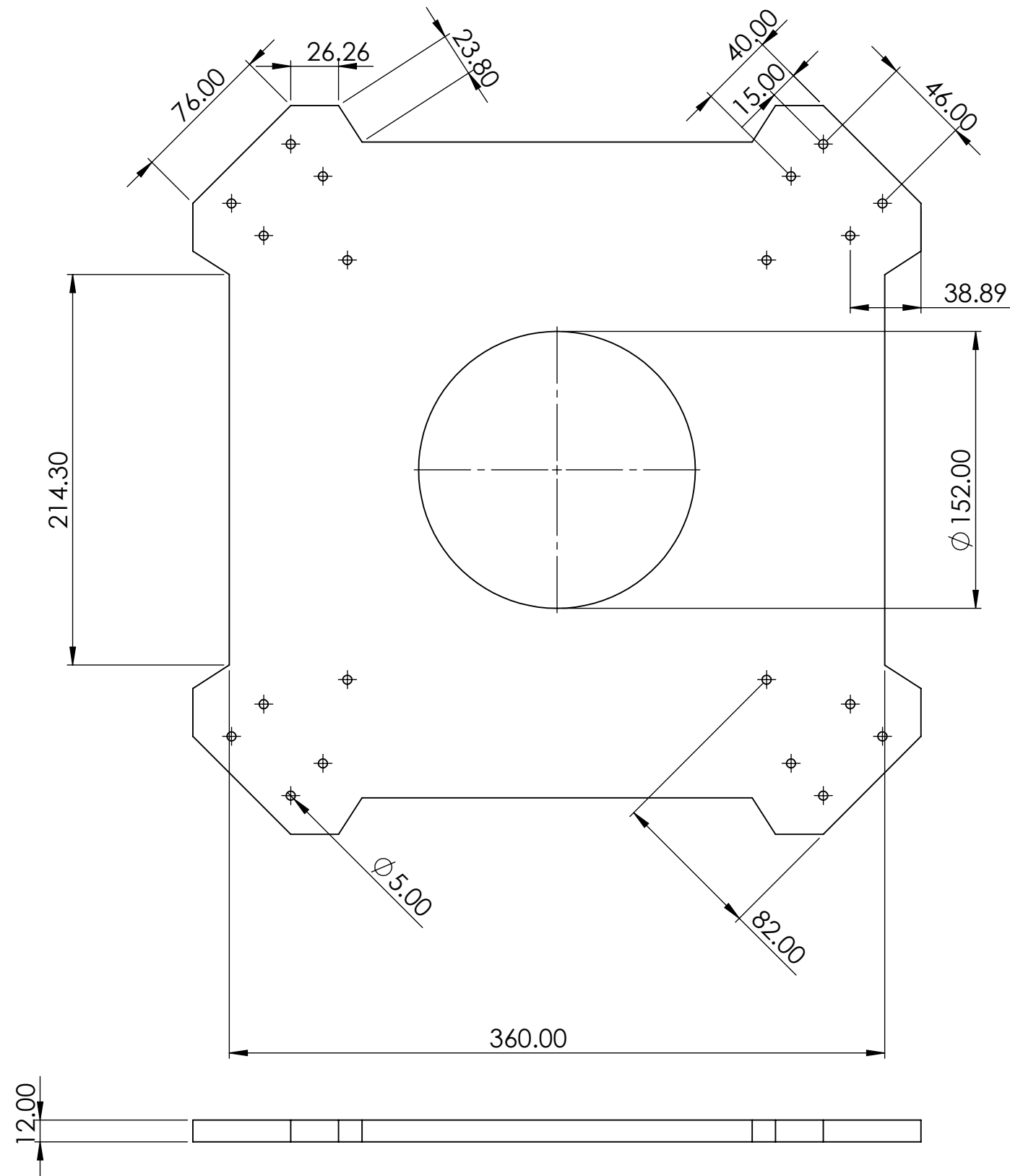


ITEM NO.	PART NUMBER	DESCRIPTION	QTY.
1	Top UAV frame plate		1
2	Bottom UAV frame plate		1
3	Container		1
4	UAV arm		4
5	Spacer		4
6	Leg base		2
7	Leg		2
8	Leg support 2		4
9	Leg support		4
10	Leg Base 2		2
11	Support base		4
12	Steel plate		4
13	Pixhawk 5x		1
14	RC receiver		1
15	Telemetry Radio		1
16	GPS M8N		1
17	Sunnysky X6215s 170Kv		4
18	Stepper Control Circuit		1
19	Battery		2
20	Flycolor_ESC_80A_HobbyWing		4
21	Propeller 2255		4
22	Power Module		1
23	Circuit Spacer		2

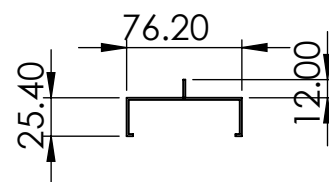
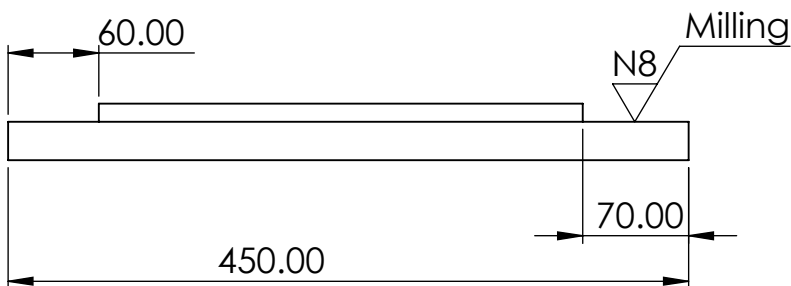
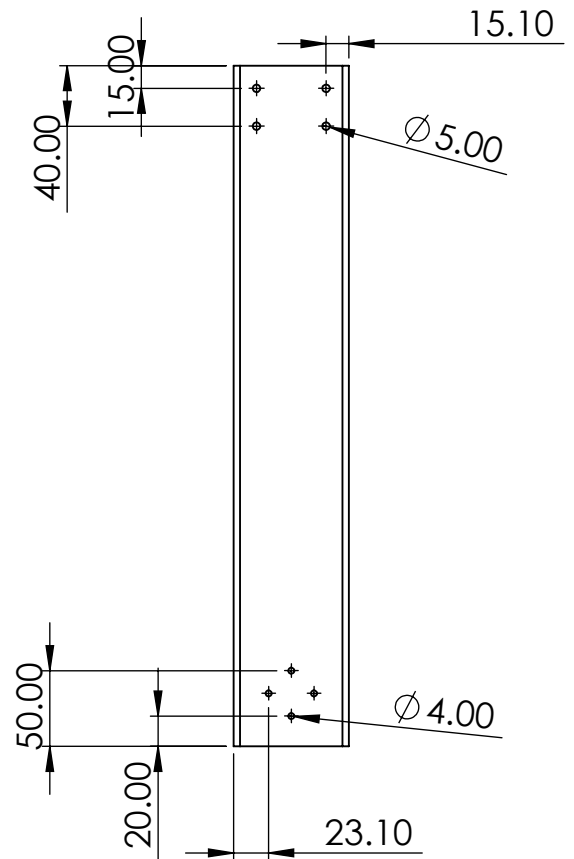
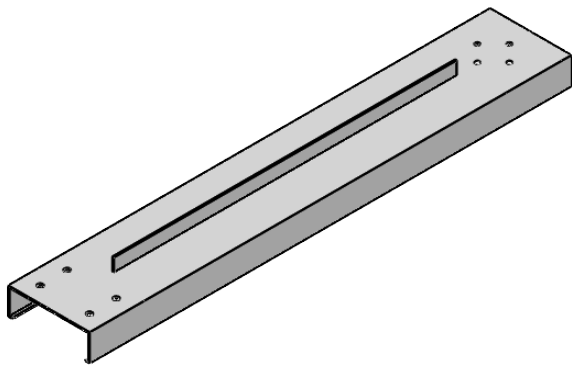
Tolerance: 0.1		Weigth: 13.5			
Date: 14/05/2022		Name: Gabriel Gómez			
Drawn: 14/05/2022		Checked: 18/05/2022		Code: A-001	
Checked: 18/05/2022		Approved:			Finish: Sheet No.: 1






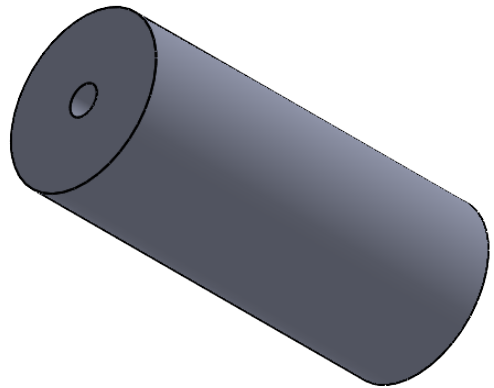
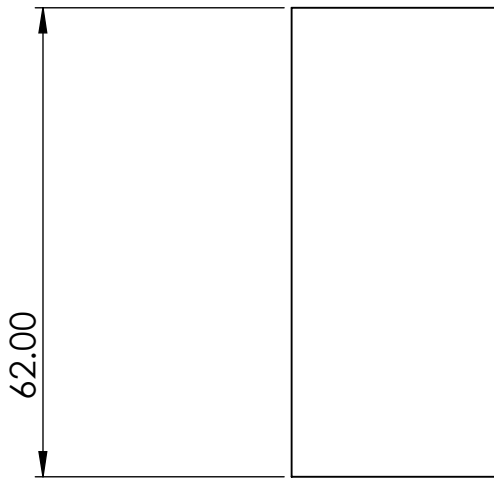
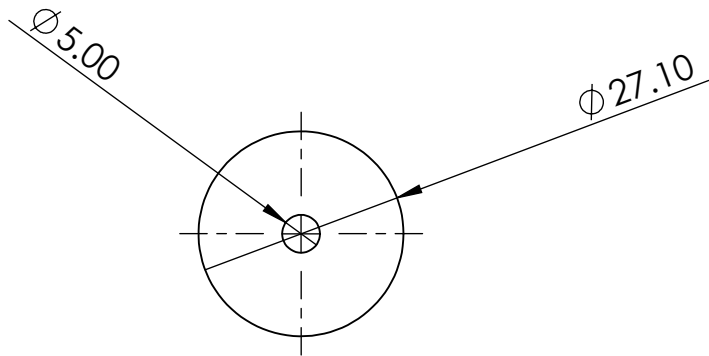
Tolerance: 0.1	Weight: 1.44	Plywood	
Drawn: 17/04/2022	Date: 17/04/2022	Bottom UAV Plate	Scale: 1:5
Checked: 20/04/2022	Name: Mateo González		
Approved:	Name: Gabriel Gómez		
		Code: S-001	Finish: Sheet No.: 2






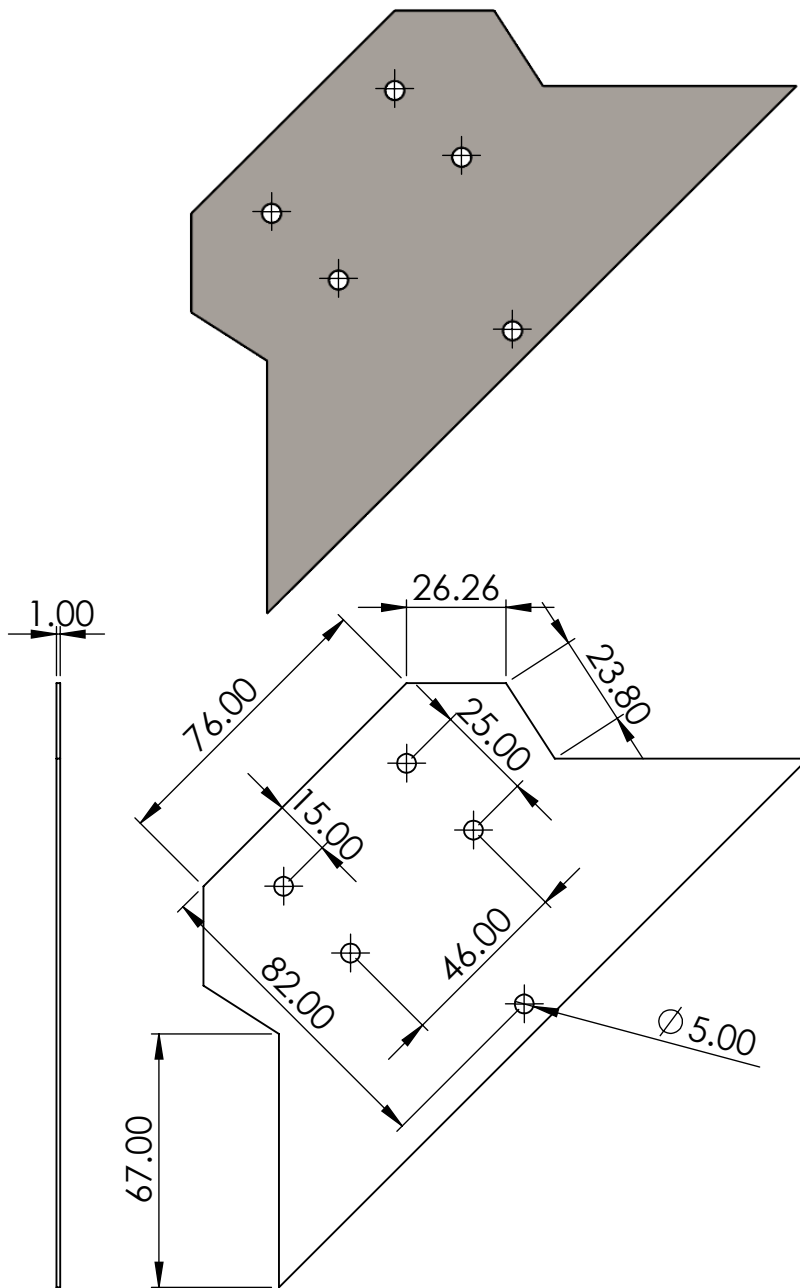
Tolerance: 0.1		Weight: 0.85		Plywood			
Date: 7/04/2022		Name: Mateo González		Top UAV Frame Plate		Scale: 1:3	
Checked: 8/04/2022		Gabriel Gómez					
Approved:							
				Code: S-002		Finish:	
						Sheet No.: 3	



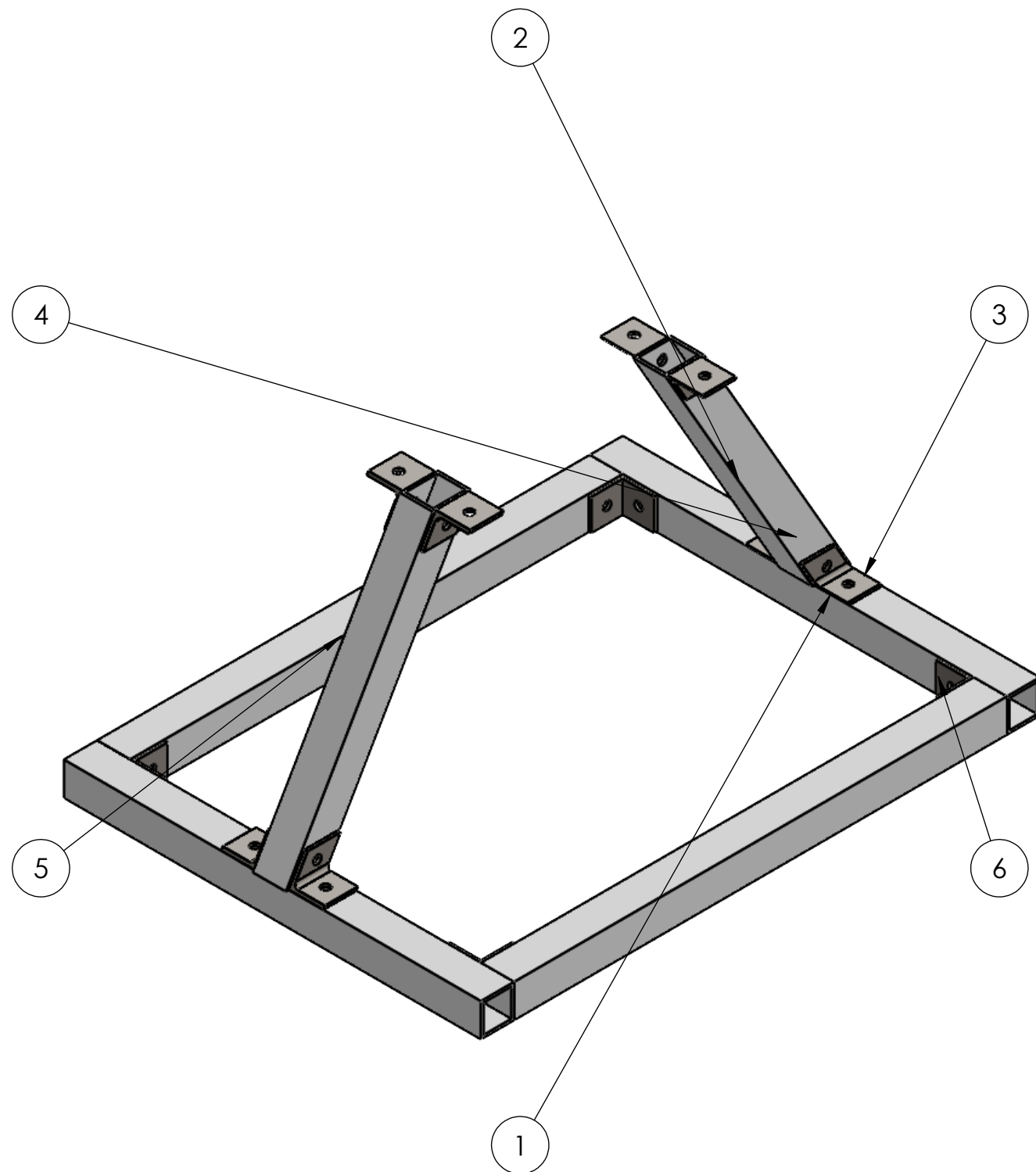
Tolerance: 0.1		Weight: 234.99		Aluminum 2011		 		
Date: 17/04/2022		Name: Gabriel Gómez		UAV Arm				Scale: 1:5
Checked: 18/04/2022		Nicolás Herrera						
Approved:								
				Code: S-003		Finish:		Sheet No.: 4



Tolerance: 0.1		Weight: 0.04		Nylon 101		 	
Date:		Name:		Spacer		Scale: 1:1	
Drawn:	11/04/2022	Gabriel Gómez					
Checked:	12/04/2022	Nicolás Herrera					
Approved:							
		Code: S-004		Finish:		Sheet No.: 5	

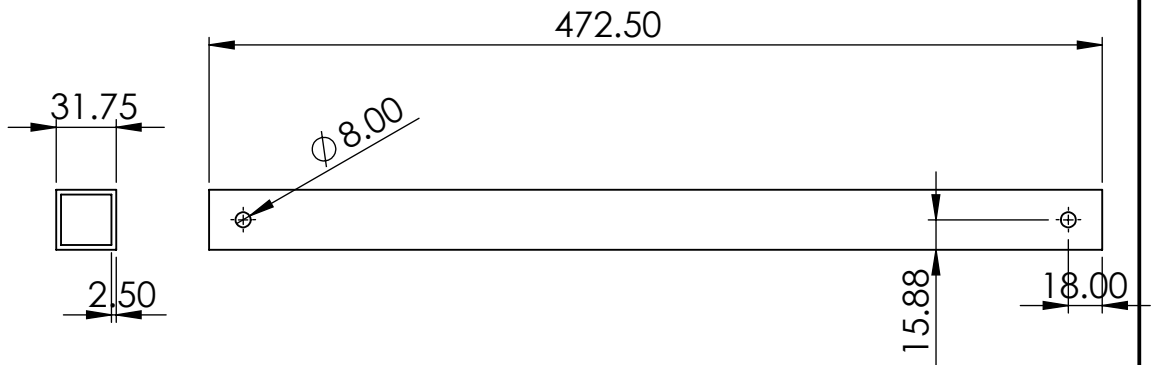
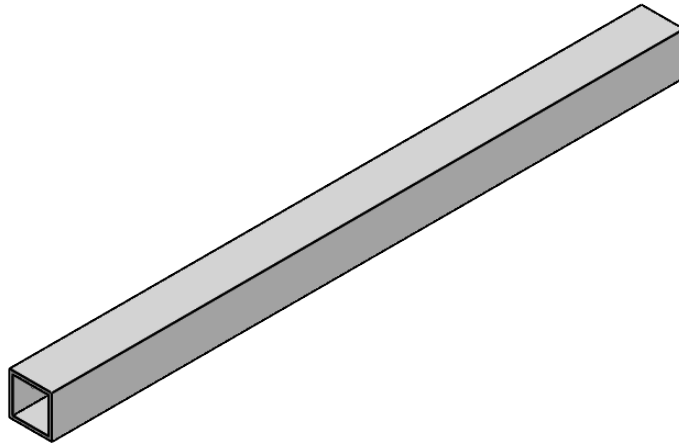





Tolerance: 0.1		Weight: 0.09		AISI 1015 Steel, Cold Drawn (SS)					
Date:		Name:		Steel Plate				Scale: 1:2	
Drawn:	11/05/2022	Gabriel Gómez							
Checked:	11/05/2022	Mateo Ormazá							
Approved:									
				Code: S-005		Finish:		Sheet No.: 6	

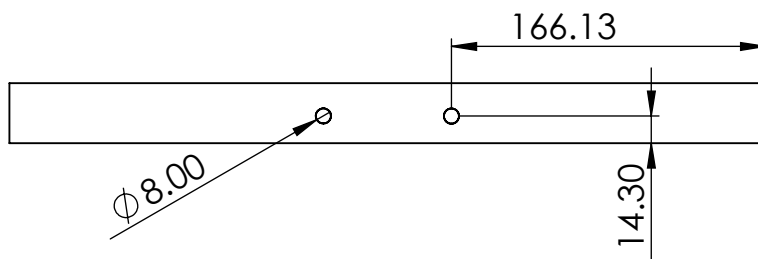
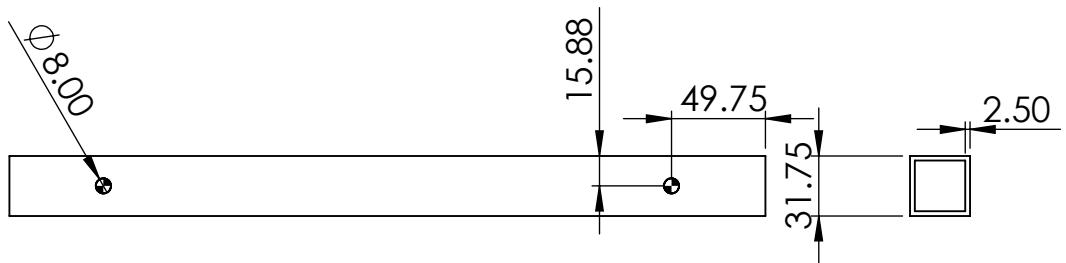
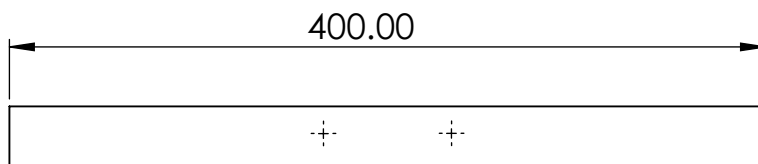
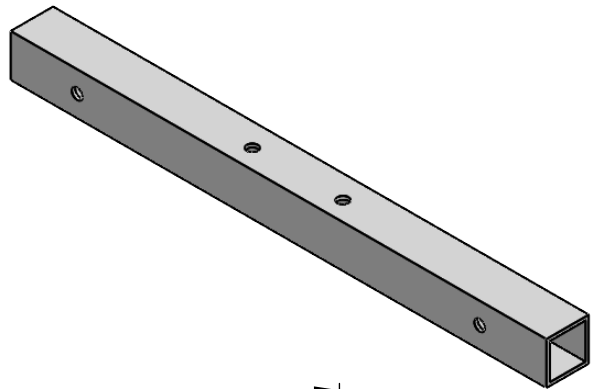


ITEM NO.	PART NUMBER	DESCRIPTION	QTY.
1	Leg base		2
2	Leg		2
3	Leg support 2		4
4	Leg support		4
5	Leg Base 2		2
6	Support base		4

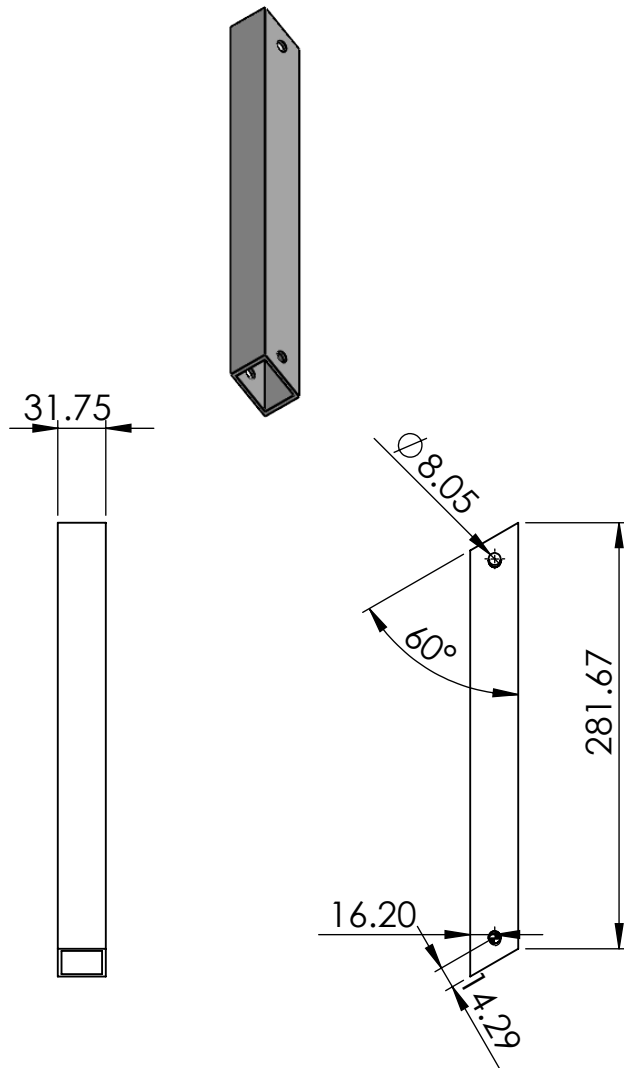
Tolerance: 0.1		Weight: 2.59			
Date:	Name:	<h3>Leg Assembly</h3>			
Drawn: 14/05/2022	Gabriel Gómez				
Checked: 15/05/2022	Mateo González				
Approved:					
		Code: L-001	Finish:	Sheet No.: 7	






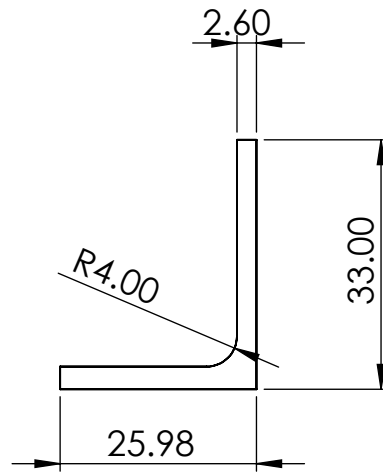
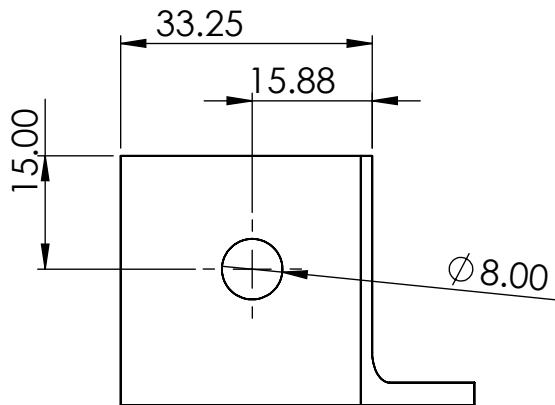
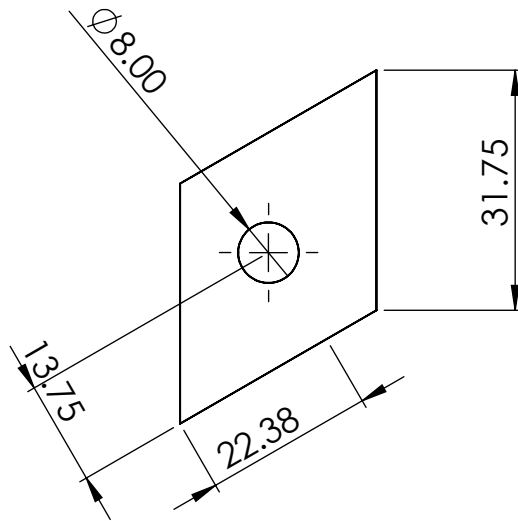
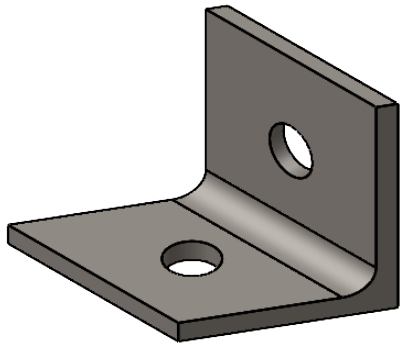
Tolerance: 0.1		Weight: 0.37		Aluminum 2011		 	
Date: 9/05/2022		Name: Gabriel Gómez		Horizontal Leg base		Scale: 1:4	
Checked: 10/05/2022		Mateo Ormaza					
Approved:							
				Code: L-002		Finish:	
						Sheet No.: 8	



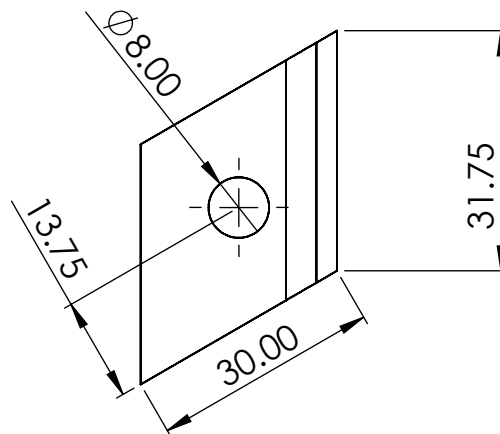
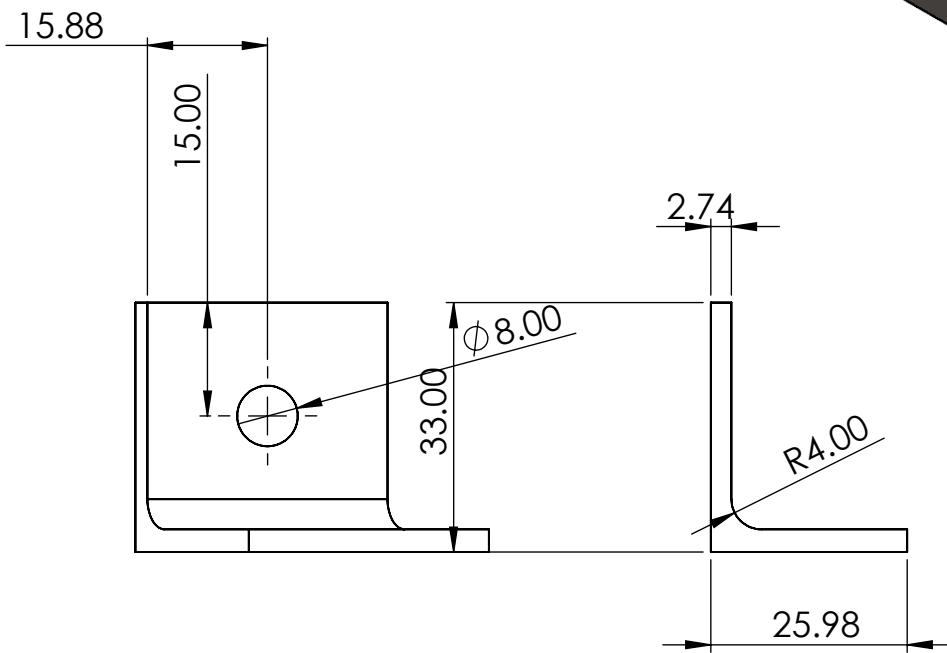
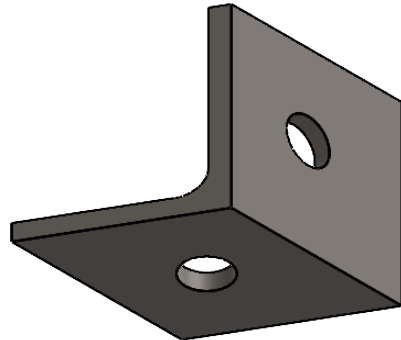
Tolerance: 0.1		Weight: 0.31		Aluminum 2011					
Date:		Name:		Vertical Leg Base				Scale: 1:4	
Drawn:	25/04/2022	Gabriel Gómez							
Checked:	26/04/2022	Nicolás Herrera							
Approved:									
				Code: L-003		Finish:		Sheet No.: 9	






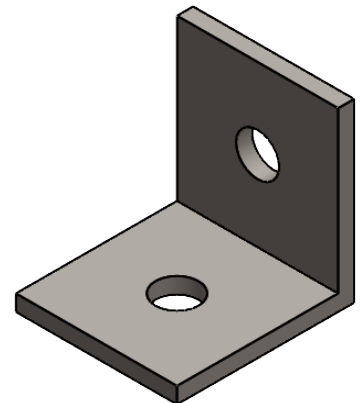
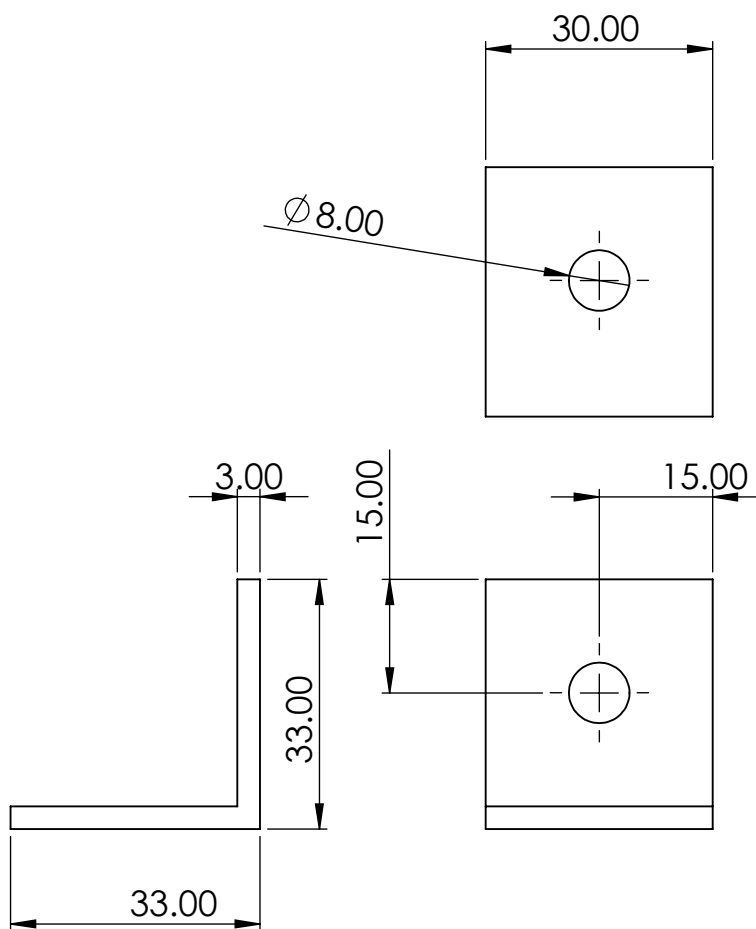
Tolerance: 0.1		Weight: 0.22		Aluminum 2011		 	
Date: 23/04/2022		Name: Gabriel Gómez		Leg		Scale: 1:5	
Checked: 24/04/2022		Nicolás Herrera					
Approved:							
		Code: L-004		Finish:		Sheet No.: 10	






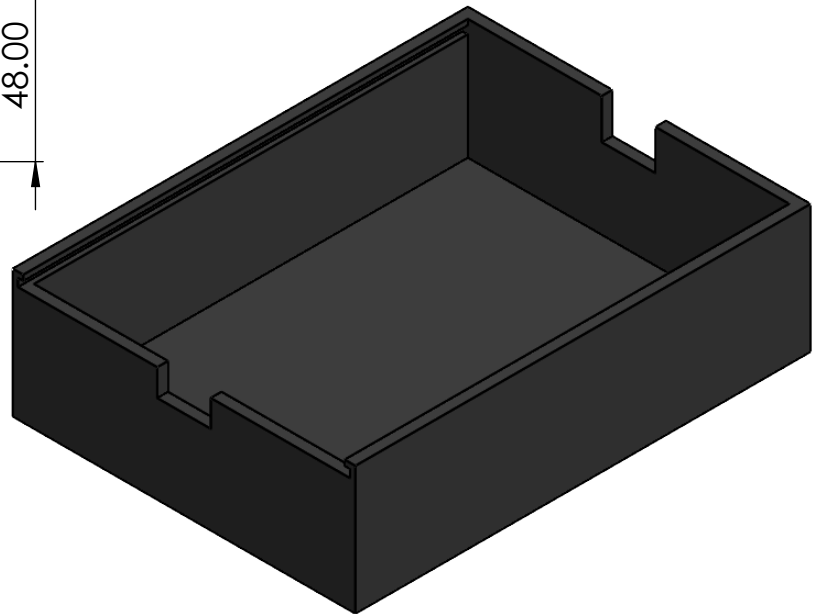
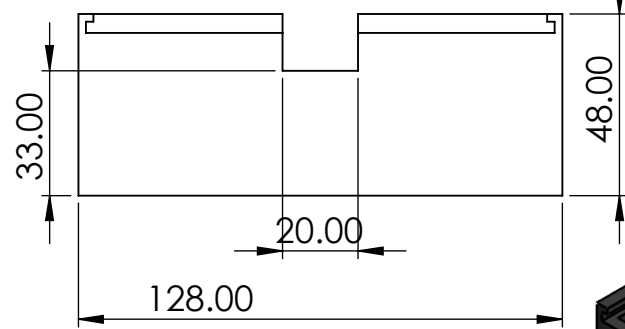
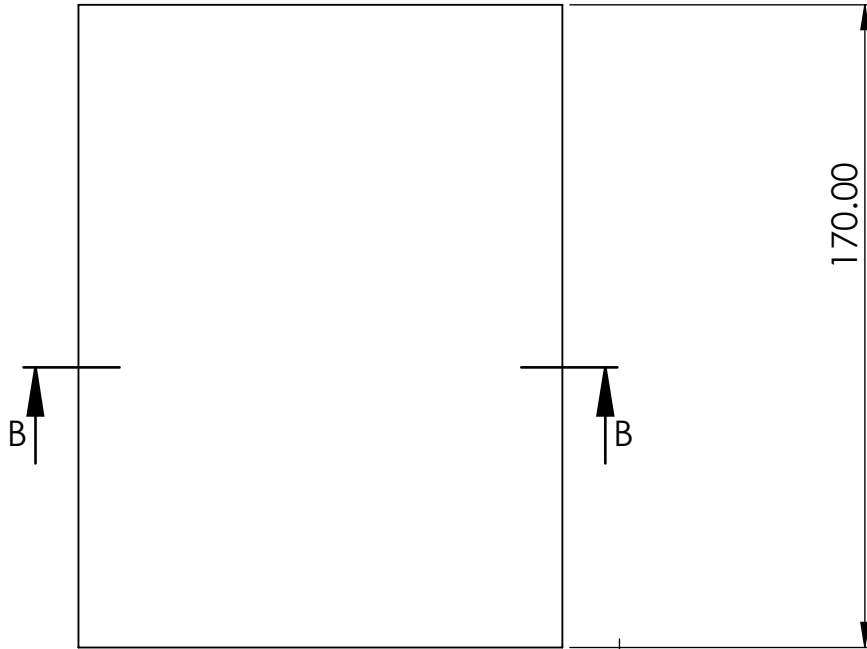
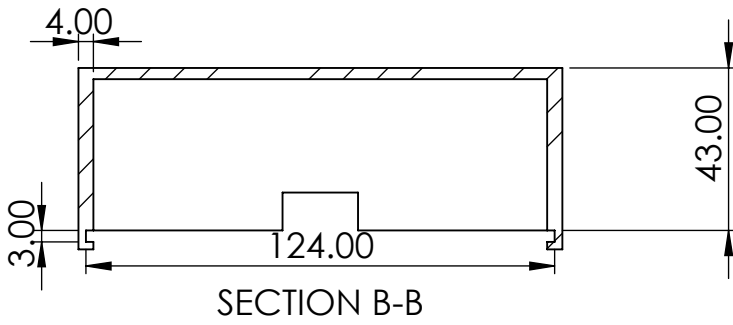
Tolerance: 0.1		Weight: 0.08		AISI 1015 Steel, Cold Drawn (SS)					
Date:		Name:		<h2>Leg Support</h2>				Scale: 1:1	
Drawn:	25/04/2022	Mateo González							
Checked:	26/04/2022	Mateo Ormaza							
Approved:									
				Code: L-005		Finish:		Sheet No.: 11	



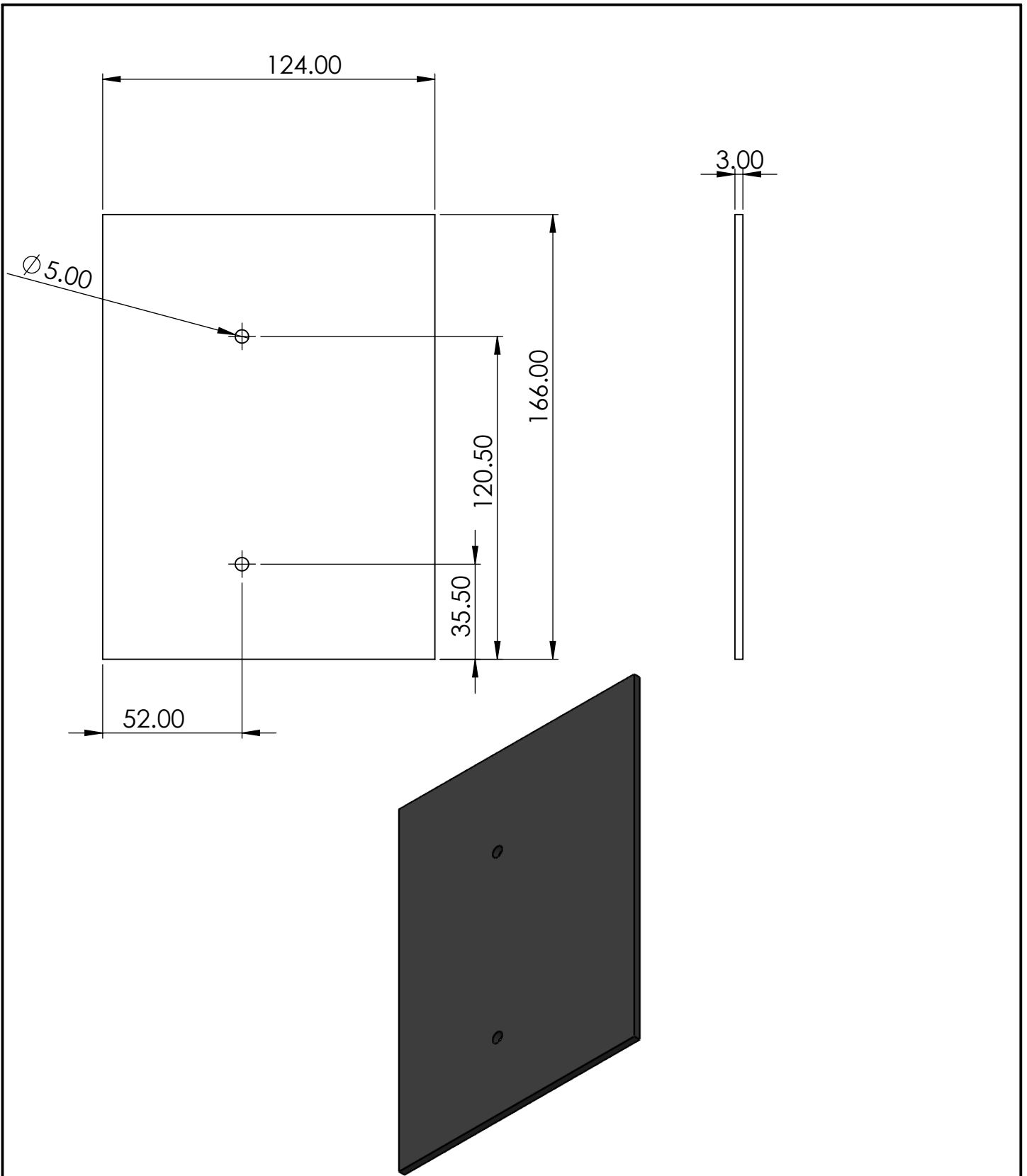
Tolerance: 0.1		Weight: 0.08		AISI 1015 Steel, Cold Drawn (SS)		 			
Date:		Name:		<h2>Leg Support 2</h2>				Scale: 1:1	
Drawn: 25/04/2022		Mateo González							
Checked: 26/04/2022		Mateo Ormazá							
Approved:									
				Code: L-006		Finish:		Sheet No.: 12	



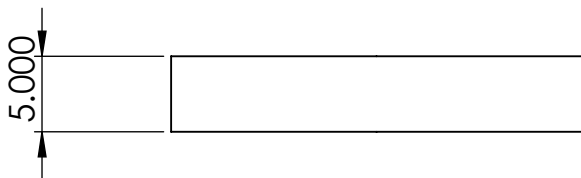
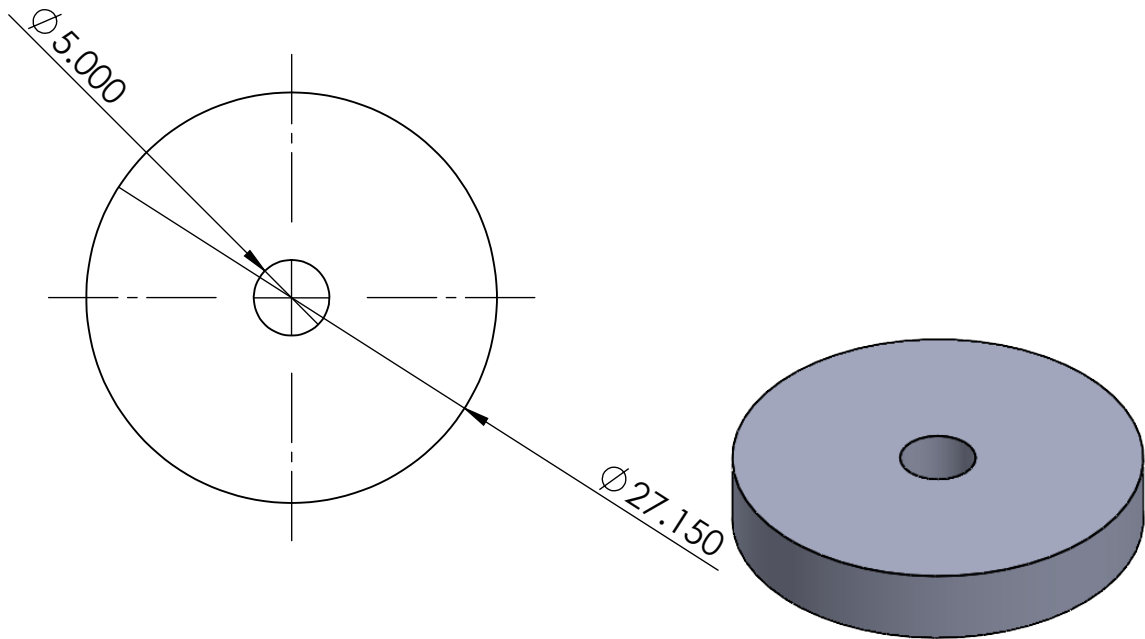
Tolerance: 0.1		Weight: 0.04		AISI 1015 Steel, Cold Drawn (SS)		 			
Date:		Name:		<h2>Base support</h2>				Scale: 1:1	
Drawn:	10/05/2022	Mateo González							
Checked:	10/05/2022	Gabriel Gómez							
Approved:									
				Code: L-007		Finish:		Sheet No.: 13	



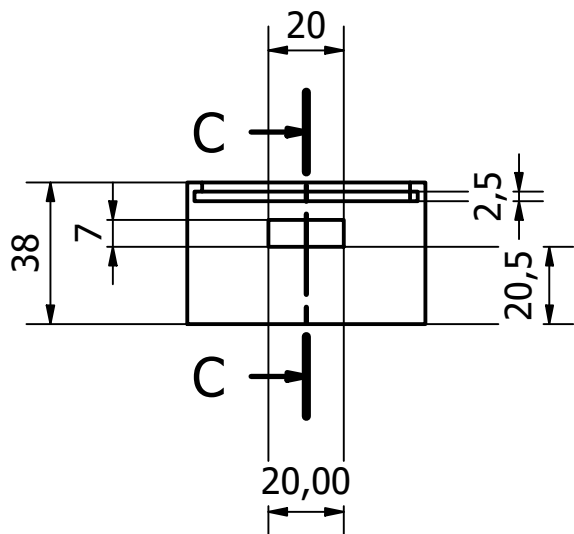
Tolerance: 0.1		Weight: 0.22		PetG			
Date: 27/04/2022		Name: Gabriel Gómez		Stepper Control Circuit Case		Scale: 1:2	
Checked: 27/04/2022		Mateo Ormaza					
Approved:							
				Code: DC-001		Finish:	
						Sheet No.: 14	



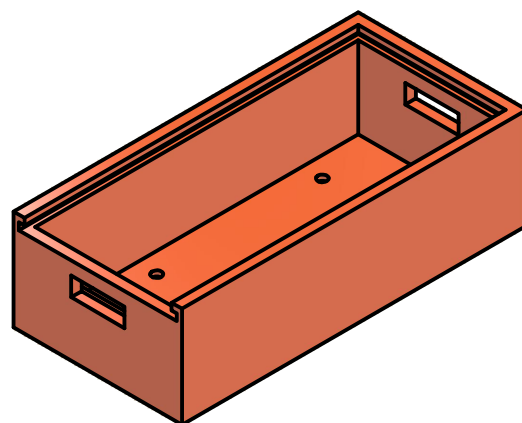
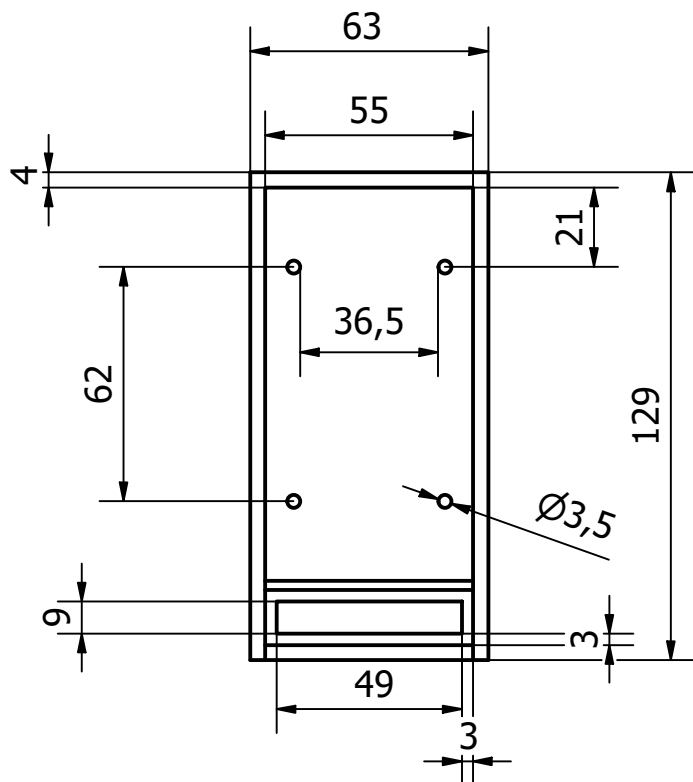
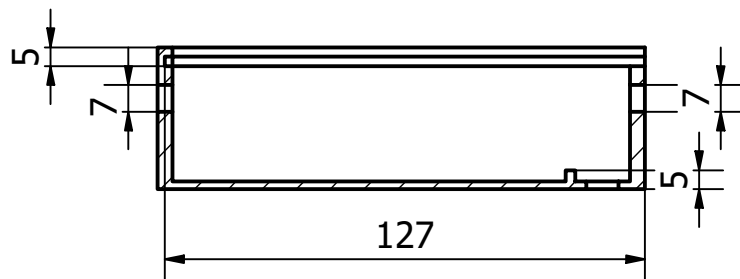
Tolerance: 0.1		Weight: 0.08		PetG					
Date:		Name:		Stepper Control Circuit Lid				Scale:	
Drawn:	27/04/2022	Gabriel Gómez						1:2	
Checked:	27/04/2022	Mateo Ormaza							
Approved:									
				Code: DC-002		Finish:		Sheet No.: 15	



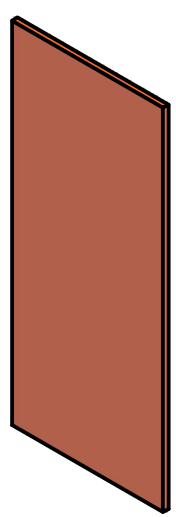
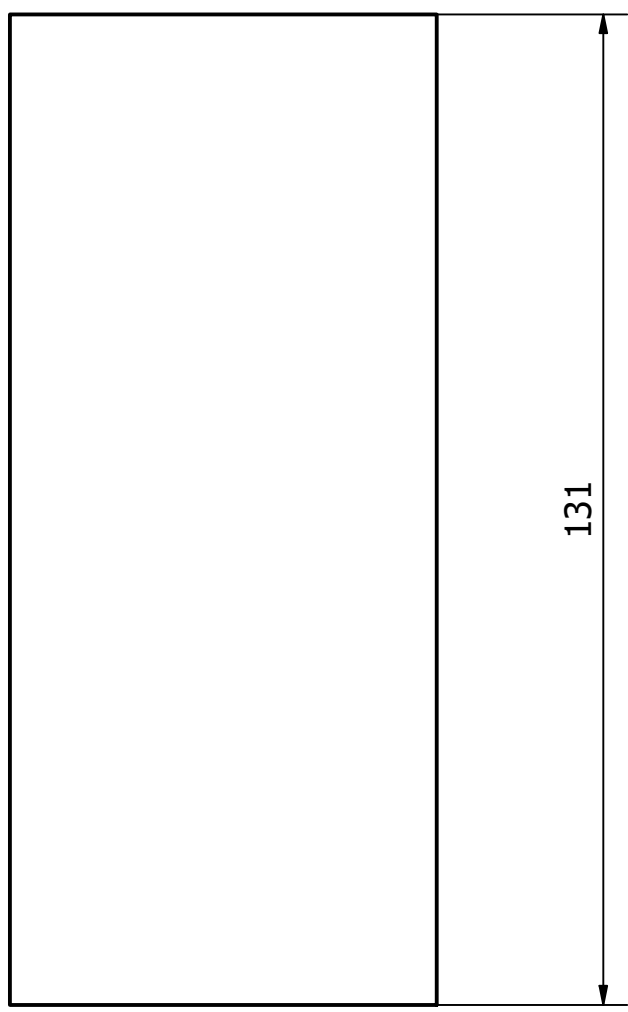
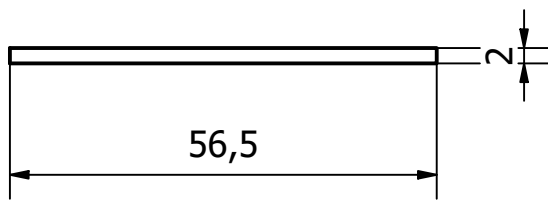
Tolerance: 0.1		Weight: 0.003		Nylon 101Nylon 101			
Date:		Name:		Circuit Spacer		Scale: 2:1	
Drawn:	26/04/2022	Gabriel Gómez					
Checked:	26/04/2022	Mateo Ormaza					
Approved:							
				Code: DC-003		Finish:	
						Sheet No.: 16	



C-C (1 : 2)

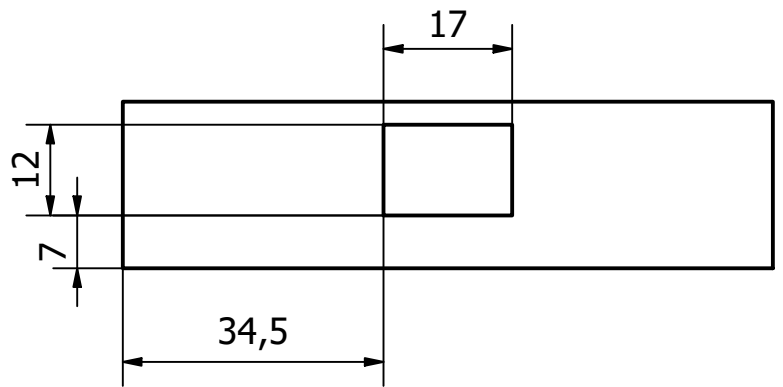
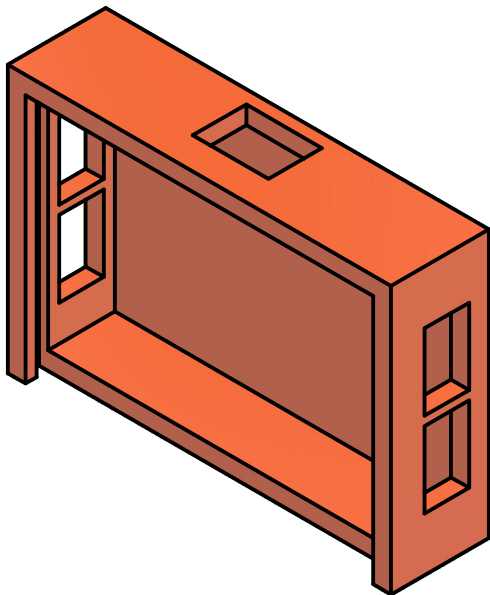
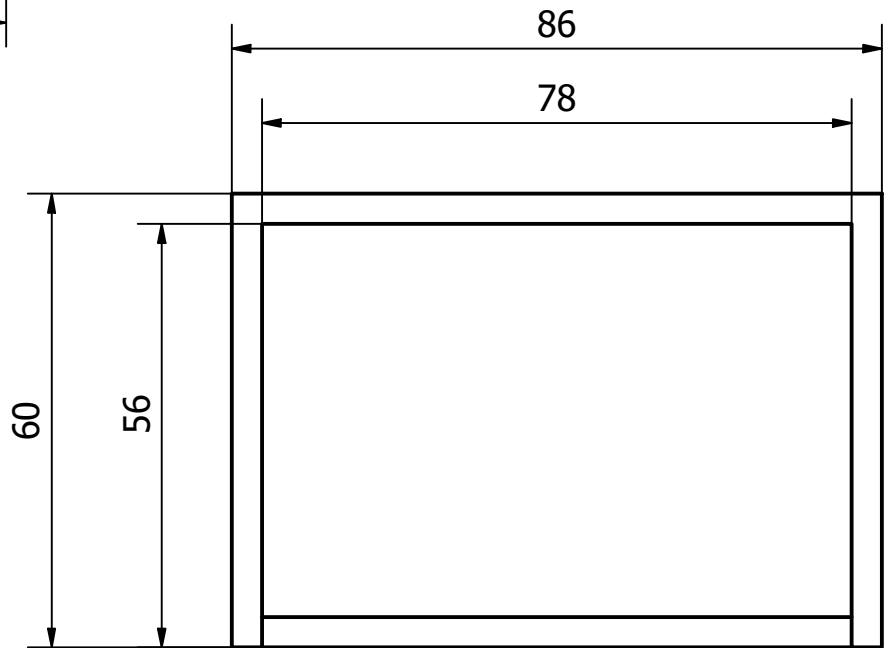
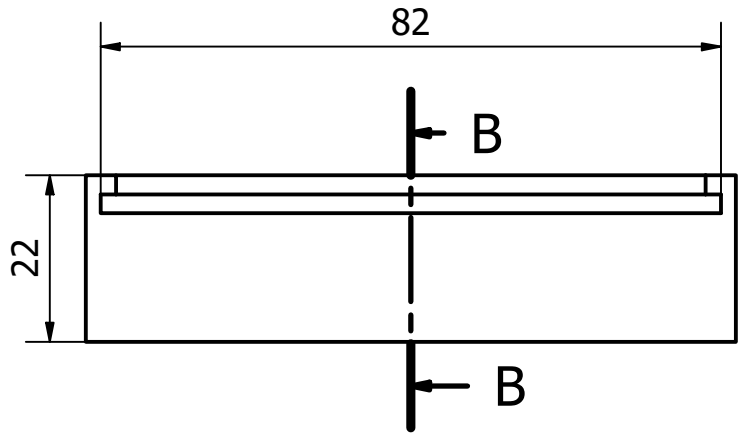
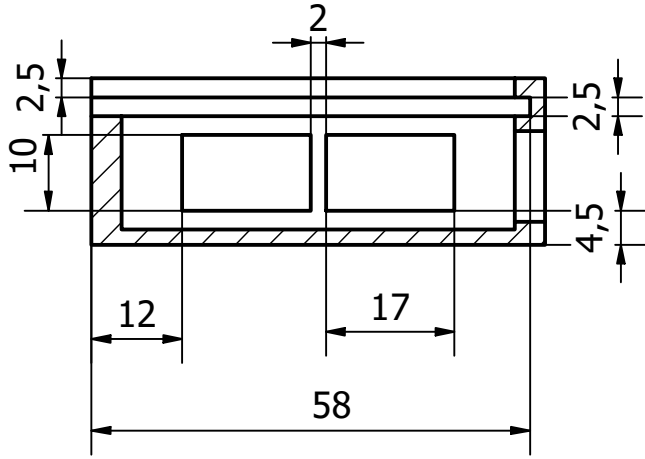


Tolerancia: +1 [mm]		Peso: 0.099 kg		PET Plastic			
Fecha		Nombre		Pixhawk Box		Escala: 1 : 2	
Dibujado	15/05/2022	Nicolás Herrera					
Revisado	15/05/2022	Mateo González					
Aprobado							
				Código: B 001		Trat. Superficial:	
						Hoja: 17	

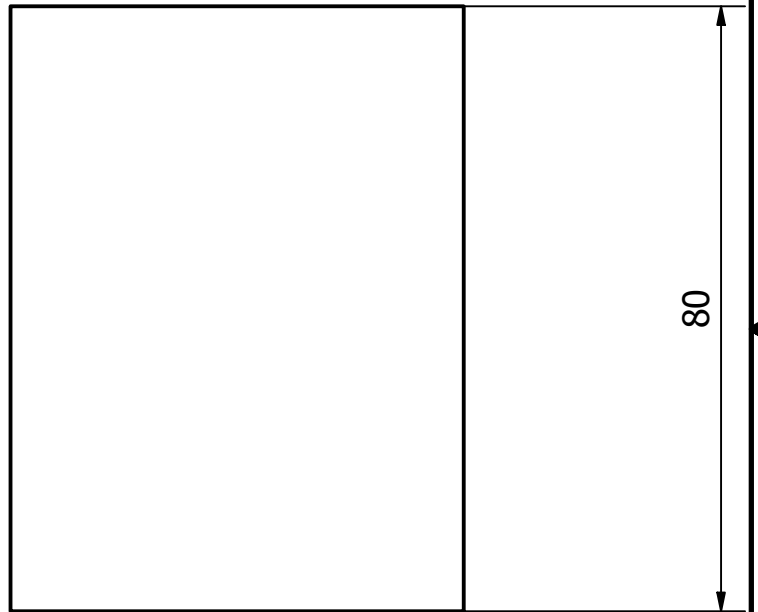
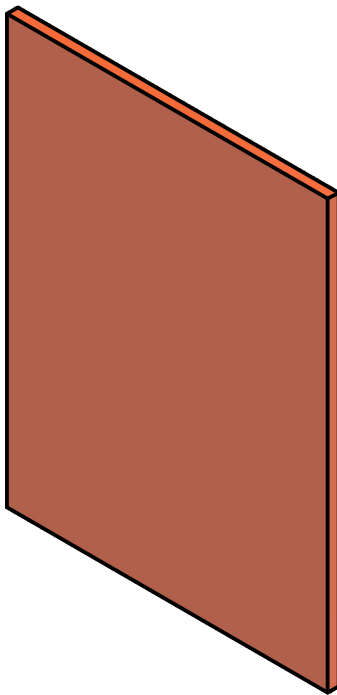
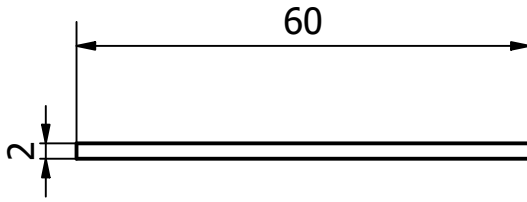


Tolerancia: +- 1 [mm]		Peso: 0.023 kg		PET Plastic		
	Fecha	Nombre		Pixhawk Lid		Escala: 1 : 1
Dibujado	15/05/2022	Nicolás Herrera				
Revisado	15/05/2022	Mateo González				
Aprobado				Código: B - 001-L		Trat. Superficial:
						Hoja: 18

B-B (1 : 1)

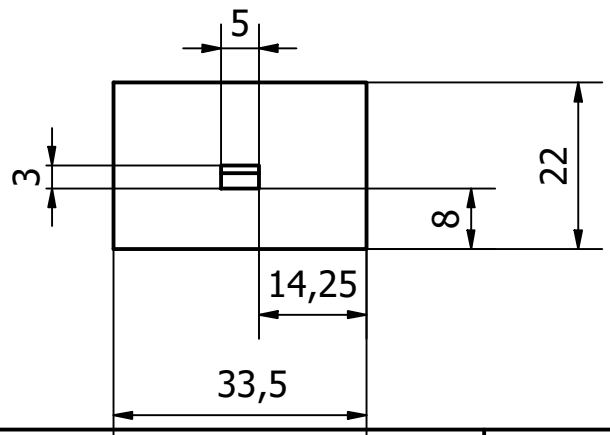
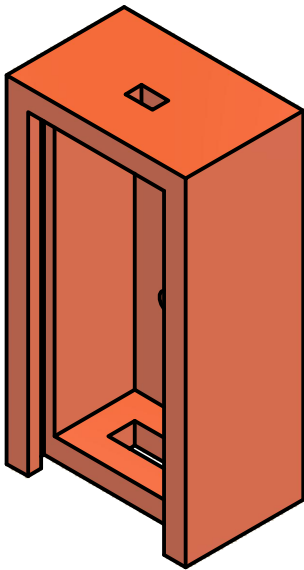
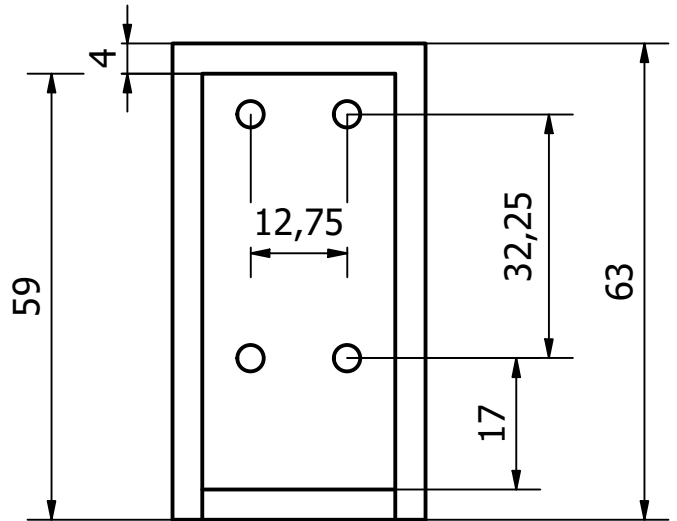
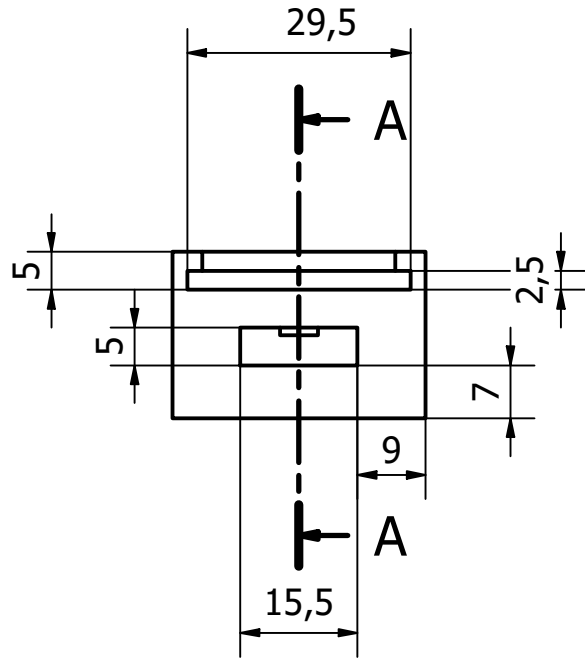
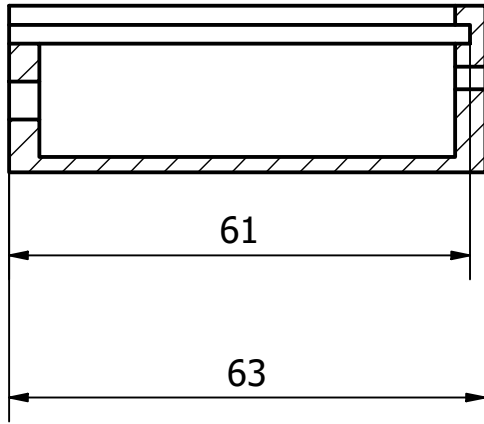


Tolerancia: +- 1 [mm]		Peso: 0.041 kg		PET Plastic			
Fecha		Nombre		Power Distributor Box		Escala: 1 : 1	
Dibujado	15/05/2022	Nicolás Herrera					
Revisado	15/02/2022	Mateo González					
Aprobado							
				Código: B-002		Trat. Superficial:	
						Hoja: 19	

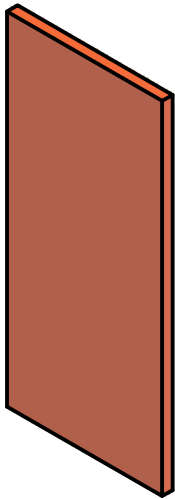
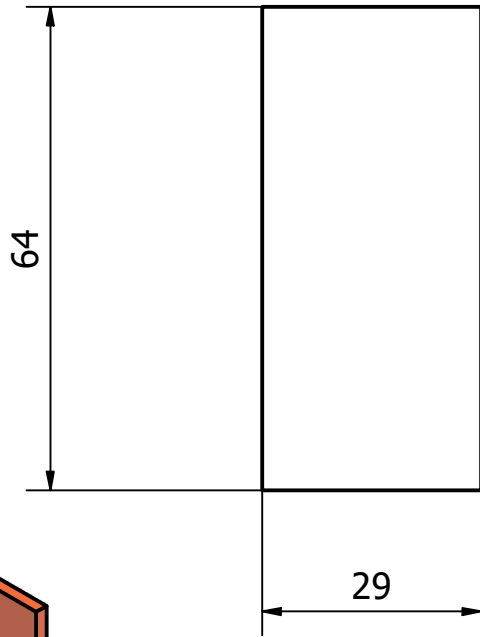
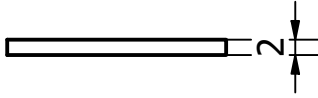


Tolerancia: +- 1 [mm]		Peso: 0.015 kg		PET Plastic			
	Fecha	Nombre		Power Distributor Lid		Escala: 1 : 1	
Dibujado	15/05/2022	Nicolás Herrera					
Revisado	15/05/2022	Mateo González					
Aprobado							
			Código: B-002-L		Trat. Superficial:		Hoja: 20

A-A (1 : 1)

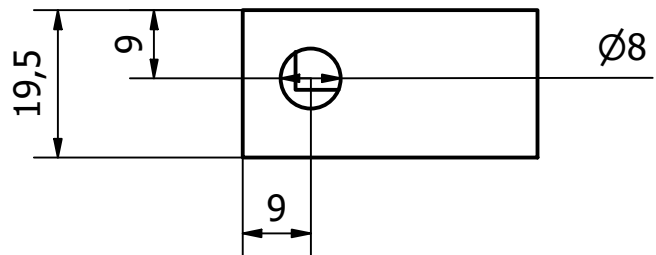
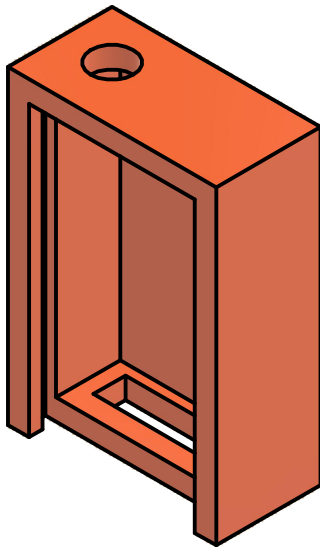
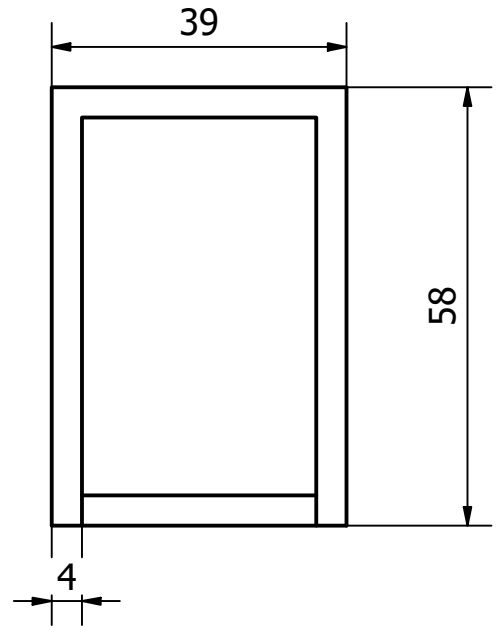
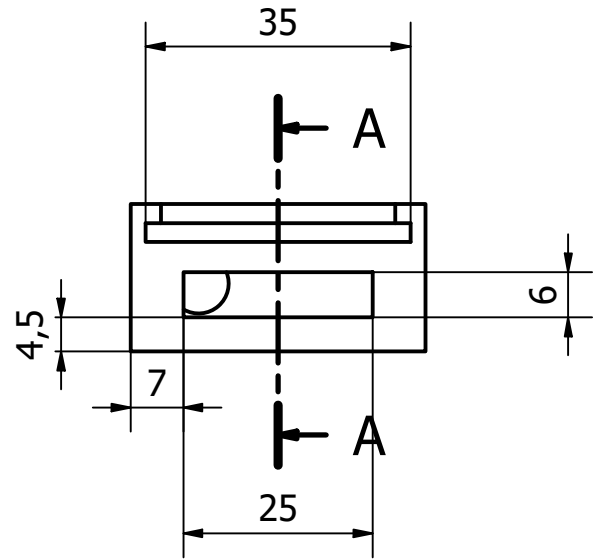
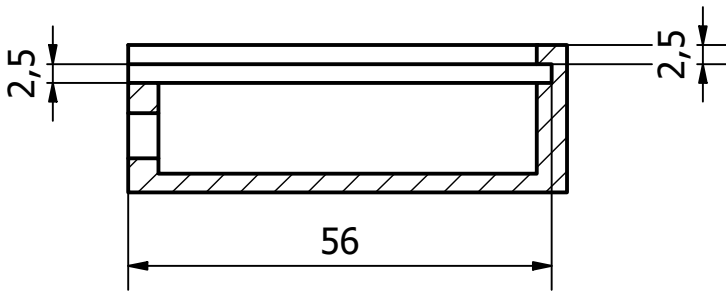


Tolerancia: +- 1 [mm]		Peso: 0.026 kg		PET Plastic			
Fecha		Nombre		Receiver Box		Escala: 1 : 1	
Dibujado	15/05/2022	Nicolás Herrera					
Revisado	15/05/2022	Mateo González					
Aprobado							
		Código: B-003		Trat. Superficial:		Hoja: 21	

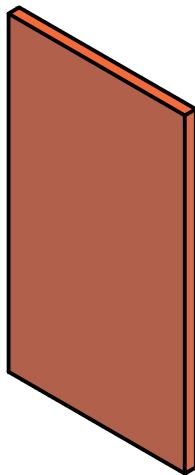
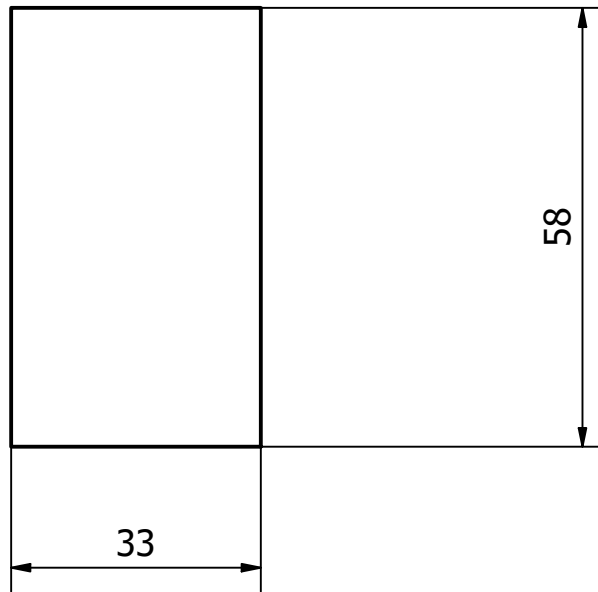
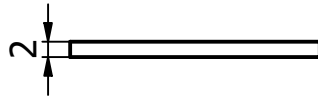


Tolerancia: +- 1 [mm]		Peso: 0.013 lbmass		PET Plastic		
	Fecha	Nombre		Receiver Lid		Escala: 1 : 1
Dibujado	15/05/2022	Nicolás Herrera				
Revisado	15/05/2022	Mateo González				
Aprobado				Código: B-003-L		Trat. Superficial:
						Hoja: 22

A-A (1 : 1)



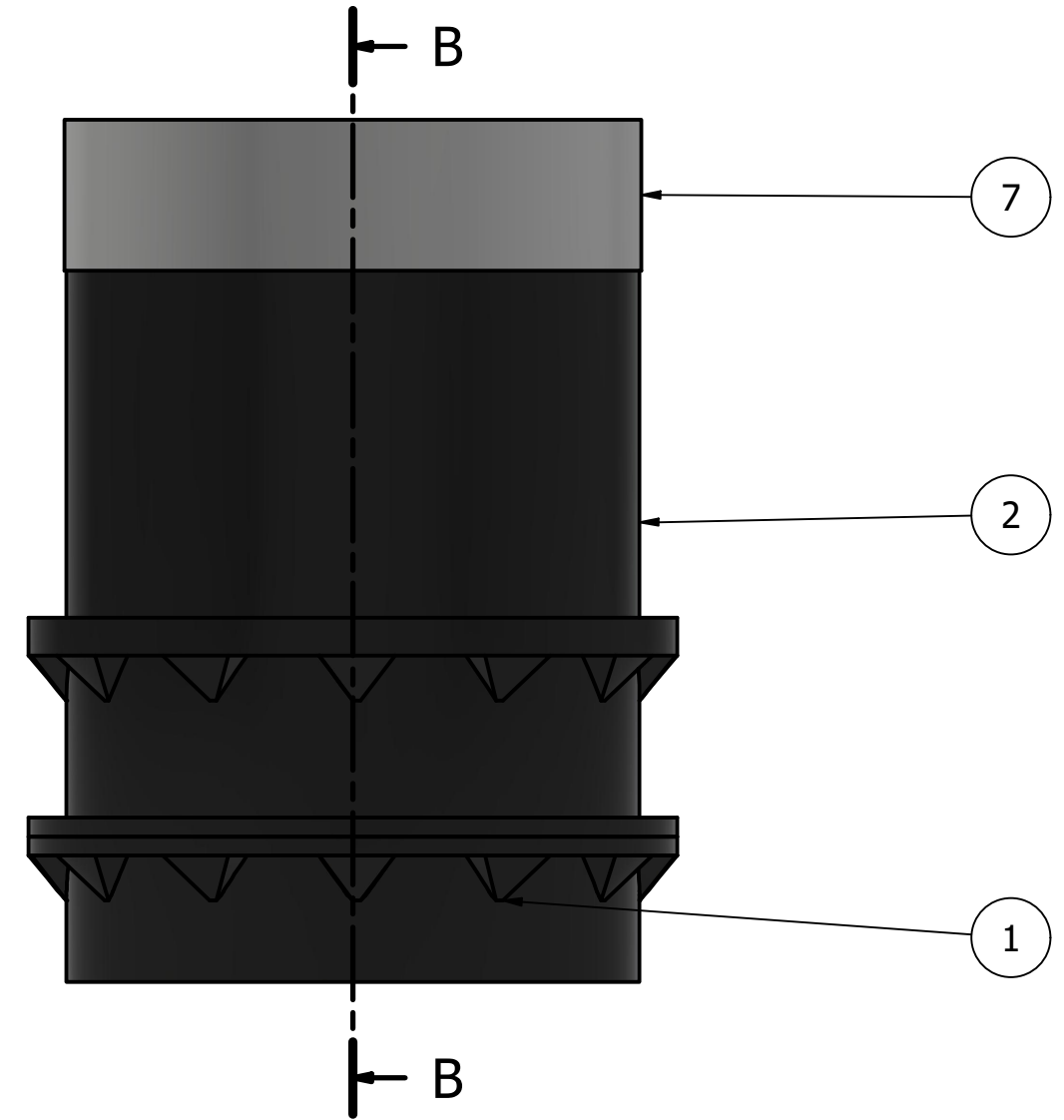
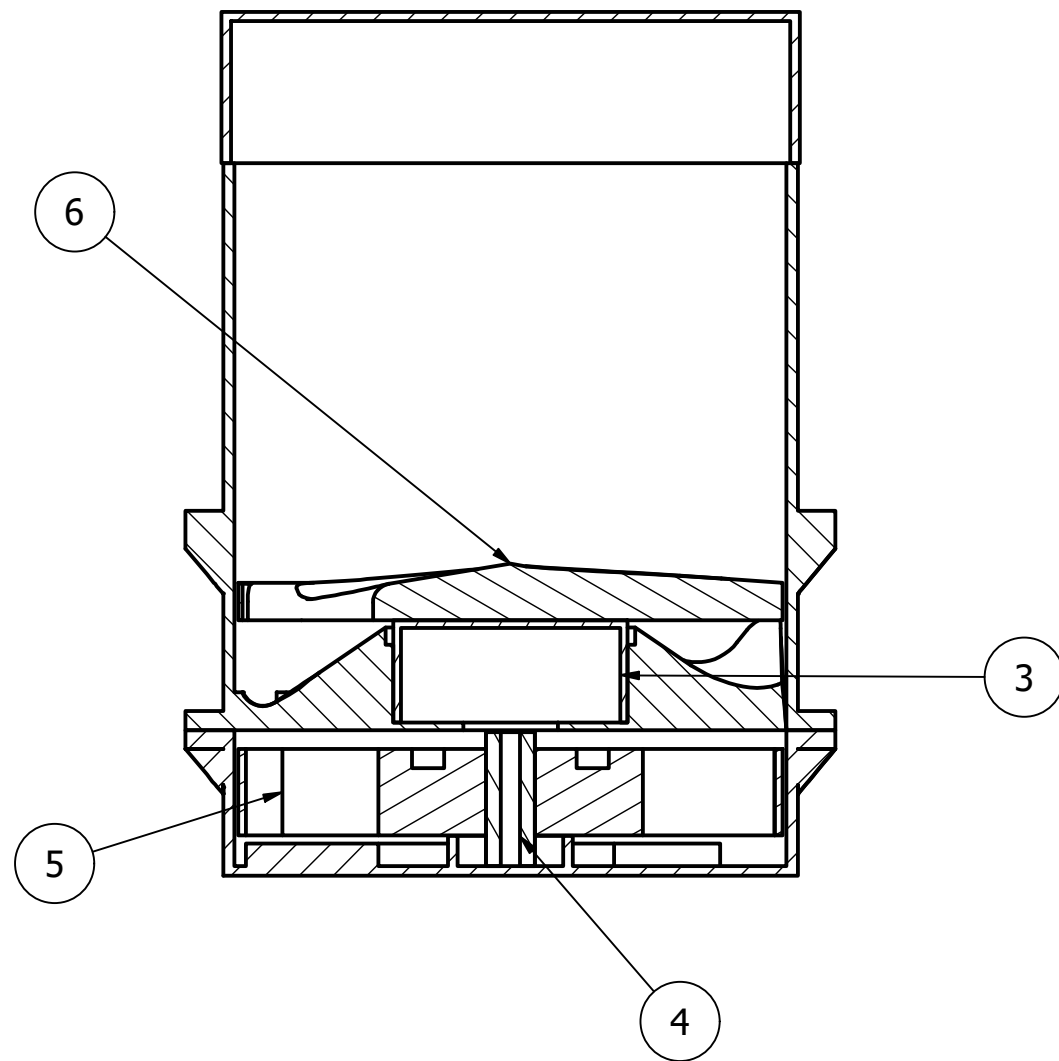
Tolerancia: +- 1 [mm]		Peso: 0.053 lbmass		PET Plastic		
Fecha		Nombre		Telemetry Box		Escala: 1 : 1
Dibujado	15/05/2022	Nicolás Herrera				
Revisado	15/05/2022	Mateo González				
Aprobado						
		Código: B-004		Trat. Superficial:		Hoja: 23



Tolerancia: +- 1 [mm]		Peso: 0.006 kg		PET Plastic		
	Fecha	Nombre		Telemetry Lid		Escala: 1 : 1
Dibujado	15/05/2022	Nicolás Herrera				
Revisado	15/05/2022	Mateo González				
Aprobado						
			Código: B-004-L		Trat. Superficial:	Hoja: 24

PARTS LIST			
ITEM	QTY	PART NUMBER	DESCRIPTION
1	1	Bottom Lid	SDS 002
2	1	Seed Tank	SDS 003
3	1	Nema Lid	SDS 005
4	1	Seed Distributor Rod	SDS 006
5	1	Seed Distributor	SDS 004
6	1	Seed Separator	SDS 001
7	1	Tank Lid	SDS 007

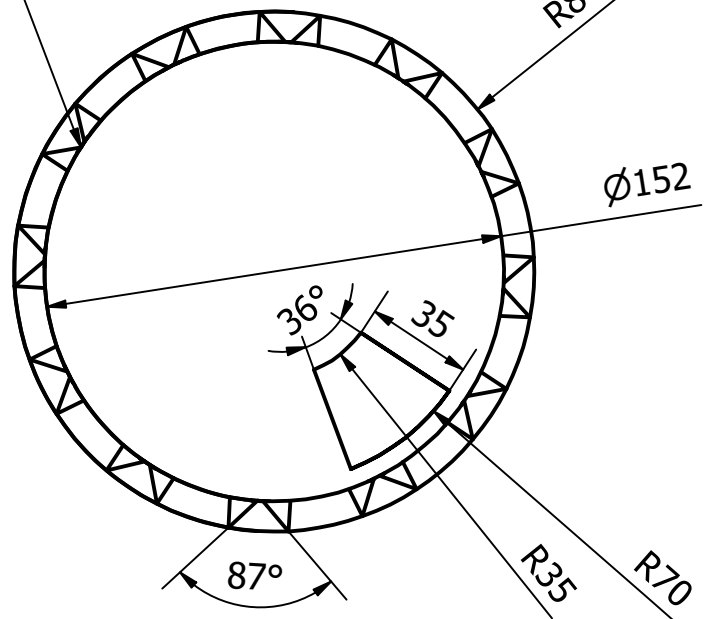
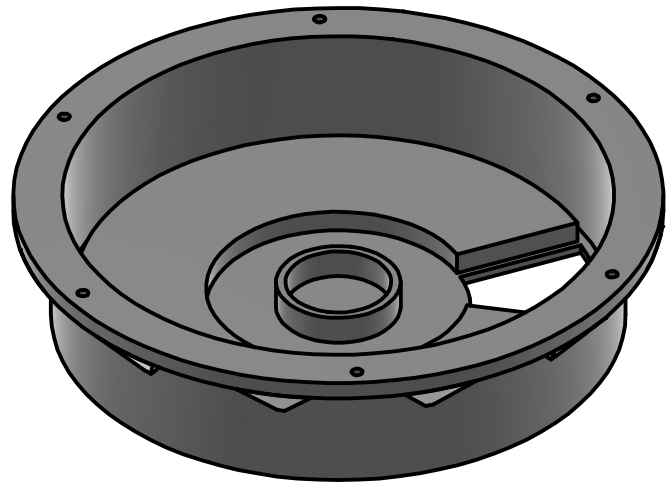
B-B (1 : 2)



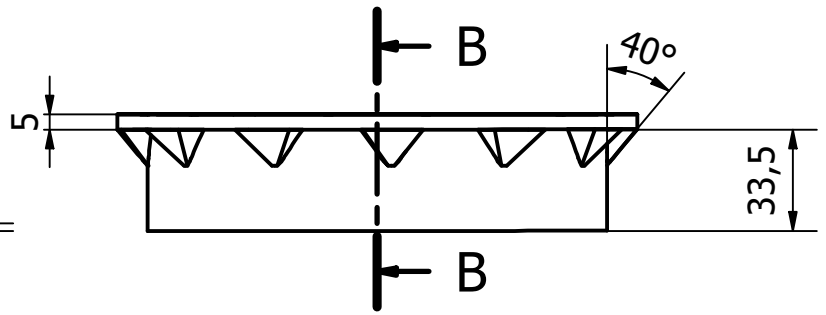
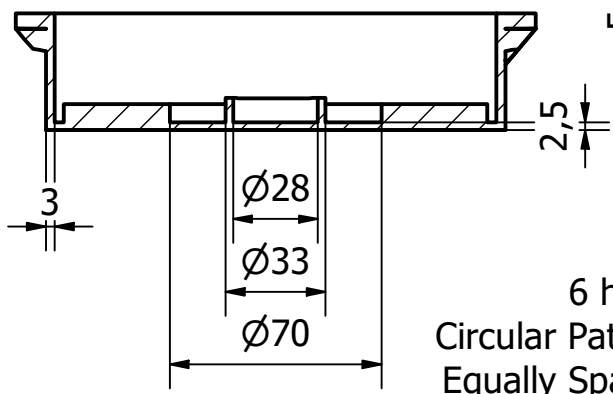
Tolerancia:		Peso: N/A		PETG			
Fecha		Nombre		Seed Distribution System Assembly		Escala: 1 : 2	
Dibujado	5/15/2022	Mateo Ormaza					
Revisado		Gabriel Gómez					
Aprobado							
				Código: SDS Assembly		Trat. Superficial:	
						Hoja: 25	



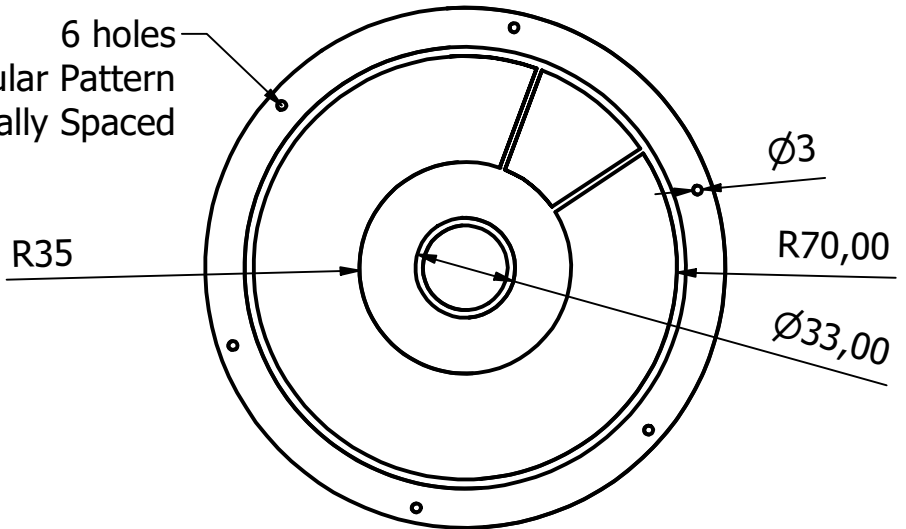
12 Supports
Circular Pattern
Equally Spaced



B-B (0.4:1)

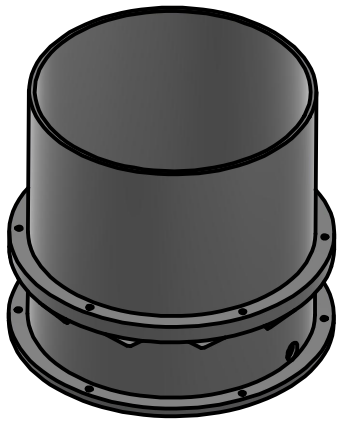


6 holes
Circular Pattern
Equally Spaced



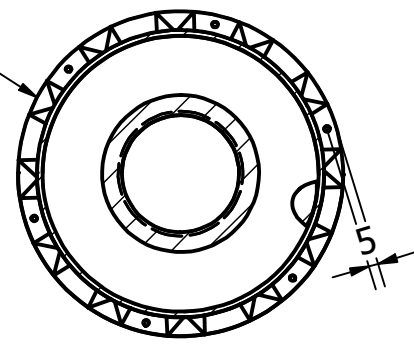
Tolerancia: +- 1 [mm]		Peso: 0.297 kg		PET Plastic			
Fecha		Nombre		Bottom Lid		Escala: 0.4:1	
Dibujado	15/05/2022	Nicolás Herrera					
Revisado	15/05/2022	Mateo González					
Aprobado							
		Código: SDS 002		Trat. Superficial:		Hoja: 26	



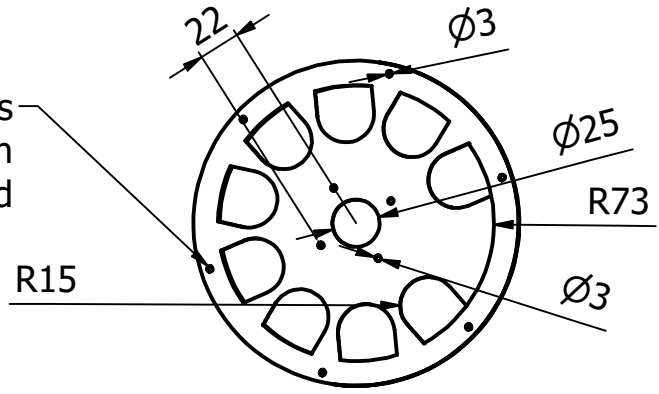


B-B (0.5 : 2)

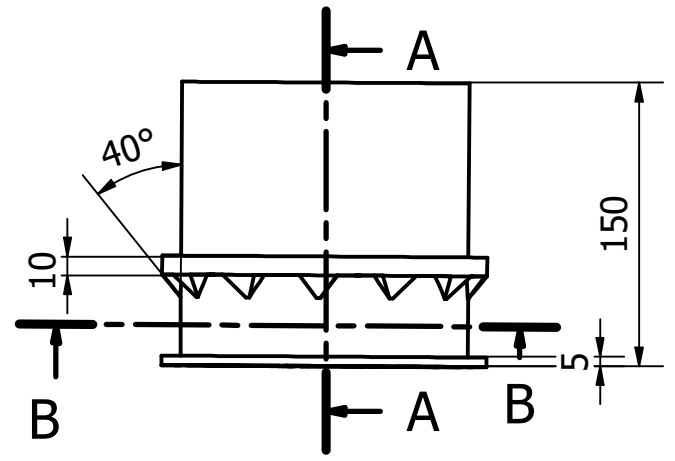
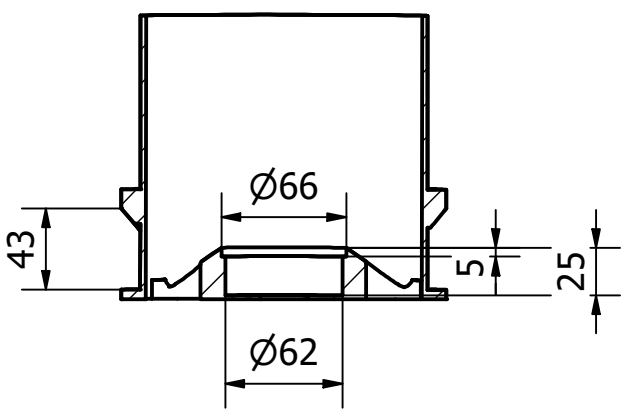
12 Supports
Circular Pattern
Equally Spaced



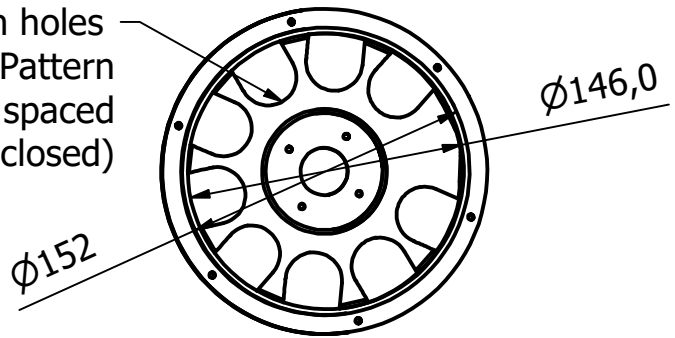
6 holes
Circular Pattern
Equally Spaced



A-A (0.5 : 2)

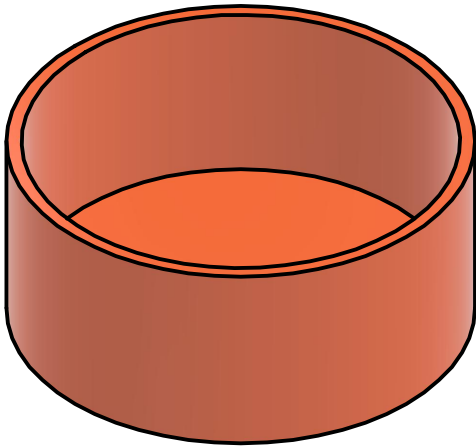
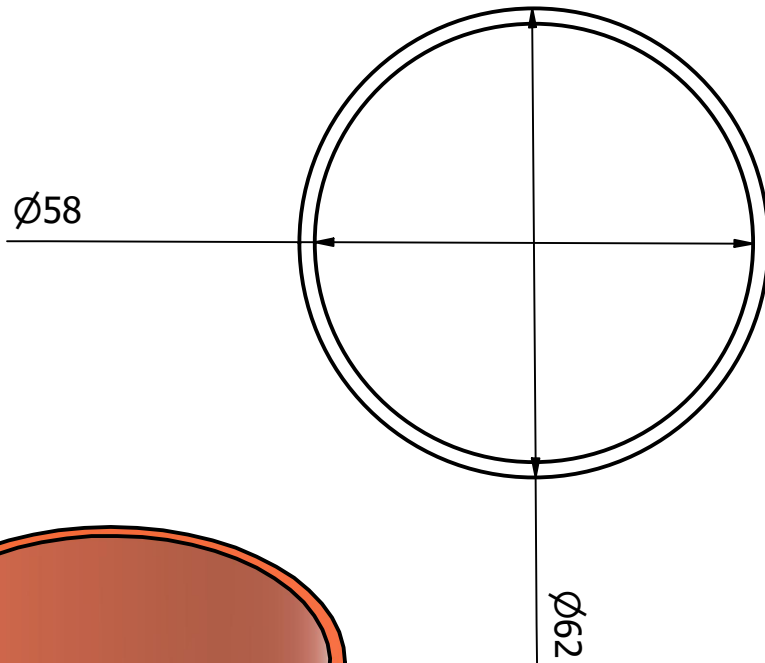
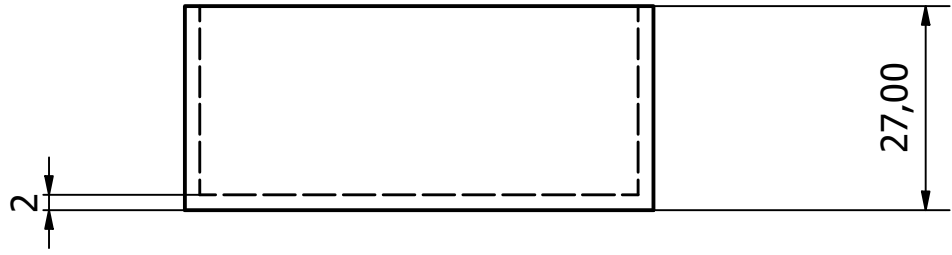


Ten holes
Circular Pattern
Equally spaced
(One is closed)



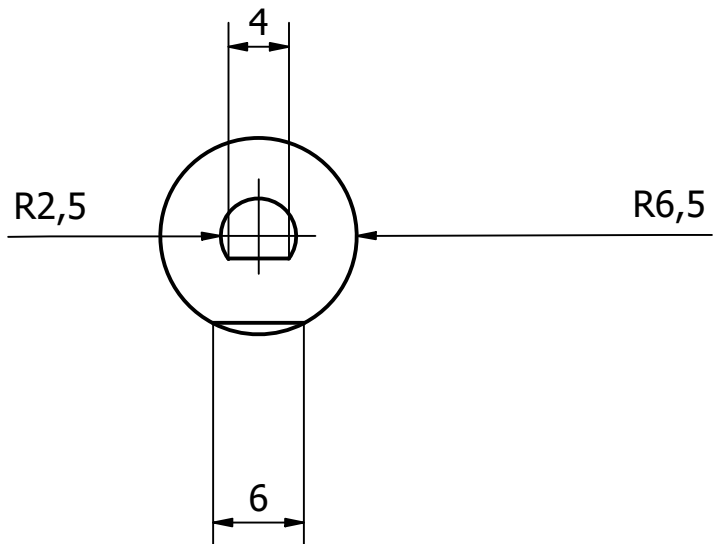
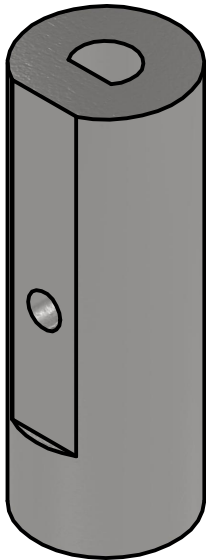
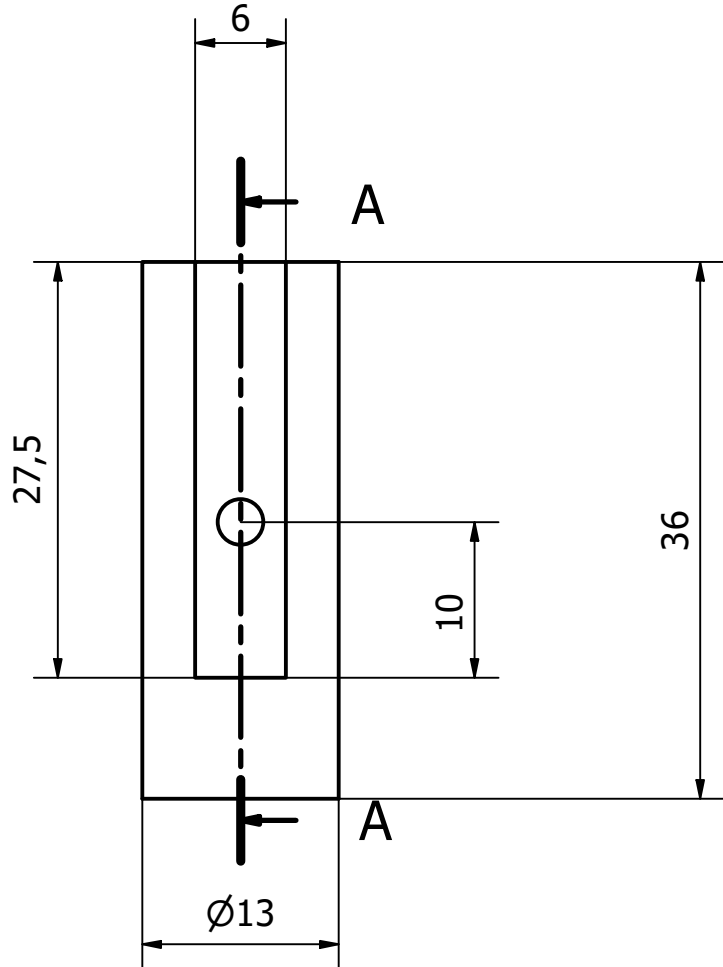
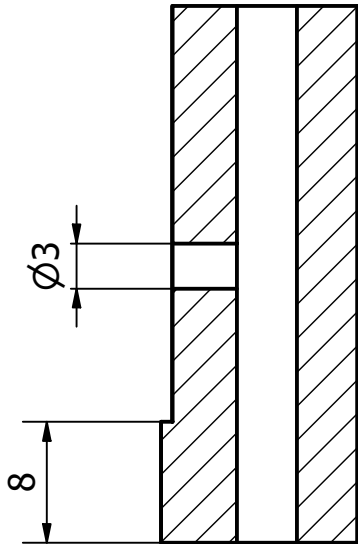
Tolerancia: +- 1 [mm]		Peso: 0.640 kg		PET Plastic			
Fecha		Nombre		Seed Tank		Escala: 0.5 : 2	
Dibujado	15/02/2022	Mateo González					
Revisado	15/02/2022	Mateo Ormaza					
Aprobado							
		Código: SDS 003		Trat. Superficial:		Hoja: 27	






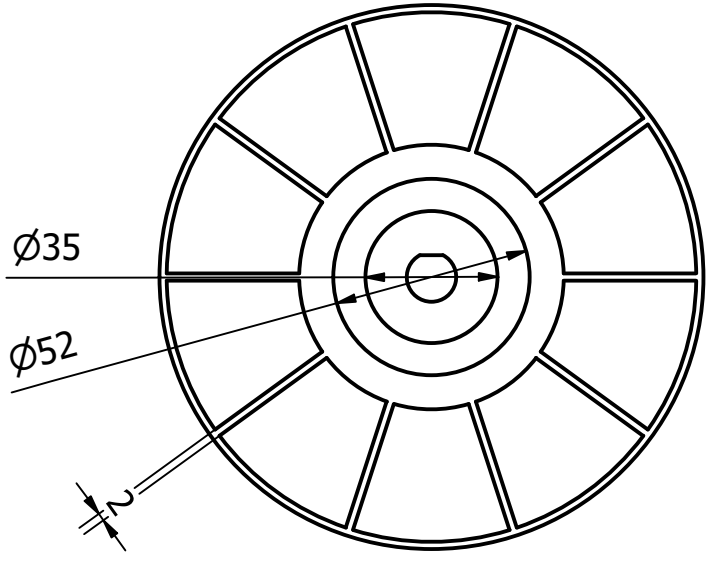


Tolerancia: +- 1 [mm]		Peso: 0.024 kg		PET Plastic		
	Fecha	Nombre		Nema Lid		Escala: 1 : 1
Dibujado	15/02/2022	Mateo González				
Revisado	15/02/2022	Mateo Ormaza				
Aprobado						
			Código: SDS 005		Trat. Superficial:	Hoja: 28

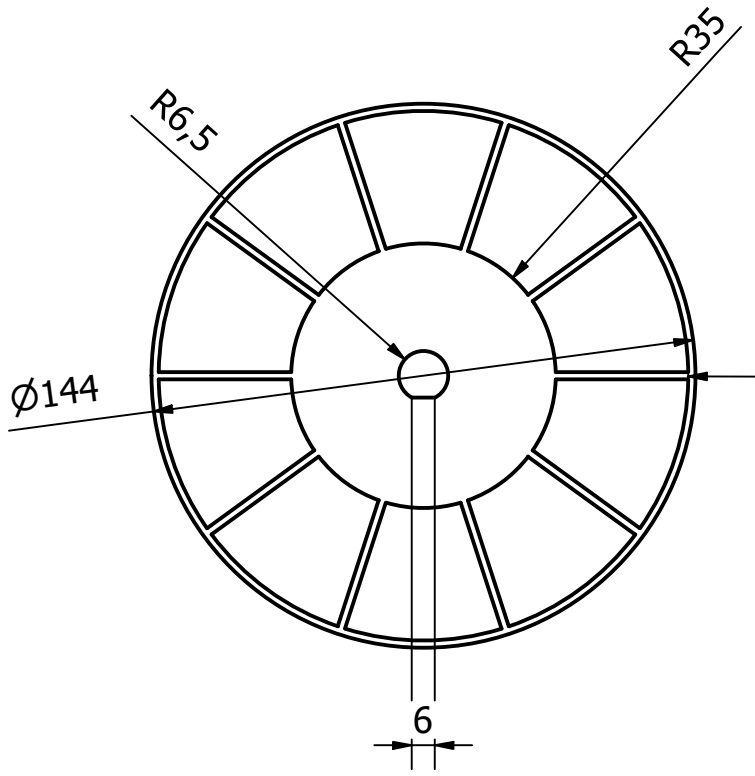
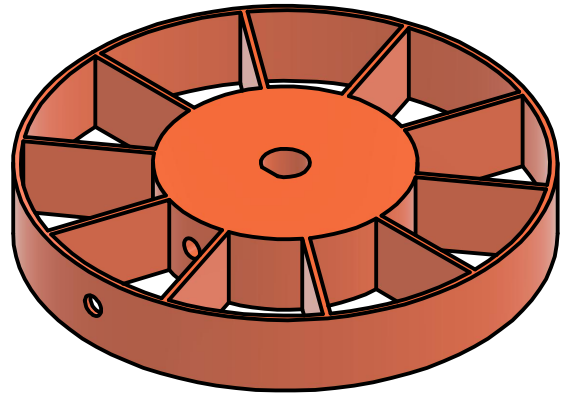
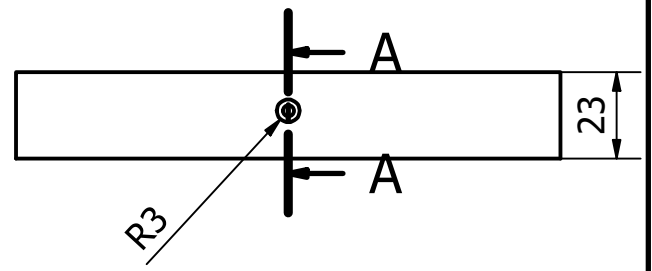
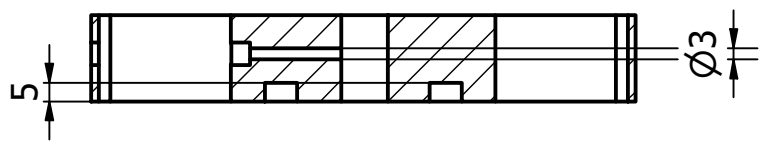
A-A (2 : 1)



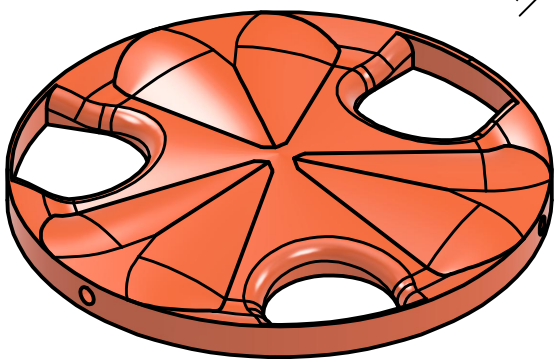
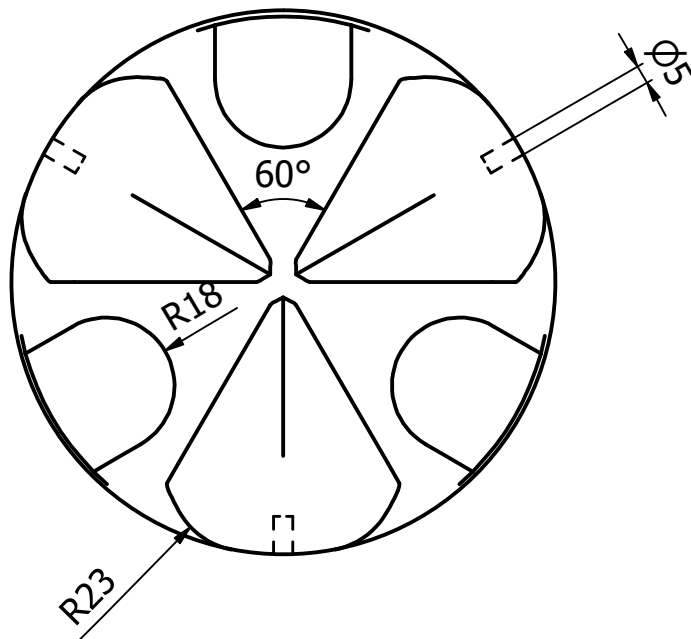
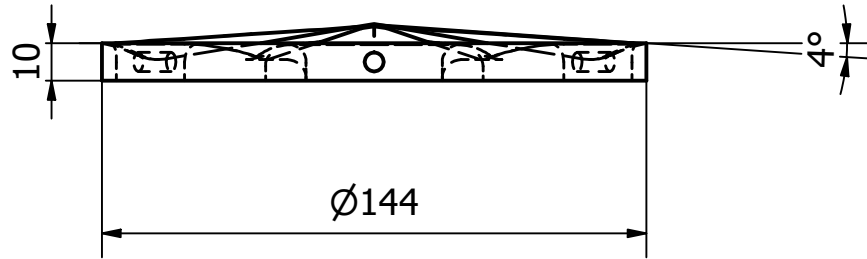
Tolerancia: +- 0.1 [mm]		Peso: N/A		Steel, Galvanized		 	
Fecha		Nombre		Seed Distributor Rod		Escala: 2 : 1	
Dibujado	15/02/2022	Mateo Ormaza					
Revisado	15/05/2022	Mateo González					
Aprobado							
		Código: SDS 005		Trat. Superficial:		Hoja: 29	



A-A (1 : 2)



Tolerancia: +- 1 [mm]		Peso: 0.178 kg		PET Plastic			
Fecha		Nombre		Seed Distributor		Escala: 1 : 2	
Dibujado	15/05/2022	Mateo González					
Revisado	15/05/2022	Mateo Ormaza					
Aprobado							
		Código: SDS 004		Trat. Superficial:		Hoja: 30	



Tolerancia: +- 1 [mm]		Peso: 0.198 kg		PET Plastic			
	Fecha	Nombre		Seed Separator		Escala: 0.5 : 1	
Dibujado	15/05/2022	Mateo González					
Revisado	15/05/2022	Gabriel Gómez					
Aprobado							
				Código: SDS - 001		Trat. Superficial:	
						Hoja: 31	